

# Lawrence Berkeley National Laboratory

## Recent Work

### Title

PREPARATIONS AND MECHANISM OF HYDROLYSIS OF ( [8] ANNULENE)ACTINIDE COMPOUNDS

### Permalink

<https://escholarship.org/uc/item/2tn049bk>

### Author

Moore, R.M.

### Publication Date

1985-07-01

c.2



# Lawrence Berkeley Laboratory

UNIVERSITY OF CALIFORNIA

## Materials & Molecular Research Division

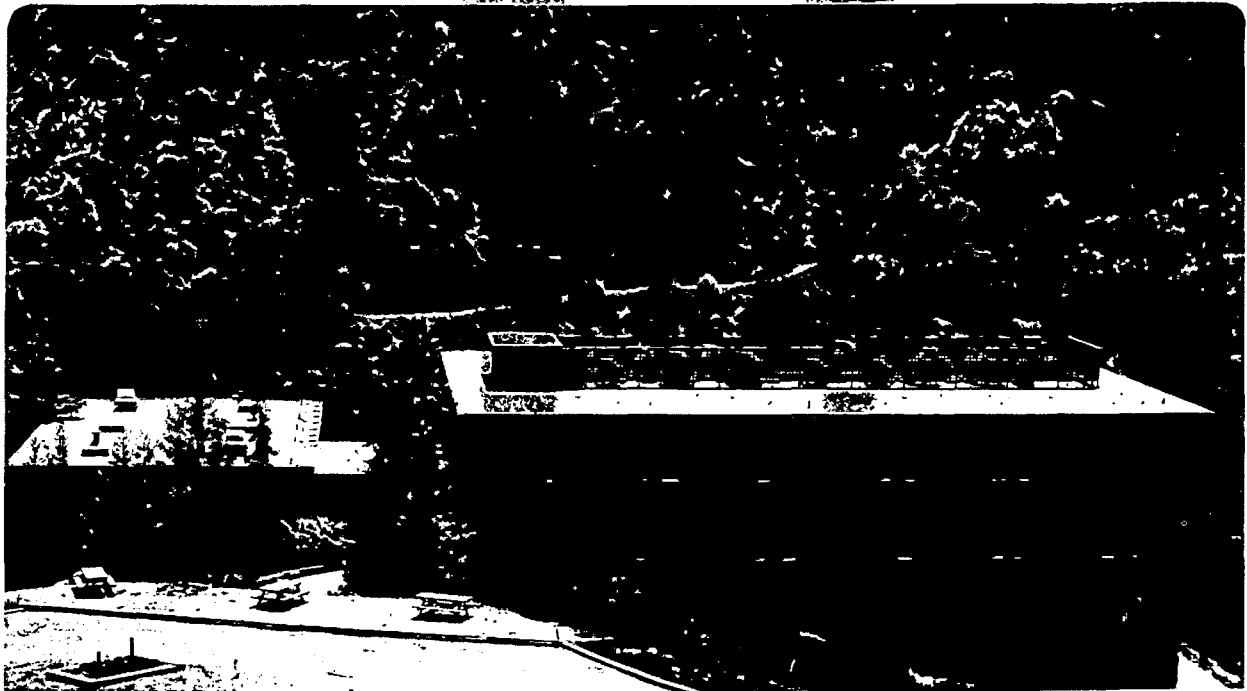
RECEIVED  
E. O. RICHARDSON LIBRARY  
SERIES 1855  
MAY 1985  
MATERIALS & MOLECULAR RESEARCH DIVISION

PREPARATIONS AND MECHANISM OF HYDROLYSIS  
OF ([8]ANNULENE)ACTINIDE COMPOUNDS

R.M. Moore, Jr.  
(Ph.D. Thesis)

July 1985

**TWO-WEEK LOAN COPY**  
*This is a Library Circulating Copy  
which may be borrowed for two weeks.*



LBL-20031  
c.2

## **DISCLAIMER**

This document was prepared as an account of work sponsored by the United States Government. While this document is believed to contain correct information, neither the United States Government nor any agency thereof, nor the Regents of the University of California, nor any of their employees, makes any warranty, express or implied, or assumes any legal responsibility for the accuracy, completeness, or usefulness of any information, apparatus, product, or process disclosed, or represents that its use would not infringe privately owned rights. Reference herein to any specific commercial product, process, or service by its trade name, trademark, manufacturer, or otherwise, does not necessarily constitute or imply its endorsement, recommendation, or favoring by the United States Government or any agency thereof, or the Regents of the University of California. The views and opinions of authors expressed herein do not necessarily state or reflect those of the United States Government or any agency thereof or the Regents of the University of California.

Preparations and Mechanism of Hydrolysis  
of ([8]annulene)actinide Compounds

Robert Michael Moore, Jr.

Ph.D. Dissertation

July, 1985

Materials and Molecular Research Division, Lawrence  
Berkeley Laboratory and Department of Chemistry,  
University of California, Berkeley, California 94720

This work was supported in part by the Director, Office  
of Energy Research, Office of Basic Energy Sciences,  
Chemical Sciences Division of the U.S. Department of Energy,  
under Contract No. DE-AC03-76SF00098.

Preparations and Mechanism of Hydrolysis  
of ([8]Annulene)actinide Complexes

Robert Michael Moore Jr.

Abstract

The mechanism of hydrolysis for bis[8]annulene actinide and lanthanide complexes has been studied in detail. The uranium complex, uranocene, decomposes with good pseudo-first order kinetics (in uranocene) in 1 M degassed solutions of H<sub>2</sub>O in THF. Decomposition of a series of aryl-substituted uranocenes demonstrates that the hydrolysis rate is dependent on the electronic nature of the substituent (Hammett rho value=2.1, r<sup>2</sup>=0.999), with electron-withdrawing groups increasing the rate. When D<sub>2</sub>O is substituted for H<sub>2</sub>O, kinetic isotope effects of 8 to 14 are found for a variety of substituted uranocenes. These results suggest a pre-equilibrium involving approach of a water molecule to the central metal, followed by rate determining proton transfer to the eight membered ring and rapid decomposition to products. Each of the four protonations of the complex has a significant isotope effect. The product ratio of cyclooctatriene isomers formed in the hydrolysis (1,3,5/1,3,6) varies, depending on the central metal of the complex. However, the general mechanism of hydrolysis, established for uranocene, can be extended to the hydrolysis and alcoholysis of all the [8]annulene complexes of the lanthanides and actinides.

A successful, reproducible preparation of ([8]annulene)-uranium dichloride (or the uranium "half-sandwich") has been achieved. The best method consists of the addition of an excess of NaH to a THF solution of  $UCl_4$  and cyclooctatetraene. Addition of alkyl and aryl lithium and grignard reagents has thus far failed to produce any isolable products. However, reaction of  $PMe_3$  with the half-sandwich did result in a trimethylphosphine coordinated complex. Exchange of free  $PMe_3$  with coordinated  $PMe_3$  is observed in the  $^1H$  NMR spectrum of the complex. Line shape analysis of the coalescing peaks results in a  $\Delta G^\ddagger$  of  $12.1 \pm 0.5$  kcal/mol for the process.

Finally, line shape analysis of the  $^1H$  nmr spectrum of 1,1'-diphenyluranocene as a function of temperature gives the activation parameters  $\Delta H^\ddagger = 4.4 \pm 0.3$  kcal mol $^{-1}$  and  $\Delta S^\ddagger = -4.7 \pm 1.3$  e.u. for the rotation of the phenyl group about the bond to the eight-membered ring.

## Acknowledgements

As is usually the case in a dissertation, I am unable to acknowledge all those people who have helped me grow both personally and professionally. There are a number of people, however, who have had a major role in my development as a chemist.

Thanks go to Ms. Ballance and Mr. Stevens at Largo High for developing my interest in science. I must also express my appreciation to my mentor at Rice, W. E. Billups. I am grateful to Dr. Billups for granting me my first opportunity to carry out chemical research. His lucid teaching style and jovial, down-to-earth personality brought organic chemistry within the grasp of most Rice students, while at the same time making the course both interesting and dynamic.

I also owe an enormous debt of gratitude to my research advisor at Berkeley, Andrew Streitwieser, Jr. Besides the always dependable financial support, he has provided a positive learning environment for a graduate student to grow into a creative thinking scientist. Any progress that I have made in this regard can be attributed to his desire for me to bring out the best in myself. Thanks also to all the Streitwieser group members for all the socializing, theorizing, and Romancing. The camaraderie enriched the Berkeley graduate school experience for all of us and contributed towards the pleasant atmosphere in our labs.

I won't list specifically the names of my friends who have made these years so memorable, but I am an open person and

they have been told how much their friendship is valued. I do wish to acknowledge my family and in particular, my parents, for all their love and support. Ever since I can remember, they have encouraged me in a way I don't think can be equaled. They have always trusted my decisions, whether or not they agreed or understood them, and that has given me the strength and confidence to grow. I am truly blessed.



..... to my brother, Ed

## Table of Contents

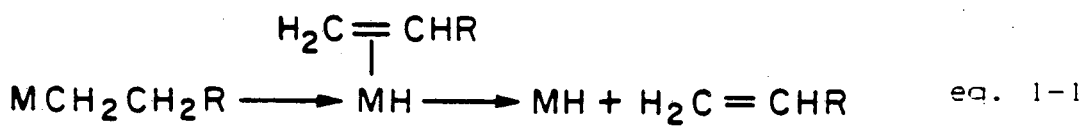
Chapter 1. The Mechanism of Hydrolysis of	
Bis-( $\pi$ -[8]annulene)actinide Complexes-----	1
Introduction-----	1
Results: Kinetic Experiments-----	19
Results: Product Analysis-----	53
Results: Half-Sandwich Hydrolysis-----	71
Conclusions on the Product Analyses-----	76
Experimental-----	77
Footnotes and References-----	92
 Chapter 2. The Preparation of ([8]Annulene)uranium	
Dichloride Bistetrahydrofuran-----	96
Introduction-----	96
Results: Preparation of the Half-Sandwich-----	101
Results: Preparation of a Substituted Uranium	
Half-Sandwich-----	112
Results: Reactions of the Uranium Half-Sandwich-----	114
Conclusions on the Chemistry of the Half-Sandwich-----	130
Experimental-----	131
Footnotes and References-----	139
 Chapter 3. The Phenyl Rotational Barrier in	
1,1'-Diphenyluranocene-----	140
Introduction-----	140
Results-----	144
Experimental-----	150
Footnotes and References-----	153

CHAPTER 1. THE MECHANISM OF HYDROLYSIS OF  
BIS-(π-[8]-ANNULENE)ACTINIDE COMPLEXES

Introduction

Over the last twenty years, a large amount of research effort has been dedicated towards the elucidation of reaction mechanisms involving transition-metal organometallic complexes. In comparison, very few detailed mechanistic studies of actinide organometallic complexes have been performed. Much of the earlier work in organoactinide chemistry dealt with the preparation and characterization of kinetically and thermodynamically stable complexes. A number of excellent reviews provide extensive coverage of the methods used in preparing and isolating these compounds.<sup>1</sup> This introduction will review the few studies which have attempted to define mechanisms in the reaction chemistry of organometallic thorium and uranium complexes.

One of the first detailed mechanistic studies in organoactinide chemistry was carried out by Marks and co-workers on the thermolysis pathway of tris(η<sup>5</sup>-cyclopentadienyl)uranium(IV) alkyl and aryl complexes.<sup>2</sup> Product analysis revealed that thermal decomposition of the (C<sub>5</sub>H<sub>5</sub>)<sub>3</sub>UR compounds in toluene solution resulted in nearly quantitative yields of the alkane RH. Decomposition via β-elimination (equation 1-1) should result in substantial quantities of olefin, yet only trace



amounts of olefin products were observed. Kinetic investigations (Table 1-1) demonstrated that the primary alkyl uranium complexes, such as the *n*-butyl compound, are more stable than the neopentyl compound, which would resist  $\beta$ -elimination.

Table 1-1. Kinetic Data for the Thermolysis of  $Cp_3UR$  Compounds in Toluene Solution

R	Concn, M	Temp, °C	$k \times 10^4$ , hr <sup>-1</sup>	$t_{1/2}$ , hr	$\Delta G^\ddagger$ , kcal/mol
<i>t</i> -C <sub>4</sub> H <sub>9</sub>	0.086	72	51,000 $\pm$ 5100	0.137	24.8
C <sub>6</sub> F <sub>5</sub>	0.208	72	1890 $\pm$ 50	3.86	27.0
Allyl	0.138	72	167 $\pm$ 3	40.0	28.7
<i>i</i> -C <sub>3</sub> H <sub>7</sub>	0.292	72	34.0 $\pm$ 1	201	29.8
Neo-C <sub>5</sub> H <sub>11</sub>	0.042	97	25.7 $\pm$ 0.2	270	32.2
<i>n</i> -C <sub>4</sub> H <sub>9</sub>	0.220	97	6.10 $\pm$ 0.3	1136	33.3
	0.072	97	6.17 $\pm$ 0.1	1123	33.3
CH <sub>3</sub>	0.181	97	1.10 $\pm$ 0.1	6300	34.5
<i>trans</i> -2-Butenyl	0.303	97	1.03 $\pm$ 0.1	6730	34.6

Small amounts of deuterium incorporated in the alkane produced when the reaction was run in toluene-d<sub>8</sub> provide strong evidence for homolytic scission of the metal-alkane bond, although no isomerization of *trans*-2-butene to *cis*-2-butene was observed when its respective uranium complex was thermolyzed (free 2-butenyl radicals are known to undergo rapid inversion<sup>3</sup>). The observations were thus explained as a hydrogen transfer from the cyclopentadienyl rings to the alkane in a concerted, stereospecific fashion with some competition involving abstraction of solvent molecules (Figure 1-1).

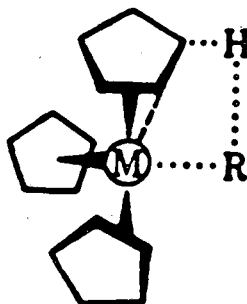


FIGURE 1-1

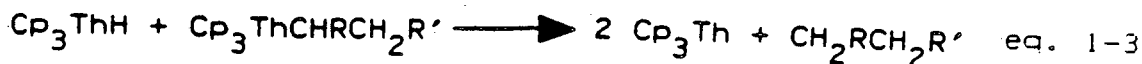
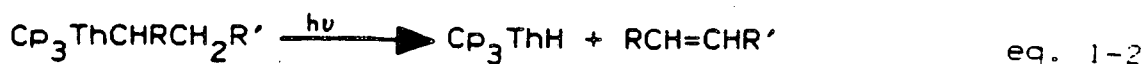
In a later study involving the analogous tris( $\eta^5$ -cyclopentadienyl)thorium alkyl complexes, or  $\text{Cp}_3\text{ThR}$ , Marks found the thermolysis pathway to be similar to the uranium complexes with molecular extrusion of R-H taking place rather than olefin elimination.<sup>4</sup> Kinetic studies were also undertaken and in all cases, considerably greater thermal stability was found for the thorium complexes in comparison to the analogous uranium compounds (Table 1-2).

Table 1-2. Comparative Data for Thermolysis of  $\text{Cp}_3\text{MR}$  Compounds in Solution

R	M = U		M = Th	
	$\Delta G^\ddagger$ (kcal/mol)	$t_{1/2}$ (hr)	$\Delta G^\ddagger$ (kcal/mol)	$t_{1/2}$ (hr)
<i>n</i> -C <sub>4</sub> H <sub>9</sub> <sup>b</sup>	33.3 (97°)	1130	37.6 (167°)	96
Neopentyl <sup>b</sup>	32.2 (97°)	270	41.4 (167°)	7500
<i>i</i> -C <sub>3</sub> H <sub>7</sub> <sup>a</sup>	29.8 (72°)	201	35.3 (167°)	7.1
Allyl <sup>b</sup>	28.7 (72°)	40	38.6 (167°)	566
<i>trans</i> -2-Butenyl <sup>a</sup>	34.6 (97°)	6730	36.3 (167°)	21

The high thermal stability of the tris-Cp complexes is remarkable considering the thermal instability of uranium tetraalkyls first noted during the Manhattan project.<sup>5</sup> The inability to suffer  $\beta$ -elimination due to partial or complete coordinative saturation of the uranium(IV) ion was offered as an explanation for the stability of the tris-Cp compounds.<sup>6</sup> In comparison, the observation of alkenes in the thermal decomposition of uranium tetraalkyls, along with their relative coordinative unsaturation suggests<sup>6</sup> that uranium tetraalkyls can decompose by  $\beta$ -hydride-elimination, although the additional presence of alkanes implies that another mechanism may also be operative. The retention of stereochemistry in the 2-butenes suggests<sup>6</sup> that free 2-butenyl radicals are not involved in the decomposition of uranium tetraalkyls.

While coordinatively saturated hydrocarbyls of the type  $\text{Cp}_3\text{ThR}$  resist  $\beta$ -hydride-elimination, the process occurs easily and cleanly for R derivatives such as isopropyl and n-butyl under photochemical excitation.<sup>7</sup> Photolysis of the thorium complexes at wavelengths shorter than 350 nm produced a 1:1 ratio of olefin:alkane. The photochemistry is consistent with a photoinduced  $\beta$ -hydride elimination reaction to yield a thorium hydride and olefin, followed by reductive elimination of alkane<sup>8</sup> (equations 1-2, 1-3).



Classical free-radical processes can be discounted as a major pathway since significant amounts of the dimer  $(-\text{CHRCH}_2\text{R}')_2$  are not observed, nor are products containing solvent abstracted deuterium. Radical processes may be operative when no  $\beta$ -hydrogens are present as in the case of  $\text{Cp}_3\text{ThCH}_3$ , when far slower methane producing reactions occur with ethane and hydrogen observed as well.

Mechanistic organoactinide studies are not completely limited to the tris-Cp complexes. A reversible ortho-hydrogen-abstraction mechanism to form an actinide benzyne complex (Figure 1-2) was proposed<sup>9</sup> to explain a rapid hydrocarbon metathesis process involving the thermally unstable bis- $[\eta^5\text{-pentamethylcyclopentadienyl}]$ -uranium diphenyl complex.

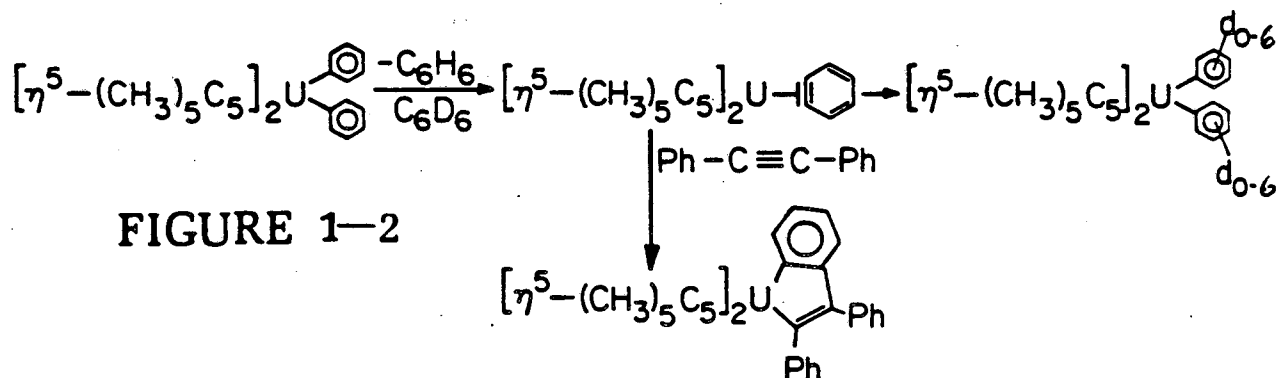
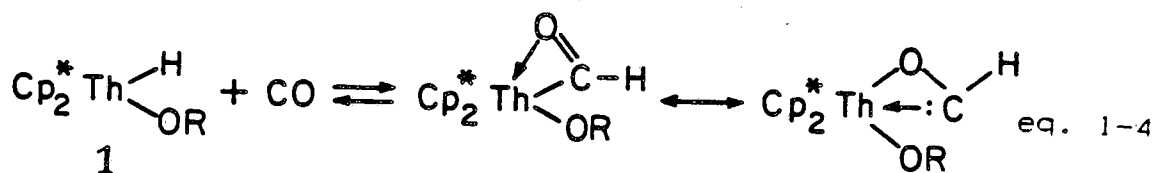


FIGURE 1-2

The intermediate benzyne can be trapped by addition of diphenylacetylene. Formation of the metalocycle occurs at a rate which is indistinguishable from the rate of decomposition of the diphenyl complex in the absence of diphenylacetylene. The thorium analog undergoes the same transformations; however, temperatures

of 100°C are required to achieve rates comparable to the uranium complex decomposition at room temperature.

After these initial mechanistic studies on the thermal decomposition of actinide-alkyl complexes, Marks and co-workers investigated migratory CO insertion into actinide-carbon and actinide-hydrogen bonds.<sup>10</sup> They found that thorium hydrides of the type  $\text{Cp}^*_2\text{Th}(\text{H})(\text{OR})$  ( $\text{Cp}^* = \eta^5\text{-C}_5\text{Me}_5$ ; OR=alkoxide) undergo a rapid, reversible migratory insertion of carbon monoxide to yield  $\eta^2$ -formyls (equation 1-4).



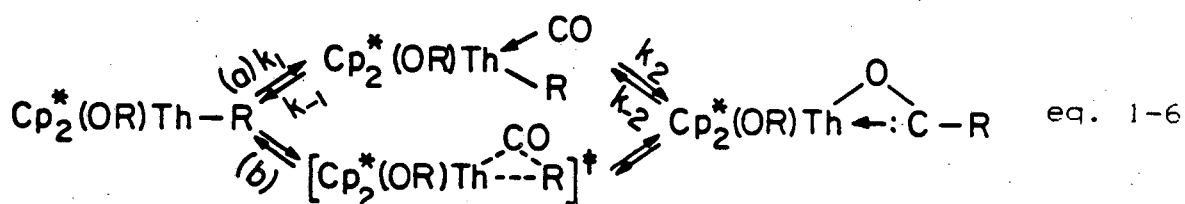
Varying the temperature causes substantial changes in the relative concentrations of hydride and formyl, with lower temperatures favoring the formyl.<sup>11</sup> Thermodynamic parameters could thus be determined for the equilibrium. In particular, large negative entropy values were determined for sterically bulky alkoxide complexes. Over a CO pressure range of 150-850 torr, the rate law for the insertion was found to obey equation 1-5, where

$$\text{rate} = k'[\text{1}][\text{CO}] = kP_{\text{CO}}[\text{1}] \quad \text{eq. 1-5}$$

$k'[\text{CO}] = kP_{\text{CO}}$  assuming Henry's law is obeyed. Varying the concentration of 1 by a factor of five causes a negligible change in the observed NMR line width near coalescence, consistent with a



first order dependence on metal hydride concentration and inconsistent with a rate-limiting intermolecular hydrogen transfer. Crossover (varying alkoxide) and labeling experiments with deuterium lend further support for an intramolecular reaction and a monomeric formyl species. On this basis, the stepwise(a) or concerted(b) pathways depicted in equation 1-6 were postulated as the most plausible scenarios for migratory insertion.<sup>11</sup>



Although the kinetic data cannot distinguish between paths a and b, it was possible to determine that if path a is operative,  $k_2$  is rate-limiting by the demonstration that the insertion process for thorium hydrides exhibits a substantial primary kinetic isotope effect.

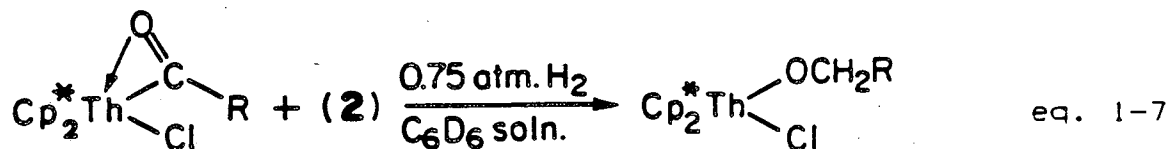
Table 1-3. Kinetic Data for  $\text{Cp}_2^*\text{Th}(\text{R})(\text{X})$   
Migratory CO Insertion

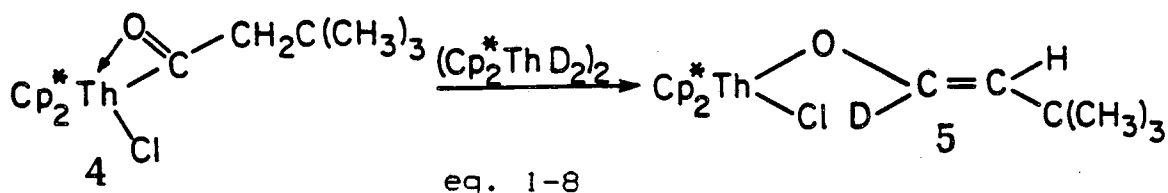
compd		temp, °C	k, min <sup>-1</sup> torr <sup>-1</sup>
R	X		
H	OCH- <i>t</i> -Bu <sub>2</sub>	-45	3.0 (3)
CH <sub>2</sub> - <i>t</i> -Bu	Cl	-54	4 × 10 <sup>-2</sup>
CH <sub>2</sub> - <i>t</i> -Bu	O- <i>t</i> -Bu	-54	4 × 10 <sup>-3</sup>
CH <sub>2</sub> - <i>t</i> -Bu	OCH- <i>t</i> -Bu <sub>2</sub>	-54	6 × 10 <sup>-4</sup>
<i>n</i> -Bu	OCH- <i>t</i> -Bu <sub>2</sub>	-54	4.6 (7) × 10 <sup>-5</sup>
Me	OCH- <i>t</i> -Bu <sub>2</sub>	0	5 × 10 <sup>-7</sup>

The kinetic data in Table 1-3<sup>11</sup> demonstrates the relative ease of migratory CO insertion for hydride.<sup>12</sup> For the series of complexes examined, hydride insertion was always found to be much more rapid than alkyl insertion. Since thorium-hydrogen bond disruption energies exceed those of thorium-carbon by approximately 15 kcal/mol,<sup>13</sup> it was concluded that the transition state is not governed by ground state parameters and that the reduced barrier for the hydride is a kinetic property of the migrating group.

Finally, it was noted<sup>11</sup> that the presence of a halide ligand (Cl) in place of alkoxide results in a further increase in the reaction rate. Since chloride is a poorer electron donor than alkoxide, the thorium(IV) is formally more unsaturated in the halide complex.

These same carbene-like,  $\eta^2$ -acyl thorium compounds were also found to react with thorium hydrides.<sup>14</sup> Homogeneous hydrogenation of the  $\eta^2$ -acyls to the corresponding alkoxide derivatives  $[\text{Th}(\eta^2\text{-COR}) \rightarrow \text{Th-OCH}_2\text{R}]$  can be carried out at room temperature and less than 1 atmosphere of  $\text{H}_2$  pressure by using the hydride  $(\text{ThCp}^* \text{H}_2)_2$  (2) as a catalyst (eq. 1-7).





Mechanistic information on the hydrogenation reaction is provided by deuterium labeling studies. Under an atmosphere of  $D_2$ , the alkoxide products are deuterated exclusively (>90% by  $^1H$  NMR spectroscopy) in the  $\alpha$  position. When no  $D_2$  is present,  $(ThCp^*_2D_2)_2$  catalyzes the isomerization of 4 to quantitatively yield the trans-enolate 5 (eq 1-8). The observations are interpreted in terms of the scheme in Figure 1-3. Insertion of the carbene-like thorium acyl complex into the thorium-deuteride bond results in the intermediate 6.  $\beta$ -elimination regenerates the catalyst 2 and yields the enolate 5. The sequence is particularly interesting because it suggests an attractive mechanism for certain types of CO reduction catalyses.

Streitwieser and co-workers have also initiated some organoactinide mechanistic studies. Grant and Streitwieser have found that uranocenes rapidly convert alkyl and aryl nitro compounds into their respective azo derivatives (eq. 1-9, 1-10).<sup>15,16</sup> The experimental results were not definitive, but they did find that azoxybenzene, which is reduced by 7 to azobenzene, reacts too slowly to be an intermediate in nitrobenzene

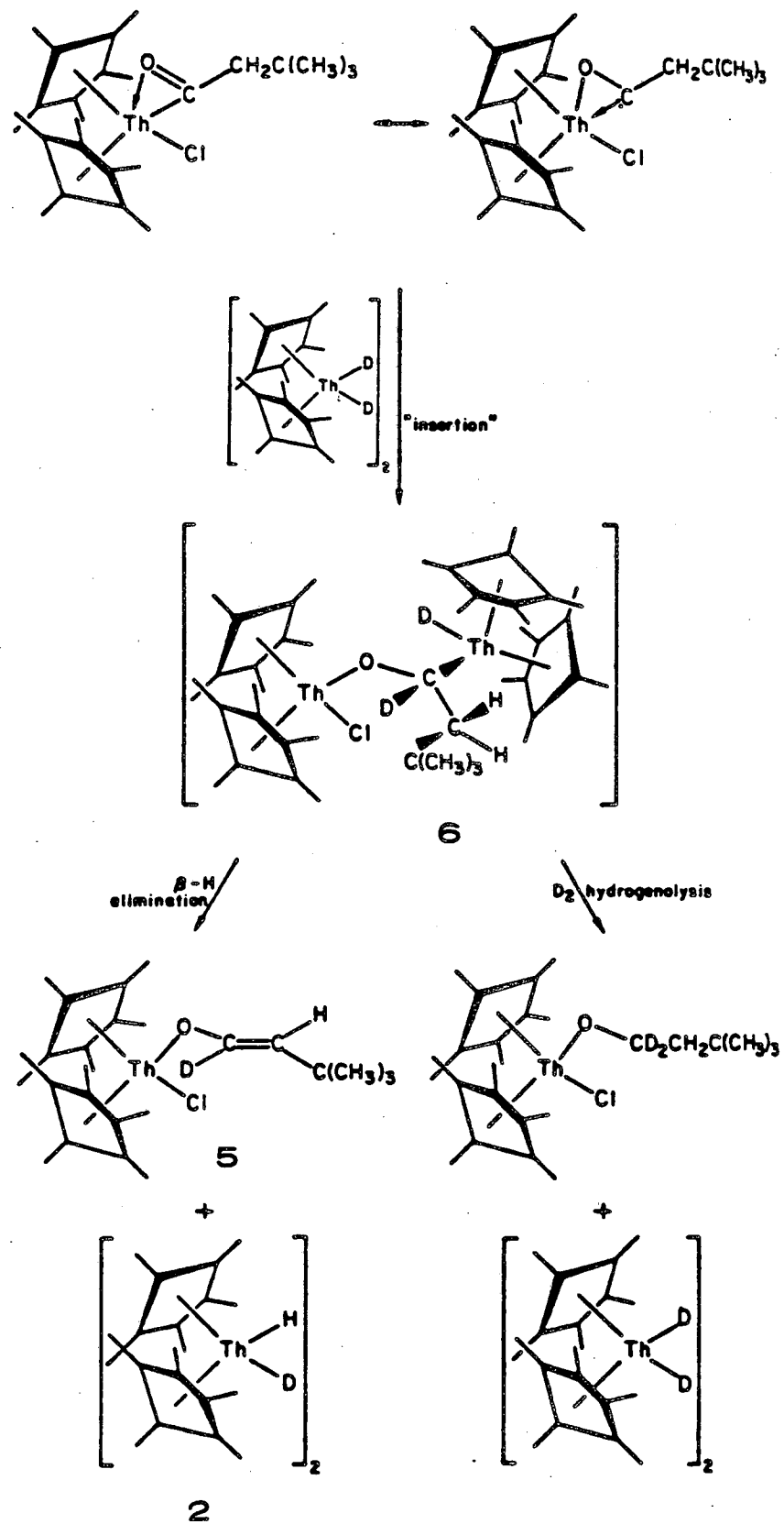
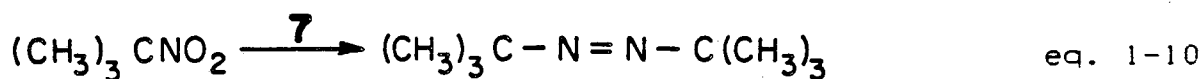
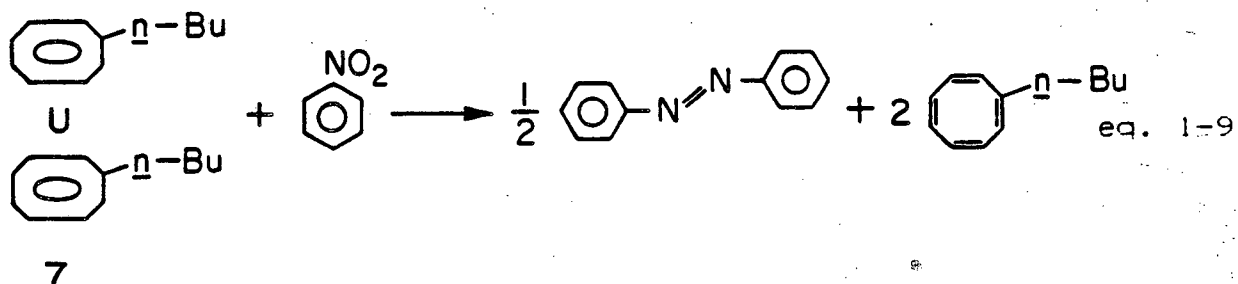
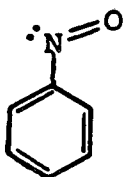


FIGURE 1-3

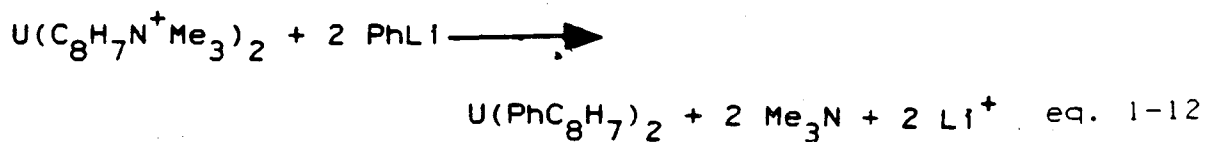


reductions.<sup>15</sup> The high rate of the reaction suggests an electron transfer from 7 to the nitro compound after direct attack by a nitro oxygen at the central actinide metal.<sup>16</sup> Free nitro radical anions or nitrenes do not appear to be involved, but free nitroso compounds such as 8 are possible intermediates.



8

Alkoxyuranocenes and uranocyltrimethylammonium ions have been found to undergo ring metallation reactions (eq. 1-11, 1-12).<sup>17</sup>



Methyl lithium is apparently too weak to metallate methoxyuranocene directly, but it does react with the 1,1'-uranocyl-bis-trimethylammonium salt. Thus, methyl lithium should react with any intermediates involved in the reaction sequence.<sup>18</sup>

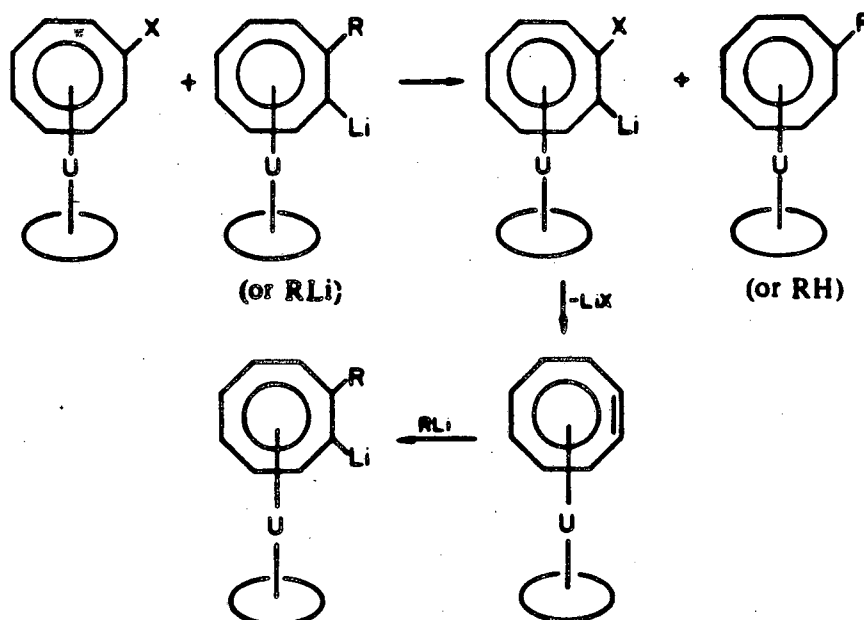
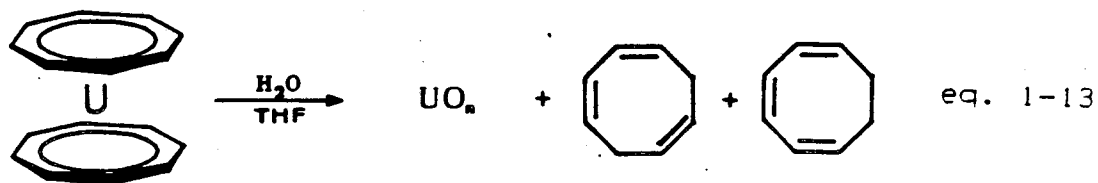


FIGURE 1-4

When 1,1'-dimethoxyuranocene was treated with a mixture of methyl lithium and *n*-butyllithium a mixture of uranocenes resulted, which gave both methyl and *n*-butylcyclooctatetraene upon oxidation. The reaction is proposed to involve metallation of the ring followed by loss of the electronegative substituent to yield a uranium derivative of cyclooctatrienyne (figure 1-4). This intermediate can react with either methyl lithium or *n*-butyllithium to give incorporation of both methyl and butyl groups.

A number of other authors have speculated on mechanisms in organoactinide chemistry, but without any competitive, kinetic or intermediate trapping experiments to back up a scheme, most of the mechanisms are mere "paper chemistry" to rationalize an observed result. Not that a detailed mechanistic study would have been trivial. Often an organoactinide reaction is complicated by significant side reactions or by the formation of intractable organometallic products. Proposing a reasonable intermediate in a reaction sequence then becomes uncertain or as is sometimes the case, elusive to the investigator.

Thus, if we are to begin to comprehend the factors which influence reactivity in organoactinide complexes, mechanistic studies of simple, unambiguous reactions are necessary. One such reaction is the hydrolysis of uranocene or bis-( $\pi$ -[8]annulene)uranium(IV) (eq. 1-13).



The hydrolysis decomposition is ideal for study because of the irreversible formation of high energy uranium-oxide bonds; reverse reaction complications are thus avoided. In addition, uranocenes possess an easily monitored absorbance in the visible region of the electromagnetic spectrum (610-635 nm, depending on the substituent), which will not be obscured by the primarily

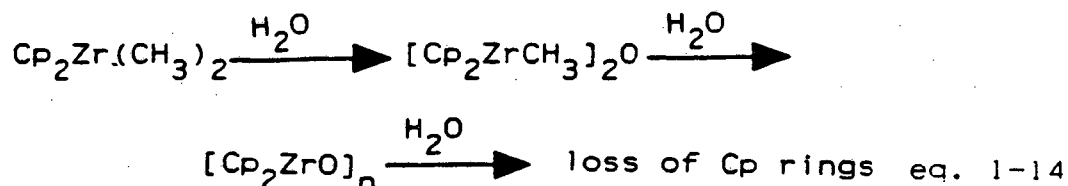
UV-absorbing products. A fortuitous opportunity is thus available to do a detailed kinetic study of the hydrolysis of an oxophilic Group IV-type metal.

A study of the hydrolysis of Group IV-type organometallic complexes would not be the first of its kind. Other authors, in briefer investigations have found certain trends in the products observed from the hydrolysis or alcoholysis of zirconium and titanium organometallic complexes.<sup>19</sup> In general, compounds of zirconium and hafnium containing a metal-carbon bond are extremely reactive toward protic reagents.<sup>20</sup> On the other hand, similarly complexed titanium compounds tend to be much more resistant to hydrolysis. The increase in stability could be due to the decrease in metal size preventing easy access of water to a coordination site. Another possibility is a decrease in Lewis acidity for titanium, discouraging coordination of a Lewis base such as an alcohol or water.

A decrease in Lewis acidity and thus, an increase in hydrolytic stability can result if more electron-donating groups are present.  $\text{CpTiCl}_3$  is destroyed by alkaline hydrolysis, but  $\pi\text{-Cp}^*\text{TiCl}_3$  is converted only to  $[\text{Cp}^*\text{TiO(OH)}]_n$ .<sup>21</sup> An additional Cp ring can also increase the compound's resistance to hydrolysis, however. Trimethylcyclopentadienyltitanium ( $\text{CpTiMe}_3$ ) liberates methane upon reaction with water or alcohol, while the bis-cyclopentadienyl titanium complex ( $\text{Cp}_2\text{TiMe}_2$ ) is stable to hydrolysis.<sup>22</sup> The trihalide complexes of titanium are generally all sensitive to hydrolysis.

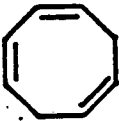

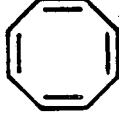


Electron-donating groups have been found to stabilize the bis-Cp<sup>\*</sup> zirconium complexes towards hydrolysis as well. The qualitative ordering<sup>23</sup> MeCp > Cp > indenyl > fluorenyl (fluorenyl complexes are most reactive towards hydrolysis), illustrates the importance of electronic over steric factors in their reaction with protic reagents. In general, hydrolysis of the  $\sigma$ -bonded alkyl groups occurs first, followed by liberation of the cyclopentadienyl (or substituted Cp) ring, sometimes requiring more vigorous reaction conditions<sup>20</sup> (eq. 1-14).



Any increase in the ionicity of the zirconium- $\eta^5$ -cyclopentadienyl bond (from  $\text{Cp}_2\text{ZrCl}_2$ ) increases its reactivity towards acidic protons. Samuel<sup>24</sup> has found that if the cyclopentadienyl protons occur further upfield than about  $\delta 6.2$  in the <sup>1</sup>H NMR, the bis-Cp zirconium complex can eliminate a Cp group upon reaction with water.

Table 1-4: Ethanolysis of the Cyclooctatetraene Complexes of Titanium

		+		+		
$\text{Ti}_2(\text{COT})_3$	12%		88%		0%	+ $\text{Ti}(\text{OEt})_n$
$\text{Ti}(\text{COT})_2$	37%		51%		12%	

Considerably less research effort has gone into the reaction chemistry of the cyclooctatetraene (COT) complexes of Group IV metals. Wilke and Breil isolated the products from the reaction of ethanol with di(cyclooctatetraene)titanium and tri-(cyclooctatetraene)ditanium (Table 1-4).<sup>25</sup> The chemical behavior of the cyclooctatetraene-titanium complexes indicate that the cyclooctatetraene molecules are bound, at least partly, as a 10  $\pi$ -electron dianion, although no explanation was offered for the 12% cyclooctatetraene observed as product. If, as is the case of di(cyclooctatetraene)titanium, one ring is bound as a 10  $\pi$ -electron ( $\eta^8$ ) molecule, and the other ring is  $\eta^4$  (see Figure 1-5), one would expect 50% cyclooctatetraene to result from protonation by ethanol. However, Schwartz and Sadler<sup>26</sup> have shown by variable temperature <sup>1</sup>H NMR spectroscopy that the two C<sub>8</sub>H<sub>8</sub> rings are fluxional, bending and flattening in turn. Perhaps the dianion ring is protonated more rapidly (i.e., cyclooctatriene forms faster) than the cyclooctatetraene ring oxidizes off the metal.

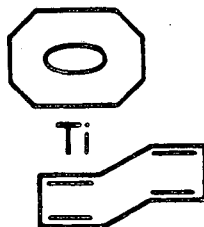
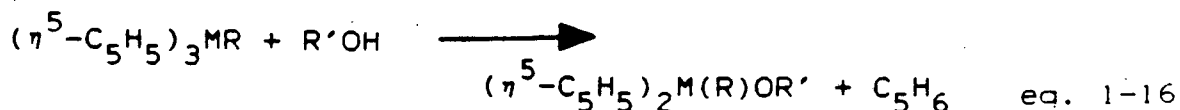
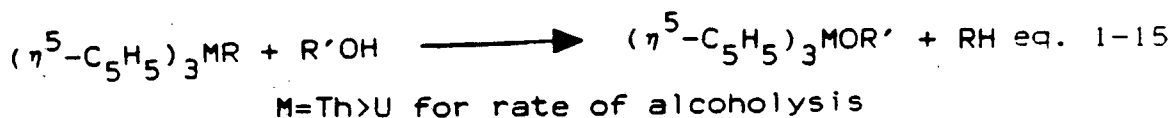


FIGURE 1-5

Other protonations of Group IV cyclooctatetraene complexes include the reaction of  $(\text{COT})_2\text{Zr-THF}^{27}$  and  $(\text{COT})_2\text{Hf}^{28}$  with two equivalents of HCl to yield  $(\text{COT})\text{ZrCl}_2$  and  $(\text{COT})\text{HfCl}_2$ , respectively. No other products were accounted for in the report. The cyclooctatetraene ligands are also replaced upon reaction of the compounds with alcohols. Reaction of  $\text{HF}(\text{COT})_2$  with alcohols results in a reported 5:1 ratio of 1,3,6-cyclooctatriene to 1,3,5-cyclooctatriene (72% yield),<sup>28</sup> an unusual result in that protonation of most COT dianion complexes results in the 1,3,5-cyclooctatriene as the major organic product isomer (see product analysis section of this chapter).

A few observations have also been made on the alcoholysis and hydrolysis of organoactinide complexes. Alcoholysis of  $\text{Cp}_3\text{Th-R}$  complexes has been found to be more rapid than reaction of the uranium complex,  $\text{Cp}_3\text{U-R}$  (eq. 1-15).<sup>2,4</sup> Curiously, for uranium there is competitive cleavage of  $\sigma$  and  $\pi$  ligands (eq. 1-16). Thorocene has been found to hydrolyze more rapidly than uranocene.<sup>29</sup> The trend of organothorium complexes reacting more rapidly than organouranium compounds with protic reagents could be due to the less covalent nature of the thorium compounds. Another possibility is the larger radius of thorium, rendering the central metal more susceptible to attack by water or an alcohol.



In the initial hydrolysis of thorocene,<sup>30</sup> Yoshida reported observing cyclooctatetraene, along with "a mixture of cyclooctatrienes" when he found two peaks from a GLPC of the products. Greco and co-workers have also reported<sup>31</sup> observation of cyclooctatetraene (20%) upon alcoholysis of cerocene,  $(COT)_2Ce$ . No explanation was offered in either case as to how COT might result from protonation of a 10  $\pi$ -electron complex.

### Results: Kinetic Experiments

As stated earlier, a detailed kinetic study of the hydrolysis of uranocene might allow for a better understanding of the factors that influence reactivity in organoactinide complexes. The ideal aspect of the hydrolysis is the ease of monitoring the distinctive  $\lambda_{\max}$  of uranocene in the visible spectrum, which usually occurs between 600 and 650 nm. Both Walker<sup>32</sup> and Lyttle<sup>33</sup> had previously found that if the concentration of uranocene is small compared to the concentration of water, then the reaction follows simple first order kinetics (eq. 1-17).

$$-d[\text{uranocene}]/dt = k_1[\text{uranocene}] \quad \text{eq. 1-17}$$

$$\text{where } k_1 = k[\text{H}_2\text{O}]$$

From Beer's law, the concentration of uranocene is directly proportional to the spectral absorbance (eq. 1-18, 1-19),

$$A_{\text{uranocene}} \propto [\text{uranocene}] \quad \text{eq. 1-18}$$

$$-d(A_{\text{uranocene}})/(A_{\text{uranocene}}) = k dt \quad \text{eq. 1-19}$$

which, upon integration gives (eq. 1-20),

$$\ln(A_t/A_0) = -kt \quad \text{eq. 1-20}$$

Thus, by simply monitoring the decrease in absorbance at  $\lambda_{\max}$  and plotting  $\ln(A_t/A_0)$  vs.  $t$ , rate constants for the hydrolysis can be determined. In general,  $10^{-3}$  M solutions of

the uranocene (or substituted uranocene) in 1M H<sub>2</sub>O-THF mixtures were used to maintain pseudo-first order conditions. Good correlations ( $r^2 > 0.999$ ) were obtained for most of the kinetic runs reported, confirming the pseudo-first order nature of the decomposition.

Before the present study was begun, it was known that the half-life for decomposition of the unsubstituted uranocene is approximately 20 to 24 hours in 1M H<sub>2</sub>O/THF solutions.<sup>32,33</sup> It was also known that the addition of an alkyl group such as *t*-butyl or ethyl resulted in a substantial increase in the half-life to approximately five days.<sup>34</sup> What was not understood was whether this decrease in hydrolysis rate is due to a steric effect, substituents such as *t*-butyl "blocking out" an incoming water molecule, or whether the effect is due to the electron-withdrawing or releasing (inductive) ability of the substituent.

Lyttle<sup>35</sup> had made an early, unsuccessful attempt at correlating the Hammett<sup>36</sup> sigma values of the substituents with their rates of hydrolysis. But most of his data consist of alkyl substituents, which are known to exert minor inductive effects and have large uncertainties in their sigma values. By hydrolyzing a larger variety of previously prepared substituted uranocenes that cover a wider range of sigma values, a better assessment of the role of the inductive effect in the hydrolysis could be made (see results, Table 1-4).

Table 1-4: Rate of Decomposition of Substituted Uranocenes  $(XC_8H_7)_2U$

X	$k \times 10^5 \text{ s}^{-1}$
t-Bu	0.22 <sup>44</sup>
H	1.1 <sup>44</sup>
NMe <sub>2</sub>	1.2
Ph	44
Ot-Bu	6100
CO <sub>2</sub> t-Bu	110,000 <sup>39</sup>

The problem with this type of correlation is in choosing the proper series of sigma values. Does one use  $\sigma_m$  or  $\sigma_p$ , with or without a resonance contribution? Since we are dealing with a ten-electron pi system and  $\sigma$  values are based on a phenyl system, the answer to this is not clear. But by looking at several correlations with standard  $\sigma$  values, we may gain some insight into the importance of electronic effects on the rate of decomposition.

As can be seen from figure 1-6, the correlation with  $\sigma_p^\circ$  values<sup>37</sup> is poor. However, a moderate improvement results from a correlation with  $\sigma_m^\circ$  constants (figure 1-7), perhaps because resonance contributions have been de-emphasized. Even though the correlation is mediocre ( $r^2=0.928$ ), a definite trend can be seen in the rates of decomposition with increasing electron withdrawing ability of the substituent. A correlation with Taft's  $\sigma_1$  values derived from aliphatic systems,<sup>38</sup> does not show a significant improvement ( $r^2=0.886$ ) (figure 1-8).

FIGURE 1-6: PLOT OF  $(C_8H_7X)_2U$  HYDROLYSIS  
RATE CONSTANTS VERSUS SIGMA PARA VALUES

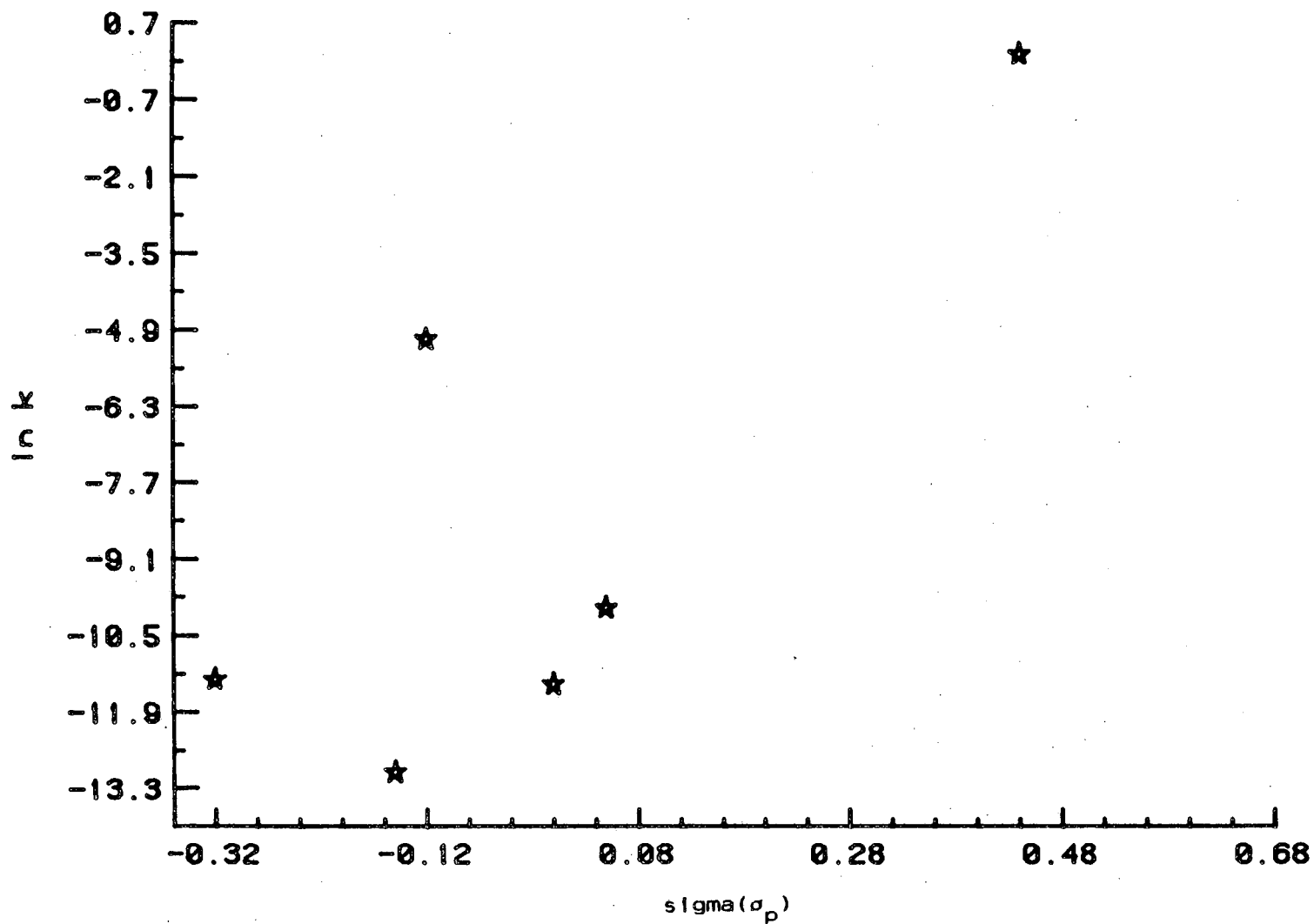




FIGURE 1-7: PLOT OF  $(C_8H_7X)_2U$  HYDROLYSIS  
RATE CONSTANTS VERSUS SIGMA META VALUES

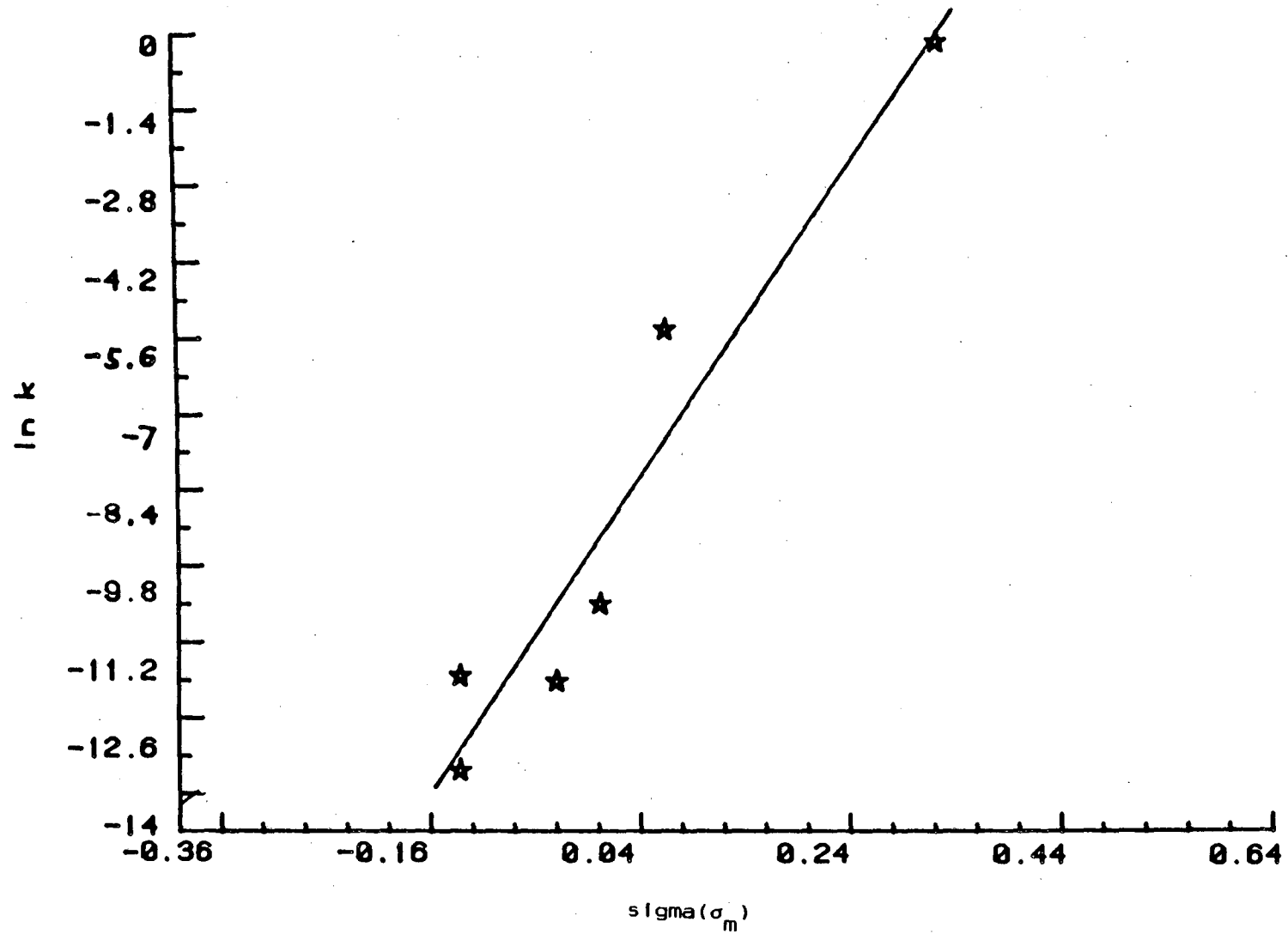
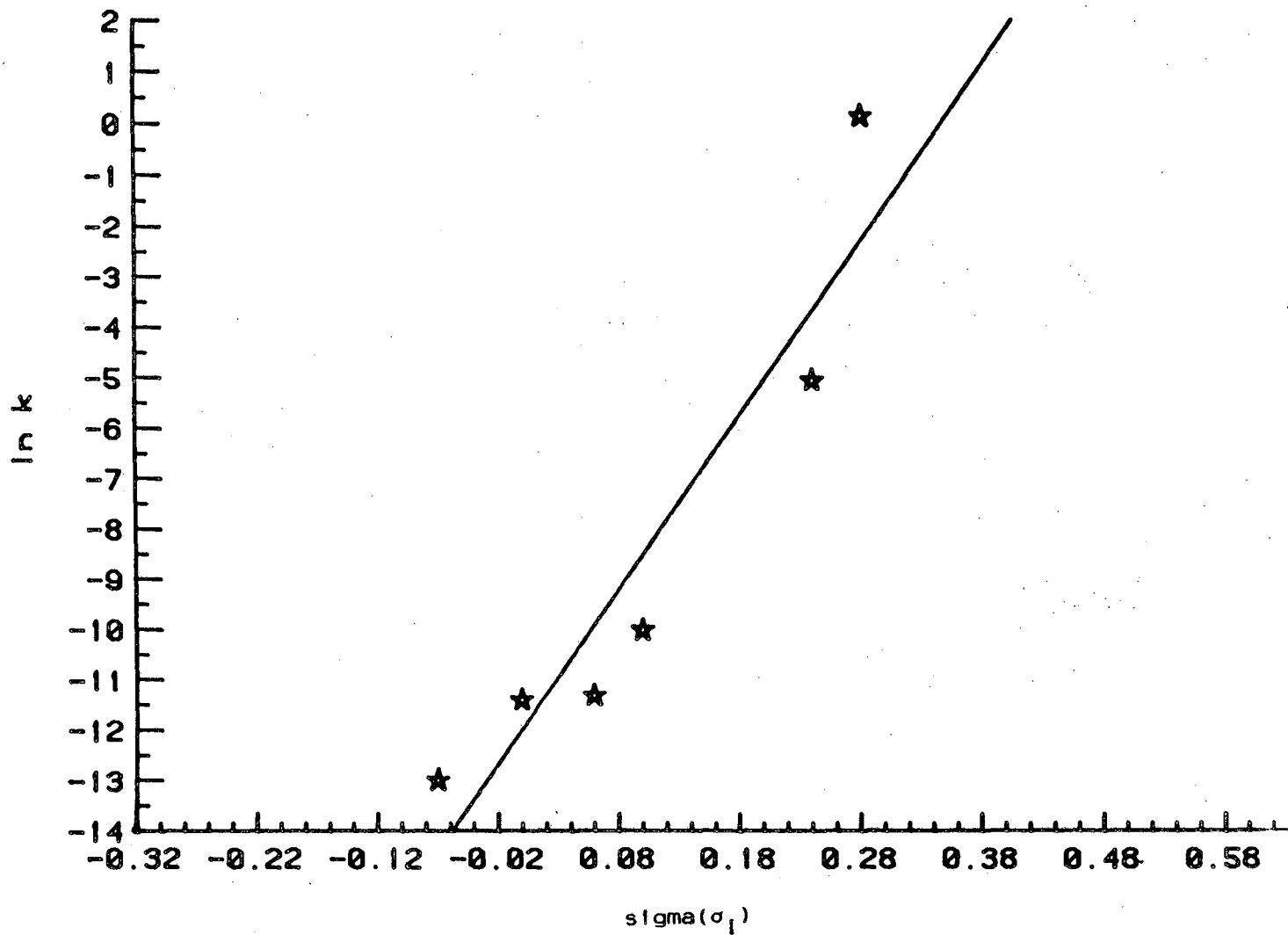


FIGURE 1-8: CORRELATION OF HYDROLYSIS RATE CONSTANTS OF  $(C_8H_7X)_2U$  WITH TAFT  $\sigma_I$  CONSTANTS



Perhaps a better way to definitively establish the importance of electronic effects in the reaction would be to correlate the rates of hydrolysis of aryl-substituted uranocenes with their respective sigma values. In this way, the type of sigma values to be used will be clearer and the reaction might better correlate with a linear free energy relationship (LFER) if the substituents are directly attached to a phenyl ring.

In order to provide a more extensive list of prepared aryluranocenes to choose from, it was necessary to develop additional cyclooctatetraene derivatives. Harmon had already developed the synthesis of a few arylcyclooctatetraene derivatives containing electron-donating substituents.<sup>40</sup> (*p*-Dimethylaminophenyl)cyclooctatetraene was prepared by refluxing cyclooctatetraene in ether for two hours under N<sub>2</sub> with the lithium reagent (Cope method).<sup>41</sup> Yields were poor (25%), probably due to the failure to allow complete formation of the dianion. To synthesize the *p*-methoxyphenylcyclooctatetraene, the same experimenter<sup>40</sup> added the lithium reagent (prepared from *p*-bromoanisole and lithium wire) to CuI-PBu<sub>3</sub> to form the cuprate. Reaction of the cuprate with bromocyclooctatetraene at -40°C for 5 h resulted in formation of the arylcyclooctatetraene in 80% yield.

The one deficiency, however, was in the availability of a substituted cyclooctatetraene that has an electron-withdrawing substituent on the phenyl ring. Initial success in synthesizing phenylcyclooctatetraene by direct coupling of phenyllithium reagent with cyclooctatetraene (via the DeKock method),<sup>42</sup>

led to the idea that a substituted-phenyllithium reagent containing an electron-withdrawing group might work as well.

To a solution of *n*-butyllithium in ether cooled to  $-78^{\circ}\text{C}$  was added *p*-bromobenzotrifluoride. Reaction was almost immediate (two minutes), producing a white solid. Aliquots were removed and quenched with freshly crushed dry ice. Acidification, after evaporation of the dry ice and standard acid work-up resulted in isolation of a white solid identified as *p*-trifluoromethylbenzoic acid. Transmetalation had occurred.

A solution of cyclooctatetraene in ether was then added to the lithium reagent and the solution was warmed to room temperature. Quenching after 24 h resulted in isolation of a large mixture of coupled products. When the reaction was run for 72 h, *p*-*n*-butyltrifluorobenzene became a major side product, apparently from displacement of bromide from *n*-butyl bromide formed during the transmetalation. It was clear that direct lithiation was not a favorable reaction, despite the preparation of phenylcyclooctatetraene by this route.

Attention was then focused on the coupling of the Grignard reagent to bromocyclooctatetraene. Reaction of *m*-bromofluorobenzene with magnesium was slow and required THF and 1,2-dibromoethane to commence the reaction. After refluxing for 1 h, however, reaction was finally complete. Titration of the solution resulted in a concentration determination of 0.25M, or approximately 0.025 moles of Grignard reagent. Cannulation of the reagent into a solution of bromocyclooctatetraene in ether, containing the insoluble nickel catalyst  $(\text{dppp})\text{NiCl}_2$ , resulted in

formation of the desired aryl product, *m*-fluorophenylcyclooctatetraene. The yield (40%) was comparable to previous Grignard coupling reactions to bromocyclooctatetraene.<sup>43</sup>

Formation of the uranocene was carried out primarily using Schlenk techniques. Reduction of the neutral ligand, *m*-fluorophenylcyclooctatetraene to the dianion with potassium in THF produced a dark red solution which was cannulated into a Schlenk vessel containing  $UCl_4$  and THF. A dark green solution resulted almost immediately, although the reaction was stirred for 1 h to ensure completion. Extraction with toluene followed by recrystallization in hexane produced a light green crystalline material, identified as *m*-fluorophenyluranocene.

Table 1-5: Hydrolysis of Diaryluranocenes  
in 1M  $H_2O/THF$ , 25°C

$U(C_8H_7-C_6H_4X)_2$	$k \times 10^5 \text{ s}^{-1}$
<u>X</u>	
<i>p</i> -NMe <sub>2</sub>	0.835
<i>p</i> -OMe	2.27
H	4.39
<i>o</i> -Me	5.10
<i>m</i> -F	21.0

Moore

The rate constants for the hydrolysis of five different aryluranocene complexes are given in Table 1-5. The use of linear free energy relationships demonstrates the principal role

electronic effects play in the decomposition reaction. The natural log of the rate constants was plotted against the Hammett  $\sigma$  values<sup>36</sup> of the phenyl substituents in the uranocenes. The plot (figure 1-9) gives only a fair correlation, but does show a definite trend of more electron-withdrawing groups causing more rapid decomposition of the uranocene complex. There is a slight problem, however, in the use of normal Hammett  $\sigma$  parameters, since the values of donor substituents contain a large component due to resonance conjugation. It would be more advantageous to use  $\sigma$  values that are based solely on inductive effects ( $I_{\sigma}$ ,  $I_{\pi}$ ). Thus, a set of  $\sigma^0$  values was chosen which had been statistically derived from a large set of reactions in which the reaction center was isolated from the aromatic nucleus by a  $\text{CH}_2$  group or another non-conjugating group.<sup>37</sup> The Hammett plot in this case is excellent (figure 1-10). The value of  $\rho$  is determined as 2.1, which indicates the sensitive nature of the transition state to changes in the polar character of the substituents. Uranocene decomposition is most certainly dominated by electronic effects, at least in the disubstituted complexes.

Lytle<sup>34</sup> had also found in preliminary experiments that the hydrolysis exhibits a substantial isotope effect (an isotope effect of greater than 20 was reported) when  $\text{D}_2\text{O}$  is used in place of  $\text{H}_2\text{O}$ . Glaser<sup>44</sup> confirmed the presence of an isotope effect when he repeated the hydrolysis, although he found the effect to be somewhat smaller (11.8). A number of substituted uranocenes have now been hydrolyzed (Table 1-7) and all have been found to

FIGURE 1-9: PLOT OF  $(XC_6H_4C_8H_7)_2U$   
HYDROLYSIS RATE CONSTANTS VERSUS SIGMA VALUES

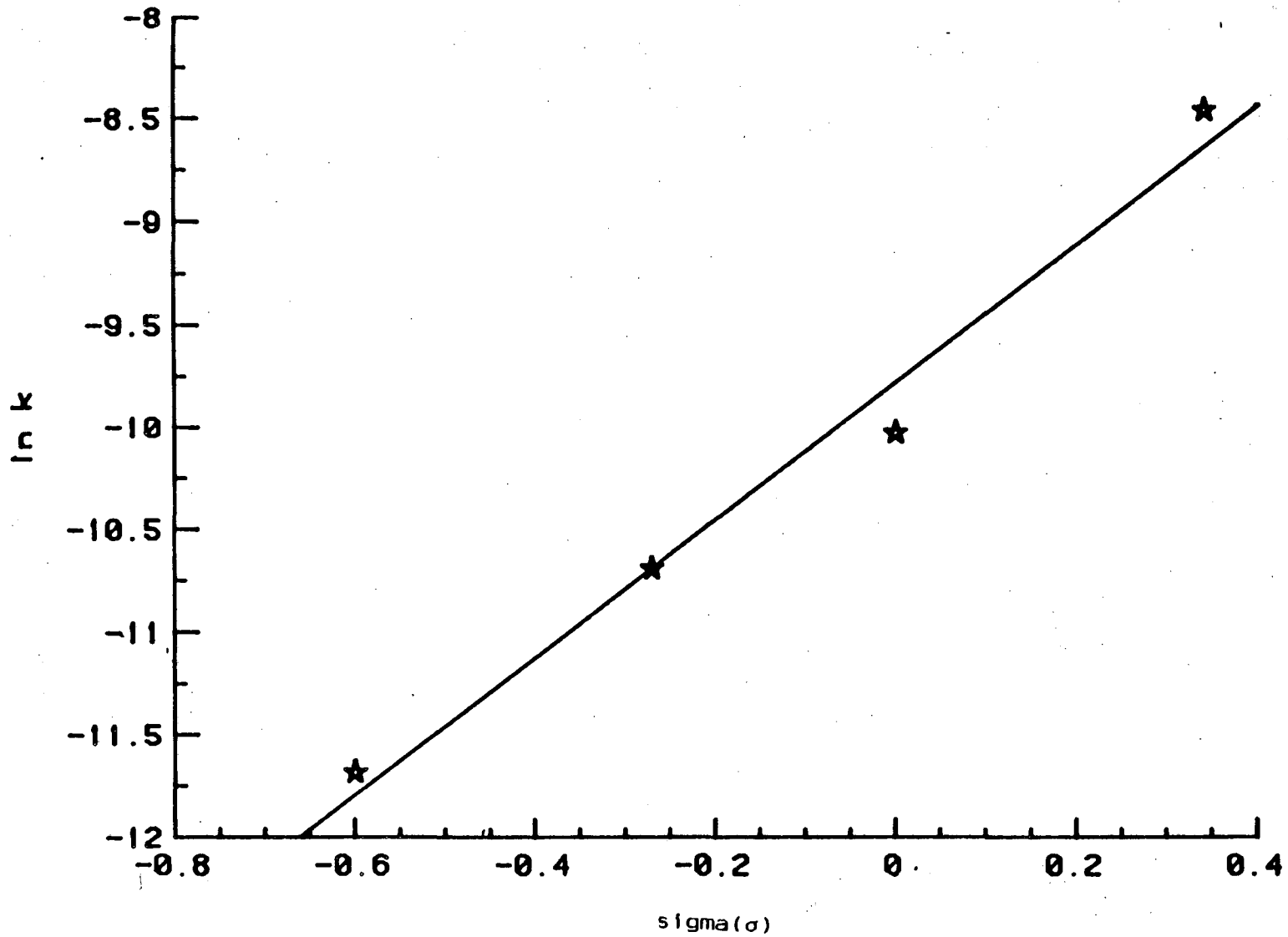


FIGURE 1-10: CORRELATION OF HYDROLYSIS RATE CONSTANTS OF  
( $\text{XC}_6\text{H}_4\text{C}_8\text{H}_7$ )<sub>2</sub>U WITH  $\sigma^\circ$  VALUES

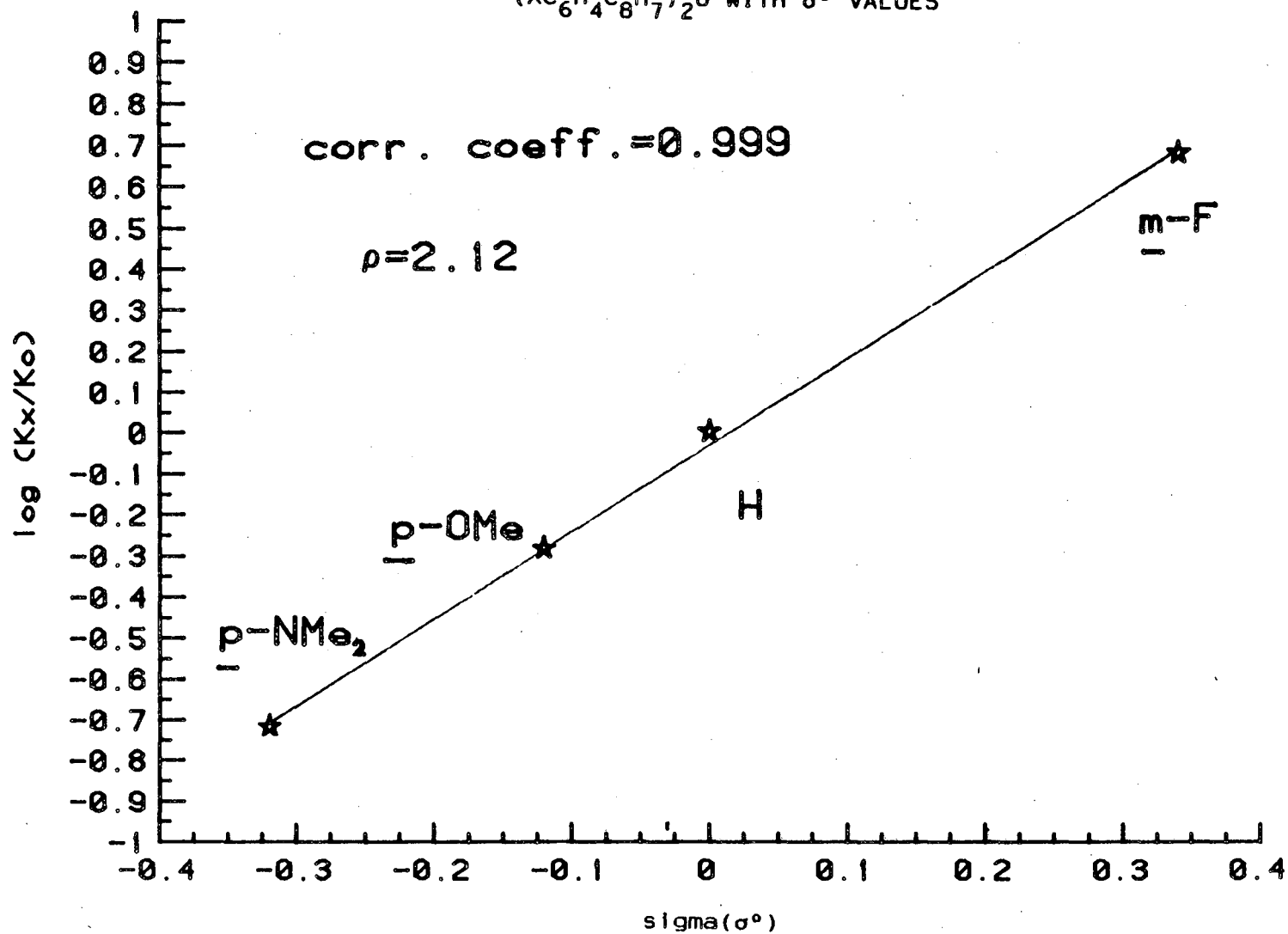




exhibit substantial (>7) isotope effects. It is thus, appropriate to conclude that proton transfer is the rate determining step in the hydrolysis.

Rate ratios this large are sometimes attributed to tunnelling effects which facilitate proton transfer. Bell<sup>45</sup> has stated that even for reactions with 'normal'  $k_H/k_D$  ratios, tunnelling may be a significant factor and that the best criteria are measurements of activation energies and A factors. Thus, in reactions involving appreciable tunnelling, the average energy of the reacting systems falls below the top of the barrier by an amount which is greater for the lighter isotope.<sup>45</sup> The ratio of A factors ( $A_D/A_H$ ) is affected as well. Bell gives a more detailed description of how this arises. Glaser<sup>44</sup> details the possible application of tunnelling theory to the large kinetic isotope effects observed for the hydrolysis of uranocene. For our purposes, it will be stated that reactions which fall outside the range  $0.6 < A_D/A_H < 1.4$  and possess activation energy differences ( $E_a^D - E_a^H$ ) of greater than 1.4 kcal/mol will be considered to demonstrate appreciable tunnelling.

Determining the extent of tunnelling involved in the hydrolysis necessitated the determination of Arrhenius Activation Parameters. Kinetic runs were carried out over a 60°C range (-5°C to 55°C), for both the H<sub>2</sub>O and D<sub>2</sub>O decomposition of m-fluorophenyluranocene. This aryluranocene was chosen because of its fairly rapid hydrolysis which could be readily monitored over short periods of time (3 h for H<sub>2</sub>O, 30 h for D<sub>2</sub>O). Figures 1-11 to 1-16 are examples of the excellent kinetic runs resulting

Figure 1-11: *m*-Fluorophenyluranocene

Decomposition in 1M H<sub>2</sub>O/THF -2°C(□), 15°C(Δ), 25°C(+)

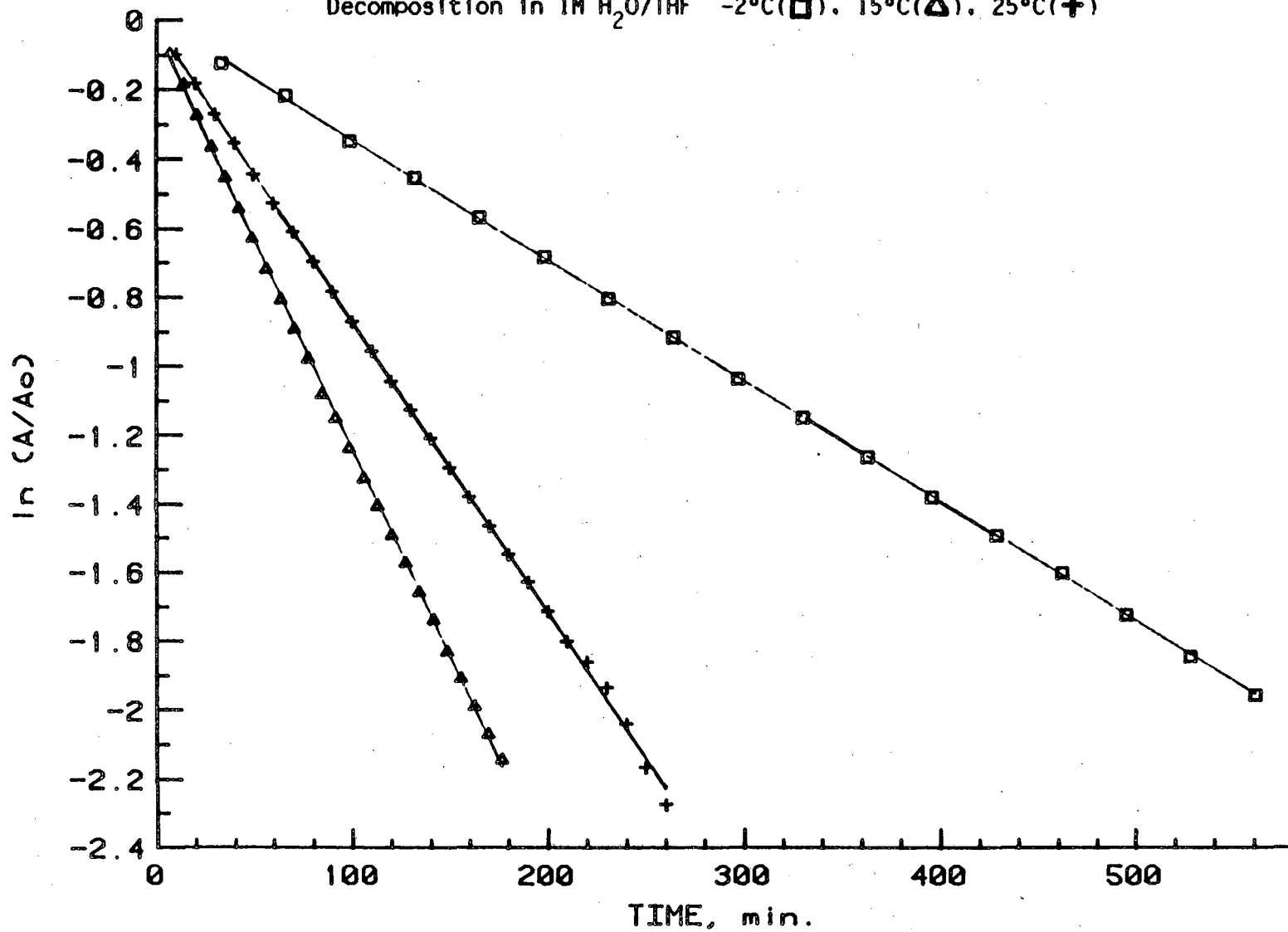


Figure 1-12: *m*-Fluorophenyluranocene

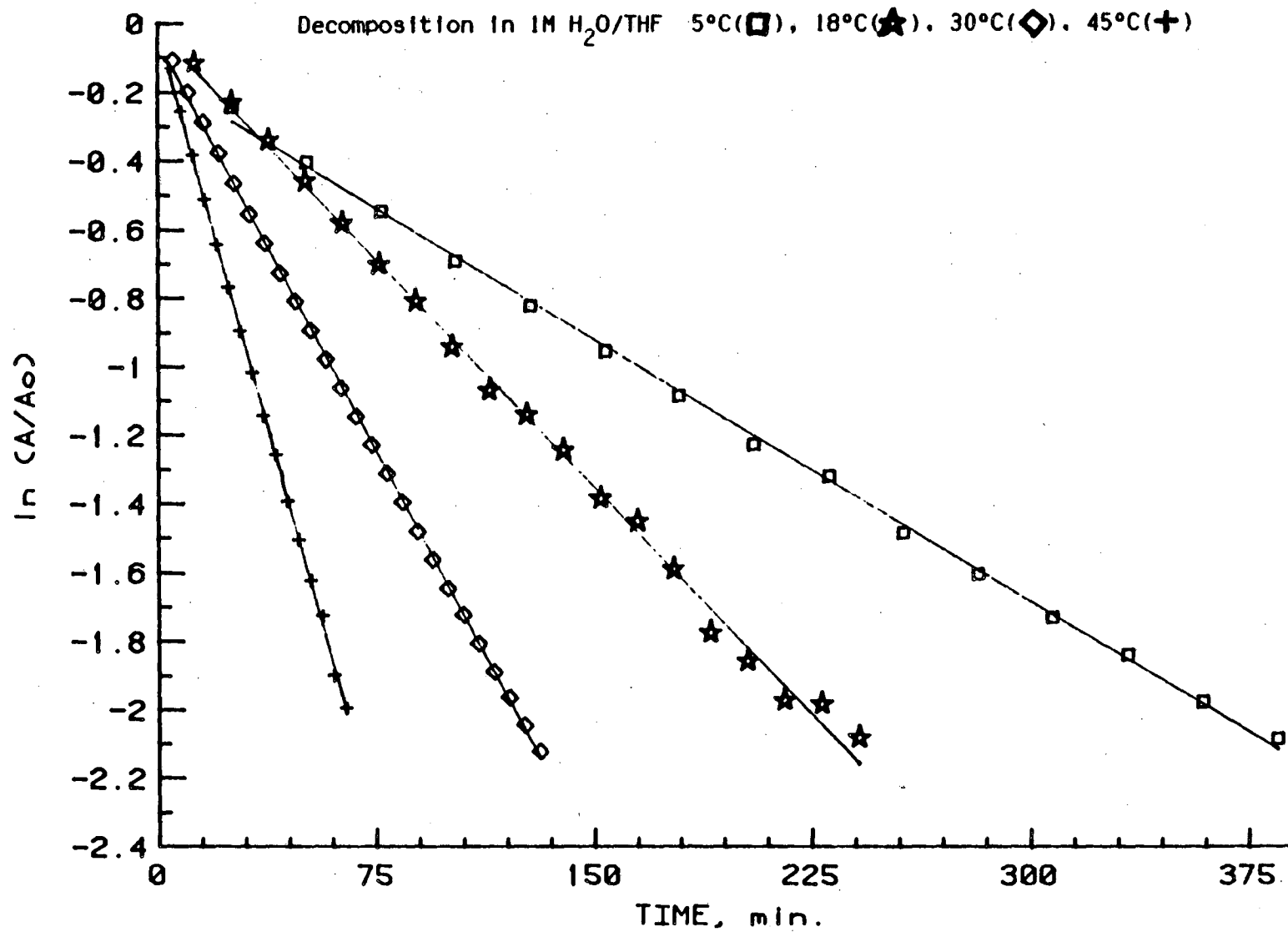


Figure I-13: *m*-Fluorophenyluranocene

Decomposition in 1M H<sub>2</sub>O/THF 12°C(□), 20°C(+), 35°C(★), 55°C(△)

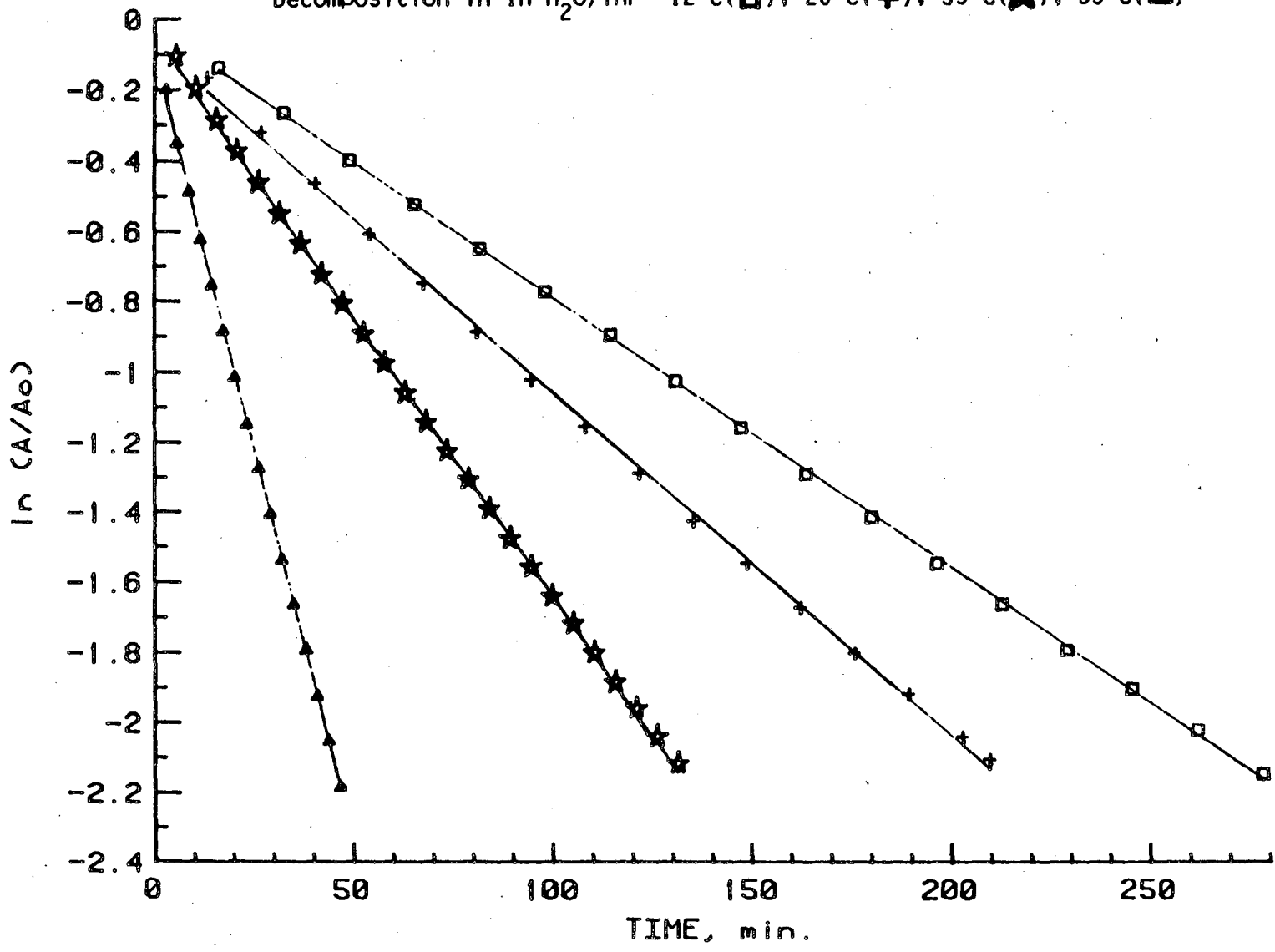


Figure 1-14: *m*-Fluorophenyluranocene

Decomposition in 1M D<sub>2</sub>O/THF 20°C(+), 35°C(Δ), 45°C(★), 55°C(□)

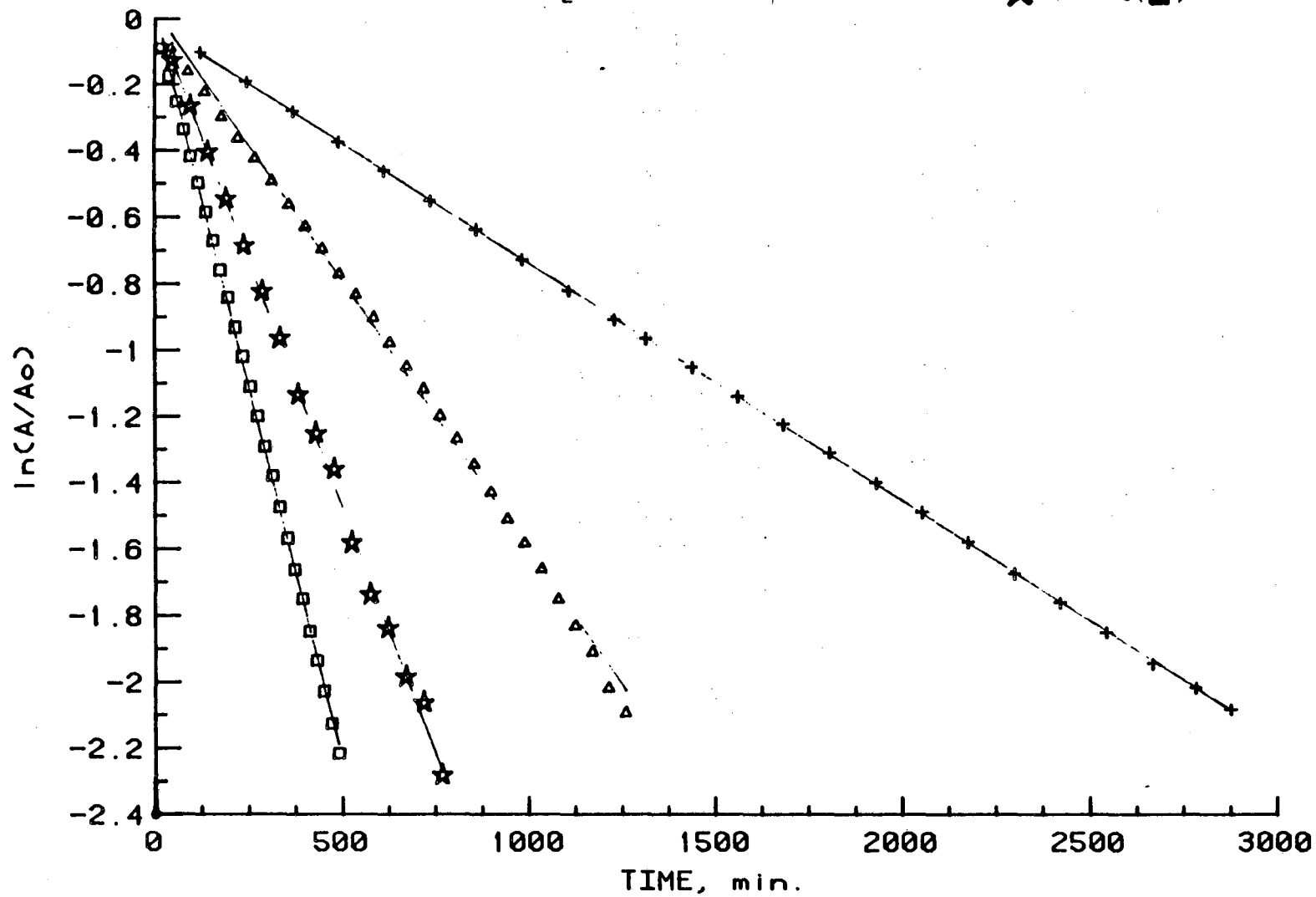


Figure 1-15: *m*-Fluorophenyluranocene  
Decomposition in 1M D<sub>2</sub>O/THF 5°C(★), 15°C(□), 30°C(Δ), 50°C(+)

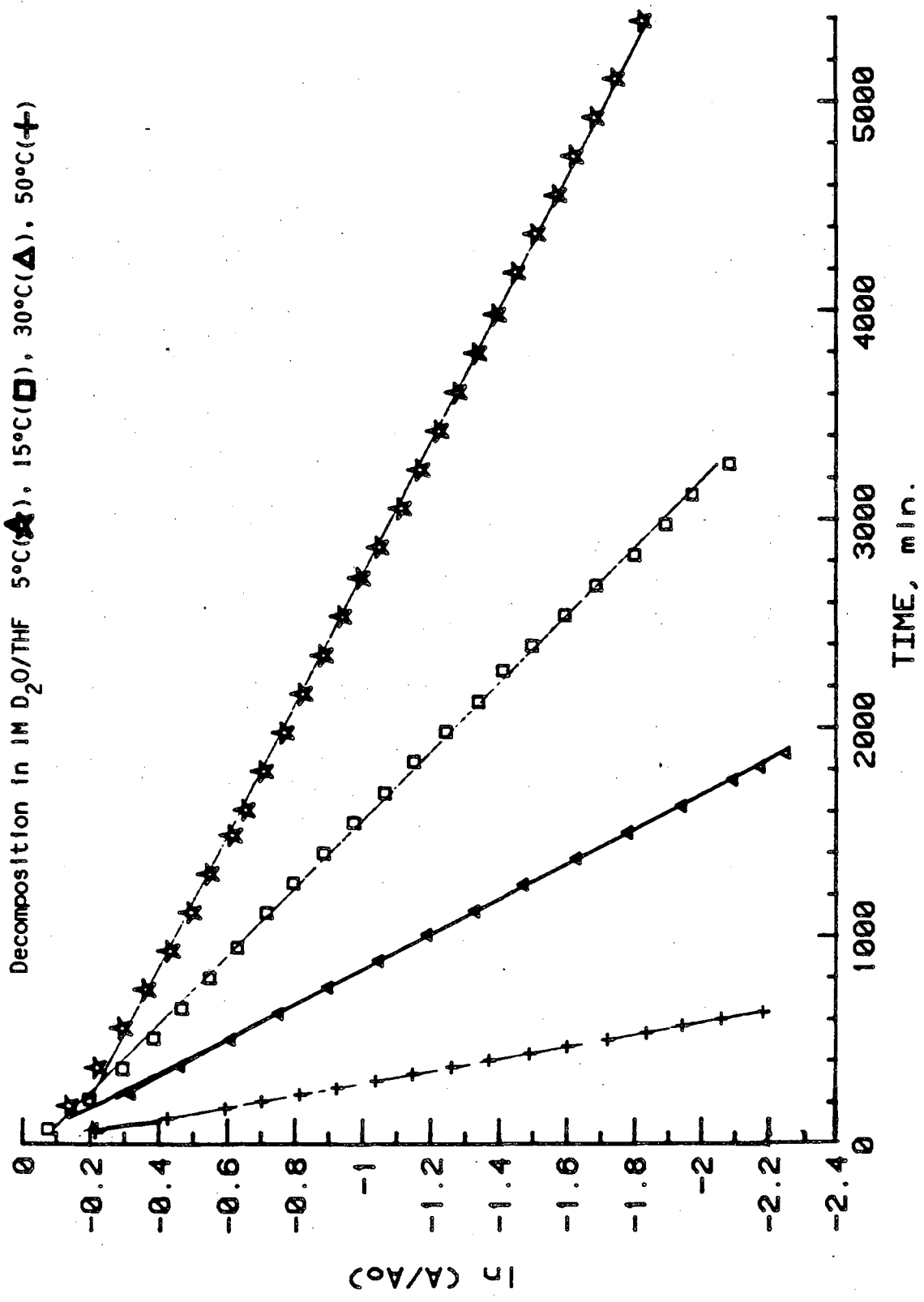


Figure 1-16: *m*-Fluorophenyluranocene

Decomposition in 1M D<sub>2</sub>O/THF 0°C(□), 10°C(★), 25°C(+), 40°C(△)

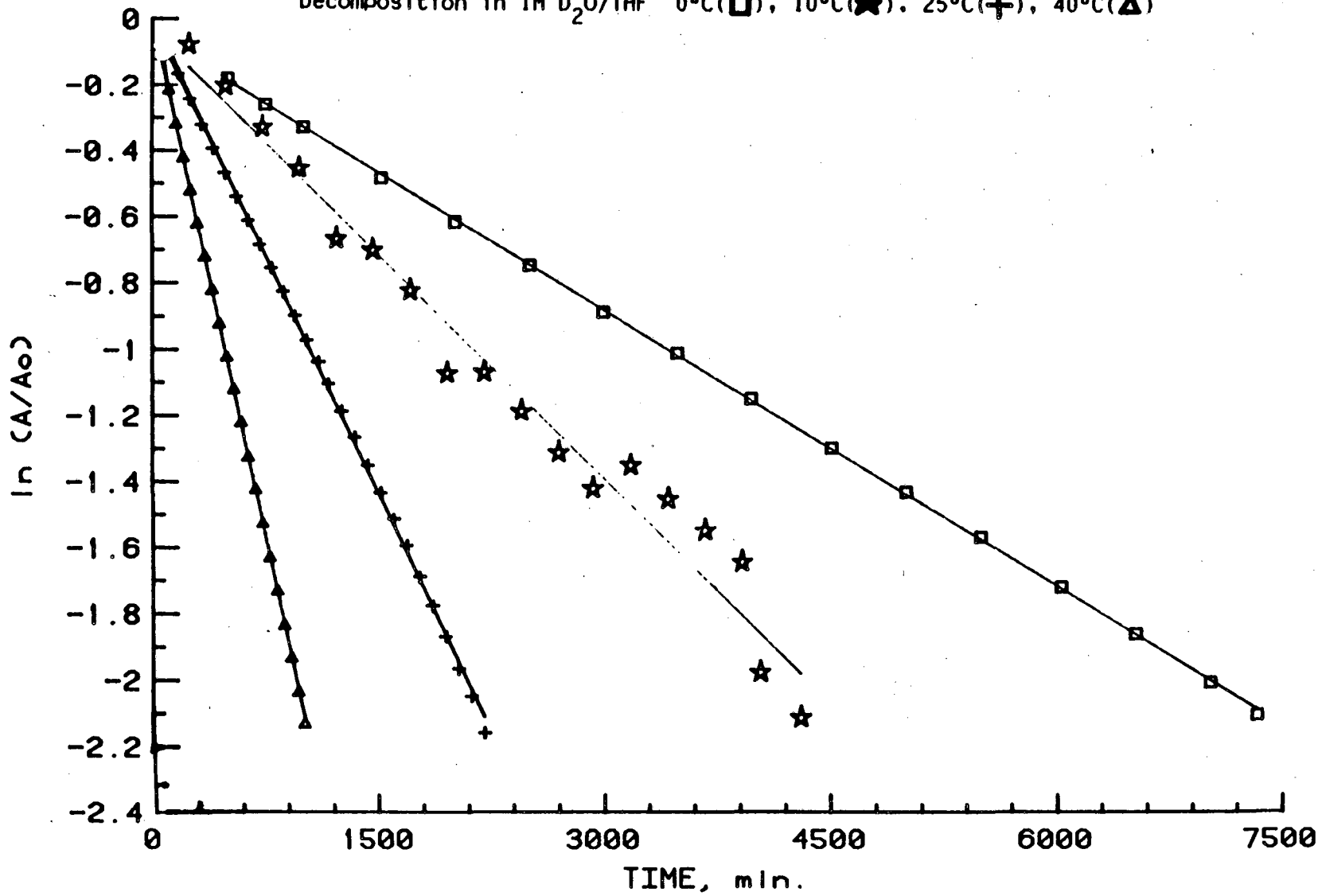


Table 1-6: Rate Constants and Isotope Effects for  
m-Fluorophenyluranocene at a series of temperatures

T°C	$k(\text{H}_2\text{O}) \times 10^5 \text{ s}^{-1}$	$k(\text{D}_2\text{O}) \times 10^5 \text{ s}^{-1}$	$k_{\text{H}}/k_{\text{D}}$
-2	5.82		
0		0.463	
5	8.42	0.529	15.9
10		0.753	
15	14.2	1.02	13.9
18	14.8		
20	16.4	1.20	13.7
25 a	20.2	1.60	
b	21.0	1.54	12.6-13.6
30	26.6	1.98	13.4
35 a	32.7		
b	32.8	2.71	12.1
40		3.53	
45 a	51.3	4.96	
b	49.0	4.99	9.8-10.3
50		5.71	
55 a	74.6	8.23	
b		7.52	9.1-9.9



from this study. A summary of the rate constants for the hydrolysis, along with isotope effects is presented in Table 1-6. Arrhenius activation parameters for the decomposition of *m*-fluorophenyluranocene in 1M H<sub>2</sub>O and 1M D<sub>2</sub>O in THF were determined by plotting ln k vs. 1/T (figure 1-17, 1-18). The results are summarized in Table 1-7.

Table 1-7: Kinetic Isotope Effect and Arrhenius Activation Parameters

U(C <sub>8</sub> H <sub>7</sub> X) <sub>2</sub> + H <sub>2</sub> O(D <sub>2</sub> O)					
X	k/k <sub>H</sub>	k <sub>H</sub> /k <sub>D</sub> (25°C)	ΔH <sup>‡</sup> <sub>H</sub> (ΔH <sup>‡</sup> <sub>D</sub> )	ΔS <sup>‡</sup> <sub>H</sub> (ΔS <sup>‡</sup> <sub>D</sub> )	A <sup>H</sup> (A <sup>D</sup> )
			kcal/mol ± 0.3	e.u. ± 1	s <sup>-1</sup> ± 20%
H	1.0	11.8	8.1(11.2)	-54(-49)	30(449)
<i>m</i> -FC <sub>6</sub> H <sub>5</sub>	19	13.1	7.2(8.9)	-51(-50)	117(144)
C <sub>6</sub> H <sub>5</sub>	3.9	12.8			
<i>p</i> -NMe <sub>2</sub> C <sub>6</sub> H <sub>5</sub>	0.74	12.4			
C(CH <sub>3</sub> ) <sub>3</sub>	0.20	8.2			
COO-(CH <sub>3</sub> ) <sub>3</sub>	100,000 <sup>39</sup>	8.5			

Moore, Glaser<sup>44</sup> (X=H, C(CH<sub>3</sub>)<sub>3</sub>)

Also summarized are the activation parameters determined for the parent complex, uranocene,<sup>44</sup> along with isotope effects for a number of substituted uranocenes. Note that the difference in the enthalpy of activation between the H<sub>2</sub>O and D<sub>2</sub>O decomposition is

Arrhenius Plot for Decomposition of  
m-Fluorophenyluranocene in 1M H2O/THF

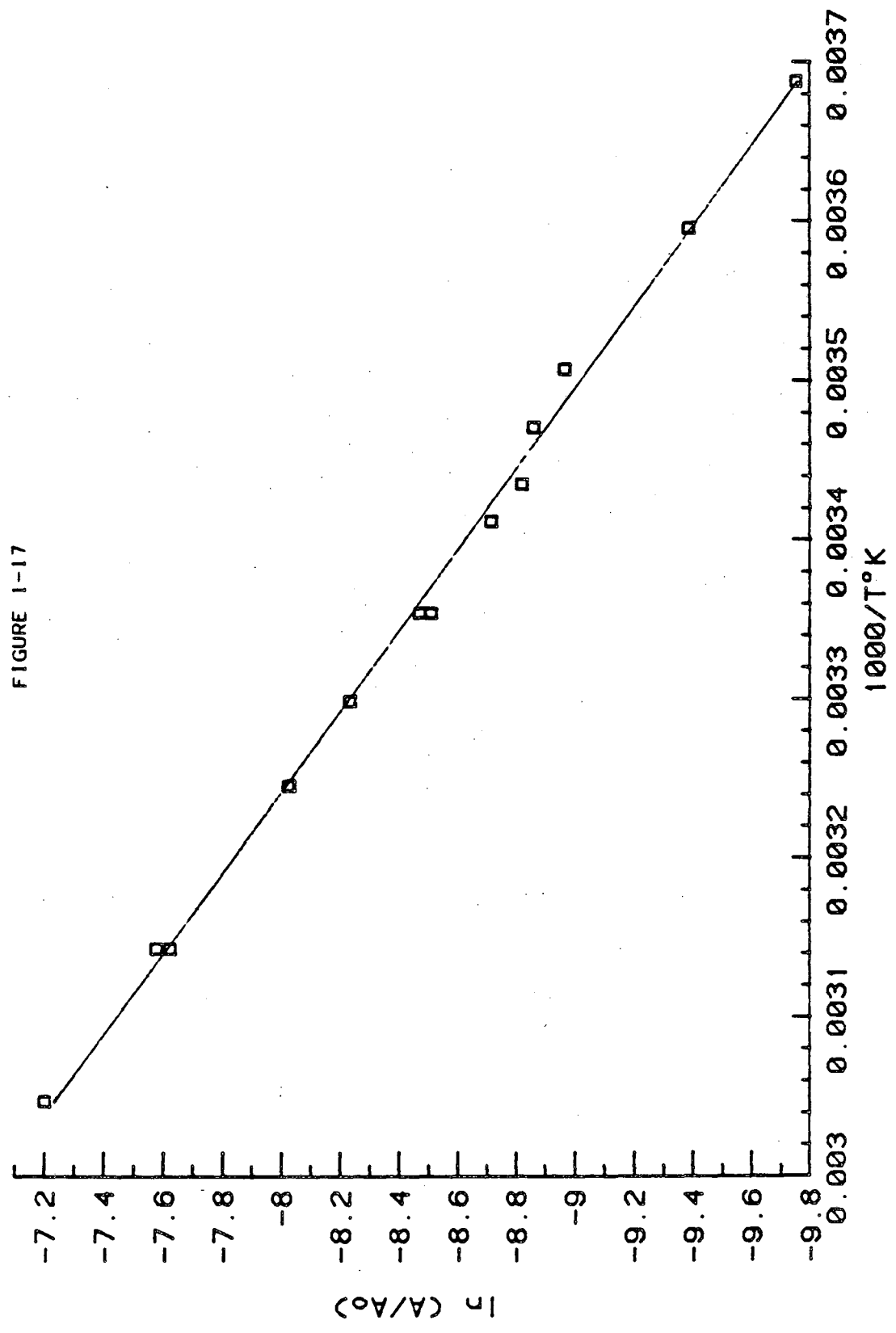
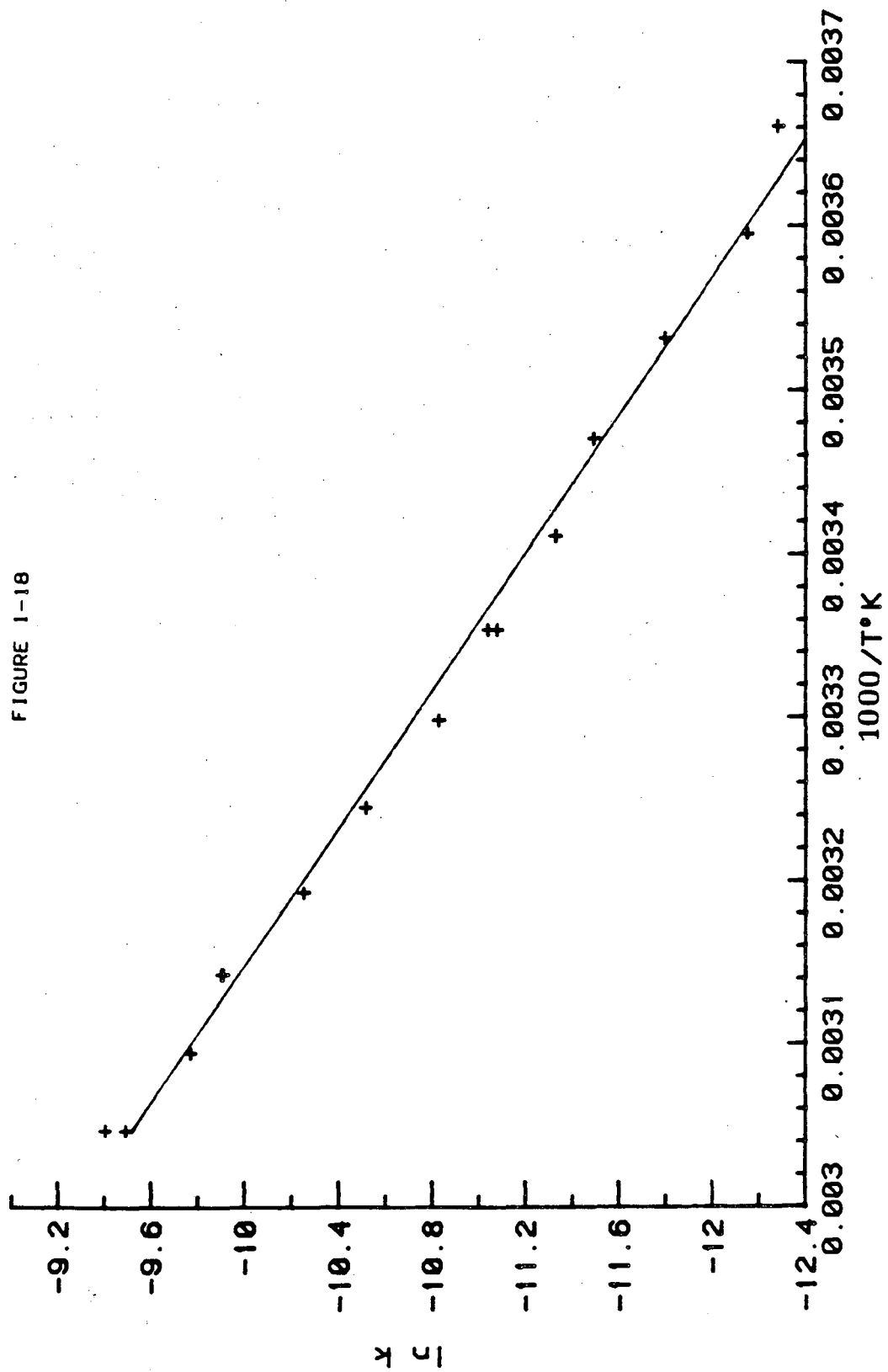


FIGURE 1-17

Arrhenius Plot for Decomposition of  
m-Fluorophenyluranocene in 1M D2O/THF

FIGURE 1-18



1.7 kcal/mol, which is just outside the range considered 'normal' by Bell for differences in enthalpies. The ratio of A factors, however, is close to 1. Thus, it does not appear that we can conclusively invoke a tunnelling mechanism for the hydrolysis of *m*-fluorophenyluranocene. Glaser,<sup>44</sup> on the other hand, did find large differences in the activation enthalpies and a large A factor ratio in his kinetic studies on the hydrolysis and deuterolysis of uranocene.

Even if we are unable to conclude that tunnelling is important in the hydrolysis of bis-([8]annulene)actinide complexes, the information we have collected thus far allows us to draw certain conclusions with regard to the general mechanism of hydrolysis. The basic mechanism presented by Lyttle<sup>33</sup> is still supported by the additional results presented in this thesis (figure 1-19). Water coordinates to the central metal of the substrate in a rapid pre-equilibrium before proton transfer to the ring commences. Coordination of water is enhanced by electron-withdrawing groups which increase the Lewis acidity of the uranium. Increased concentration of the uranium-water complex leads to an overall increase in the observed rate of reaction. Complex formation is followed by the slow rate-determining step of proton transfer to the [8]annulene ring and rapid decomposition to the uranium oxides and the cyclooctatriene mixture.

The large negative entropies ( $<-40$  e.u.) of activation determined for the hydrolysis (Table 1-7) are indicative of a highly crowded, associative-type transition state such as the water-complex postulated in our mechanism. If an intermediate

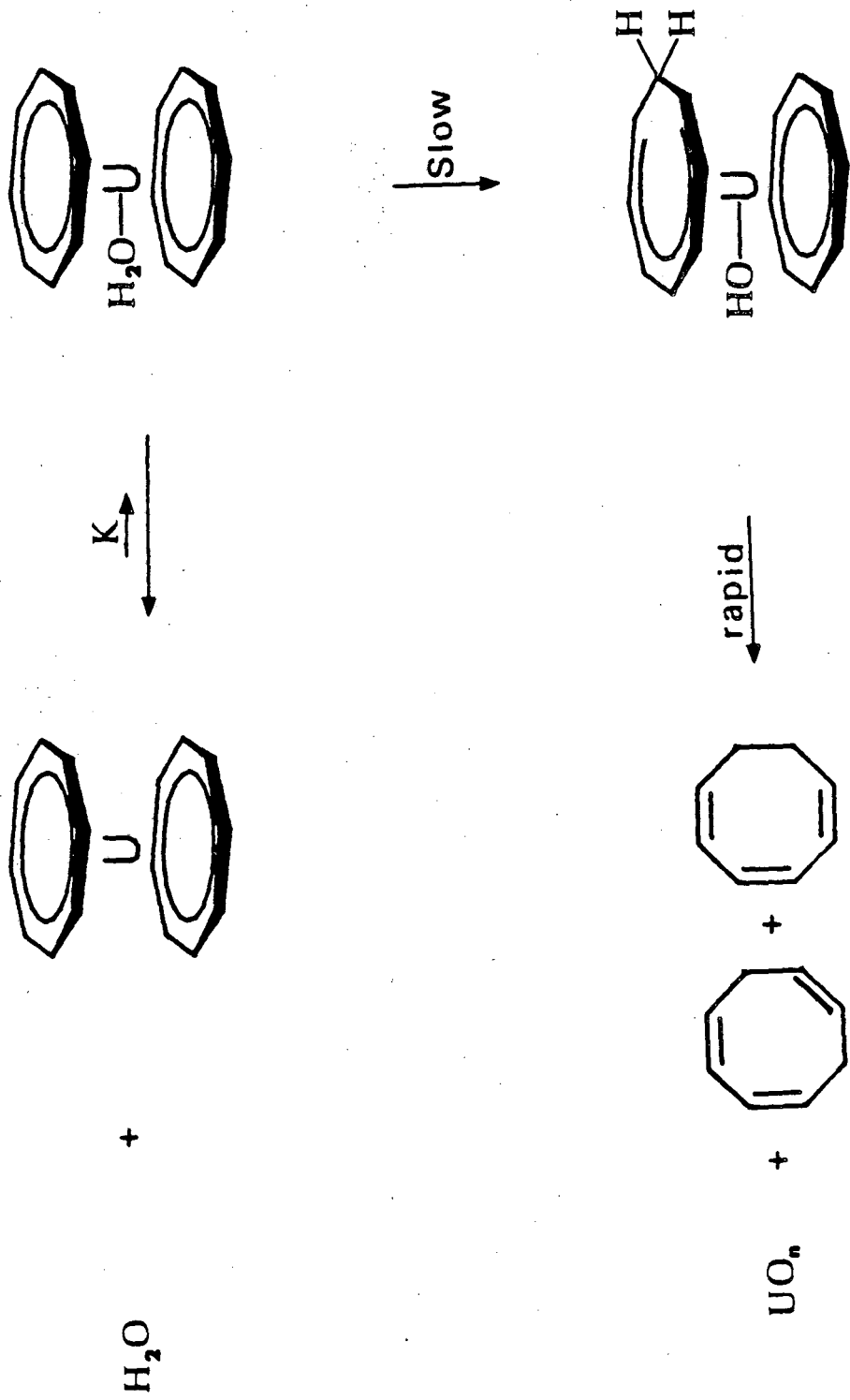


FIGURE 1-19

such as this is important in the decomposition, we would expect protic reagents containing additional steric bulk to be even slower than the hydrolysis. In fact, that is what was observed (Table 1-8). Using methanol as the protic reagent slowed the rate of decomposition by a factor of 500, and uranocene showed no signs of decomposition over a three month period when it was dissolved in a 5M solution of *t*-butanol in THF. Even using a protic reagent with a lower pKa, such as phenol, failed to increase the rate of decomposition since the bulky aryl group prevents easy coordination to uranium. Acidity does play a minor role in the rate of decomposition, however, as demonstrated by the acetic acid results.

Table 1-8: Relative Rates of Protonation of Uranocene with ROH

ROH	$k_{\text{ROH}}/k_{\text{HOH}}$
H <sub>2</sub> O	1
D <sub>2</sub> O	0.09
CH <sub>3</sub> COOH	1.4
CF <sub>3</sub> COOH	5.0
C <sub>6</sub> H <sub>5</sub> OH	0.005
CH <sub>3</sub> OH	0.002
(CH <sub>3</sub> ) <sub>3</sub> COH	NR after 3 mo.

If the hydrolysis is following good first-order kinetics with respect to uranocene (eq. 1-21), what is the effect of the concentration of H<sub>2</sub>O on the rate of decomposition? If we

$$-d[U_c]/dt = k'[U_c] \quad \text{eq. 1-21}$$

$$[U_c] = \text{concentration of uranocene, } k' = k[H_2O]^x$$

expand equation 1-21 by replacing  $k_1$  with  $k[H_2O]^x$ , we get equation 1-22.

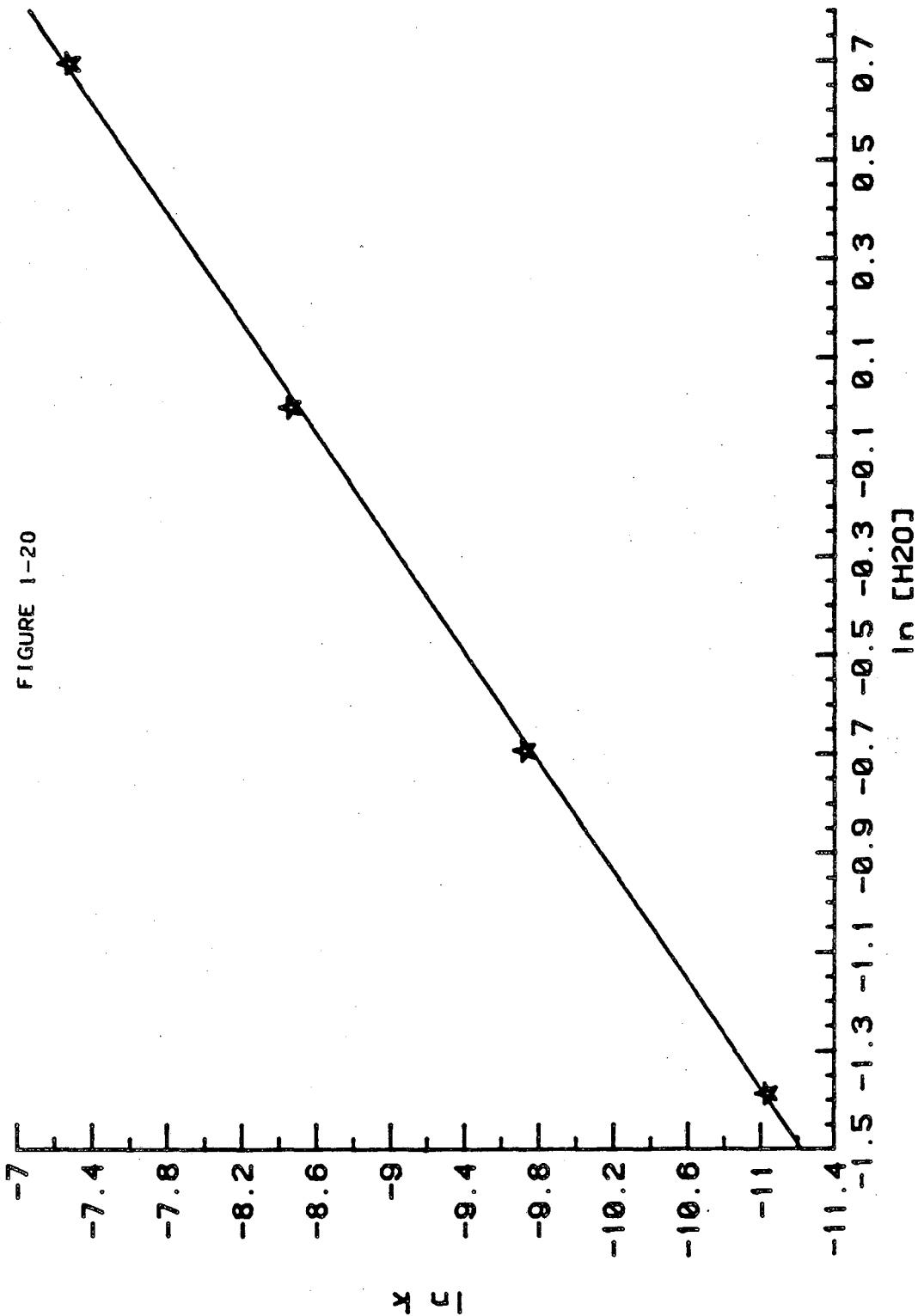
$$-d[U_c]/dt = k[H_2O]^x[U_c] \quad \text{eq. 1-22}$$

The rate order,  $x$ , for water can then be determined from the slope of the log of the water concentration vs. the log of the pseudo-first order rate constant. The intercept will be  $\ln k$ , the log of the rate constant at 1M concentration, which can usually be determined, but in the case of extremely rapid reactions the rate at 1M concentration must be extrapolated from lower water concentrations. The rate data for *m*-fluorophenyluranocene decomposition with various concentrations of water are given in Table 1-9. The plot of  $\ln k$  vs.  $\ln [H_2O]$  (figure 1-20) results in an order ( $x$ ) of 1.8 with respect to water in the rate expression. Approximate rate orders (1M, 2M runs only) were determined for other aryluranocenes (*p*-dimethylamino, *p*-methoxy). It appears as if the rate order for water in most of the hydrolyses of substituted uranocenes will range from about 1.5 to 2.

Table 1-9: Rate of Hydrolysis Decomposition of *m*-Fluorophenyluranocene with respect to concentration of water

$[H_2O], M$	$k \times 10^5 s^{-1}$
0.25	1.60
0.5	5.92
1.0	21.0
2.0	68.8

Plot of  $\ln k$  vs.  $[\text{H}_2\text{O}]$  to Determine Rate Order of Water  
in the Decomposition of m-Fluorophenyluranocene





Quite a bit was learned about the mechanism from the effect of substituents on the rate of hydrolysis. A purely ionic model, which considers the [8]annulene ring to be a full dianion, would predict more rapid protonation of rings which contain electron donating substituents. However, as described earlier, the opposite effect is observed; electron-withdrawing groups increase the rate of hydrolysis by increasing the Lewis acidity of the central metal.

To better establish that transfer of electron density from the metal to the ring does occur, a complex containing two different cyclooctatetraene substituents was prepared (a "mixed" uranocene). If direct protonation of the ring does occur, one would expect the mixed complex to decompose at the same rate as the di-substituted uranocene decomposes, since only the initial protonation will be rate determining. In the case where electron density at the metal is determined by the substituents at the ring, the rate of decomposition should be in between the hydrolysis rates of the di-substituted complexes.

The mixed uranocene chosen for the study was 1-t-butyl-1-phenyluranocene, since rates of di-t-butyluranocene<sup>44</sup> and diphenyluranocene are well established, and because the large difference in hydrolysis rates would simplify distinguishing rates should there be a gross mixture of products. Preparation of the mixed complex was straightforward. Addition of one equivalent of phenylcyclooctatetraene dianion and one equivalent of t-butylcyclooctatetraene to  $UCl_4$  in THF produced a mixture of the two di-substituted uranocenes and the mixed uranocene. The

mixture was washed with hexane to extract any remaining ligand and grease. However, di-*t*-butyluranocene is also soluble in hexane, thus the solid remaining after washing was primarily the mixed uranocene and di-phenyluranocene(45:55) with only a trace of di-*t*-butyluranocene.

The mixture was then decomposed in 1M H<sub>2</sub>O/THF and the decomposition reaction was monitored by observing the decrease in visible absorbance for the complex (figure 1-21). The first few hours of observed decreasing absorbance is due to both diphenyluranocene and the mixed uranocene; however, after 13 hours, most of the diphenyluranocene has decomposed, leaving primarily the mixed complex and simplifying determination of the decomposition rate for the mixed uranocene. Purified *t*-butylphenyluranocene was obtained by partially decomposing 500 mg of the above mixture in 1M H<sub>2</sub>O/THF and recovering the mixed uranocene. The kinetics of decomposition for the pure complex was also followed and the resulting rate constant was similar to the mixture value.

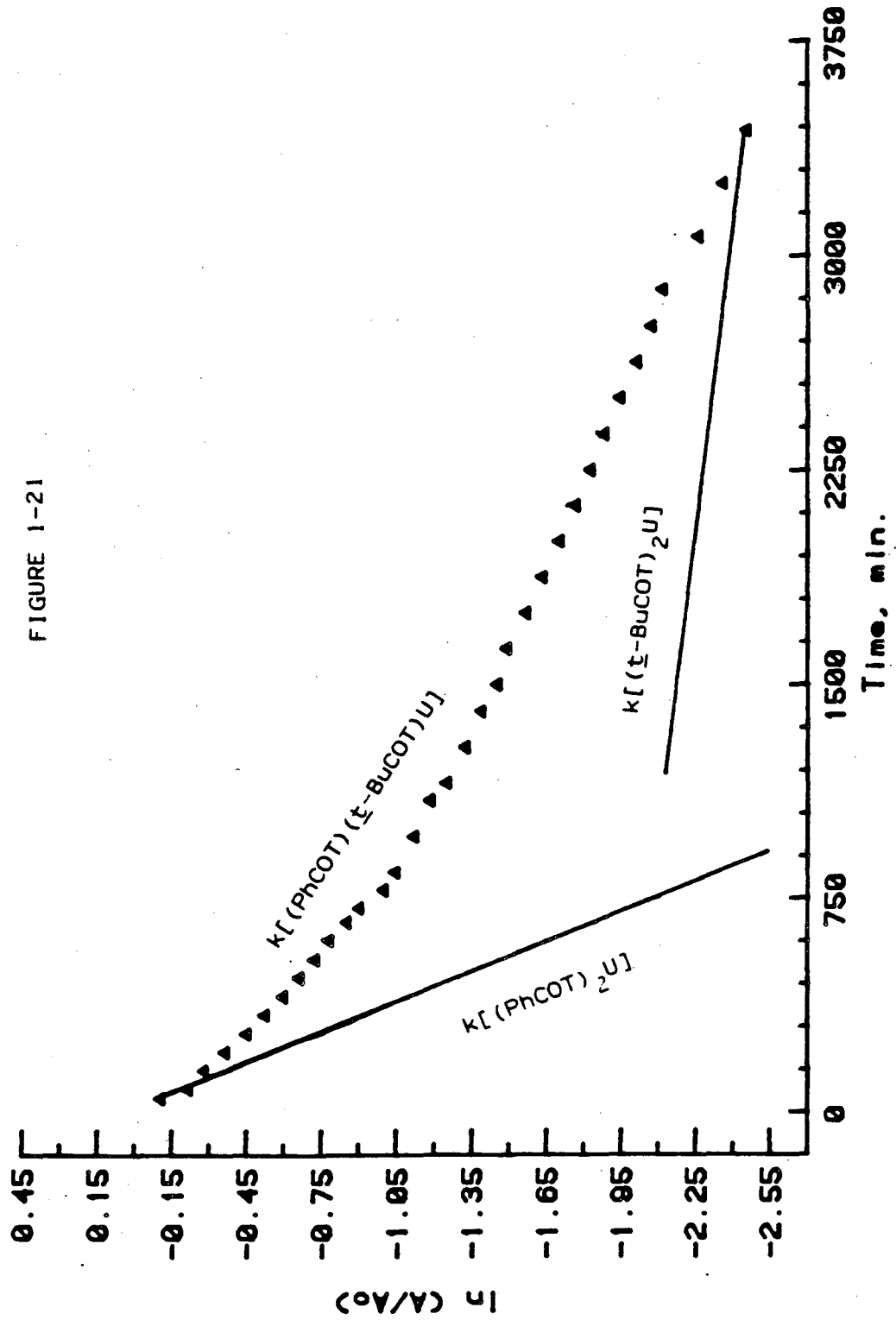
$$k_{\text{mix}} = 8.8 \times 10^{-6} \text{ s}^{-1} \text{ (figure 1-21)}$$

$$k_{\text{pure}} = 9.13 \times 10^{-6} \text{ s}^{-1} \text{ (figure 1-22)}$$

Comparison of this rate constant to those of the di-substituted uranocenes (Table 1-10) demonstrates that each substituent contributes to the electron density at the metal, since the hydrolysis rate is approximately the geometric mean of the disubstituted uranocenes.

Decomposition of diphenylurancene and mixed complex  
(55:45) in 1M H<sub>2</sub>O/THF

FIGURE 1-21



Decomposition of *t*-butylphenyluranocene  
in 1M H<sub>2</sub>O/THF

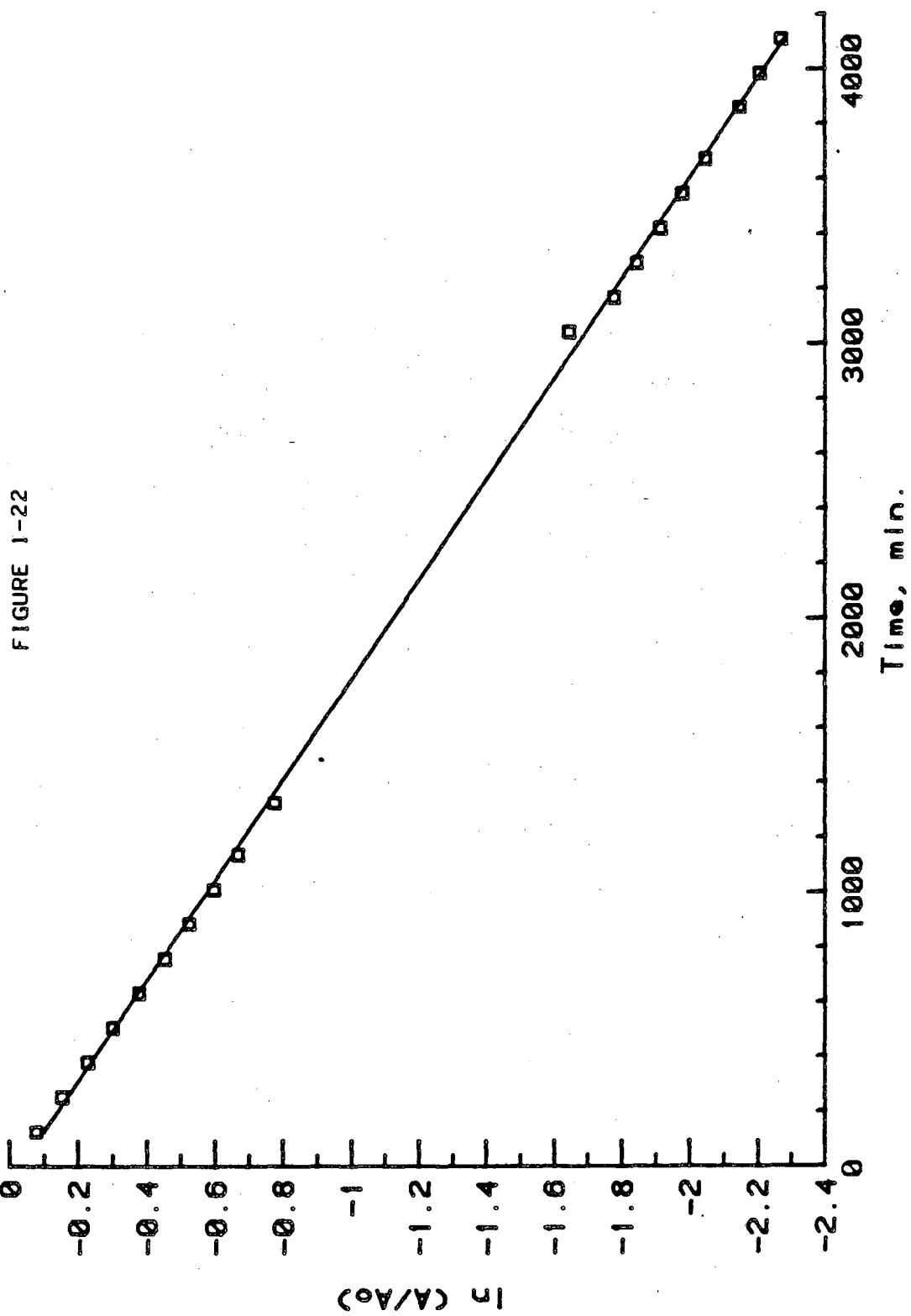


Table 1-10: Rate data for di-substituted uranocenes  
and mixed uranocene

complex	$k \times 10^5 \text{ s}^{-1}$	$\ln k$
$(\text{PhCOT})_2\text{U}$	4.4	-10.03
$(\text{PhCOT})(t\text{-BuCOT})\text{U}$	0.91	-11.61
$(t\text{-BuCOT})_2\text{U}$	0.22	-13.03

Though it is apparent from the above data that each substituent contributes to the electron density at the central metal, it is not clear as to which ring is preferentially protonated after coordination of water. One way of determining this preference is to examine the isotope effect of the mixed complex and compare it to the ratio observed for the bis-substituted complexes.<sup>46</sup> Glaser<sup>44</sup> has found the isotope effect for the hydrolysis of di-t-butyluranocene to be 8.2. Earlier (Table 1-7), it was reported that the isotope effect for the hydrolysis of diphenyluranocene is 12.8. The deuterolysis rate for t-butylphenyluranocene was measured and found to be  $7.2 \times 10^{-7} \text{ s}^{-1}$ , which results in a ratio of 12.7, close to the isotope effect observed for diphenyluranocene.

One would then be tempted to conclude that the first proton is being transferred to the ring containing the phenyl group. Unfortunately, this is in contrast to what one would predict. The electron-releasing group, t-butyl, should increase the local

electron density at the one ring and therefore, increase the proton affinity of the ring. To verify this hypothesis, two equivalents of  $D_2O$  were added to one equivalent of t-butylcyclooctatetraene dianion and one equivalent of phenylcyclooctatetraene dianion (four equivalents of protons are needed for complete quenching), followed by quenching to completion with  $H_2O$ . Mass spectral analysis determined that 55% of the protons transferred to the t-butylcyclooctatetraene dianion upon quenching were deuterium, while the phenylcyclooctatriene products incorporated only 18% deuterium. The experiment was repeated, this time allowing additional time (15 to 20 minutes) for the two dianions to compete for deuterium, with the same 3 to 1 preference for t-butylcyclooctatetraene dianion over phenylcyclooctatetraene dianion found; 73% and 23% deuterium incorporation resulted, respectively.

Thus, in the case of the dianions, our simple picture of a t-butyl group increasing electron density and encouraging proton transfer holds true. This, however, only magnifies the inconsistency of our isotope effect experiment on the mixed uranocene, and forces us to accept the protonation of the phenyl ring as the first step or leave the matter unresolved due to some fallacy in experimental design or measurement.

### Results: Product Analysis

Quite a bit of information was obtained about the hydrolysis mechanism from the kinetic experiments just detailed. It was hoped, that by examining the products (particularly the organic products) formed in the hydrolysis, further information about the mechanism could be acquired. Is the large isotope effect unique to the first protonation in the hydrolysis? Is only one isomer of cyclooctatriene formed, or does a 50:50 mixture of the two possible isomers result? Can we label the protonations in such a way as to be able to determine their preferential protonating sites in a substituted uranocene? These are just a few of the questions we had hoped to answer in our analysis of the hydrolysis products.

The first hydrolysis of a cyclooctatetraene (COT) dianion complex was carried out by Roth.<sup>47</sup> Roth found that rapid addition of a  $K_2COT$  solution in THF to water resulted in a 4 to 1 mixture of 1,3,5-cyclooctatriene to 1,3,6-cyclooctatriene. Unfortunately, there would then appear to be an apparent conflict with the more recent results of Yoshida<sup>30</sup> and Greco<sup>31</sup> who had reported observing cyclooctatetraene in the hydrolysis of f-element complexes. To clear up some of the confusion, the hydrolysis products from the dianion were separated by GLPC, and the isomers assigned by high field (250 MHz)  $^1H$  NMR. The 1,3,6 and 1,3,5-cyclooctatriene could then be used to standardize the analytical GC retention times for each isomer. Interestingly, it was discovered that cyclooctatetraene had the same retention time on the 20% carbowax

column as the 1,3,5-cyclooctatriene isomer. Co-injection of COT and the 1,3,5 triene results in one, slightly broadened peak. This could explain why previous investigators reported COT as a product of hydrolysis,<sup>48</sup> even though it was difficult to rationalize an electron transfer product in a reaction involving a protic reagent. An example of this misinterpretation is the paper by Greco and co-workers<sup>31</sup> in which they reported an 80 to 20 ratio of cyclooctatetraene to cyclooctatriene "mixture" upon alcoholysis of cerocene. When the experiment was repeated by myself, no cyclooctatetraene was observed. Instead, the correct ratio of organic products is an 81 to 19 ratio of 1,3,5 to 1,3,6 cyclooctatriene. Separation between cyclooctatetraene and 1,3,5-cyclooctatriene can be achieved, but it requires a 15-meter fused silica capillary column.

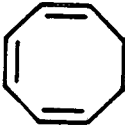

As mentioned earlier, Roth had found that hydrolysis of COT dianion resulted in a 4 to 1 ratio of the 1,3,5 to 1,3,6-cyclooctatriene isomers. As a check, the experiment was repeated by myself (twice) and a ratio of 76:24 (1,3,5:1,3,6), within 2% error, was found. Roth also found that by heating the triene mixture to 225°C, the thermodynamic equilibrium ratio of 40 to 1 (1,3,5 to 1,3,6) was reached. Thus, it was postulated that because uranocene hydrolyzed much more slowly than  $K_2COT$ , the recovered cyclooctatriene products from the uranocene hydrolysis would be in a ratio closer to that of the thermodynamic equilibrium.

Addition of 500 mg of uranocene to 100 mL of 1M  $H_2O/THF$  produced a 65:35 mixture of 1,3,6 and 1,3,5-cyclooctatriene,



respectively (see Table 1-11). Remarkably, the major product in the hydrolysis of uranocene appears to be 1,3,6-cyclooctatriene, an unexpected result, since it was believed that the slower hydrolysis would result in the more thermodynamically stable 1,3,5-cyclooctatriene as the major product.

Table 1-11: Ratio of Cyclooctatriene Products Formed During Hydrolysis

			
$K_2C_8H_8$	$\xrightarrow[\text{THF}]{H_2O}$	76	24
$U(C_8H_8)_2$	$\xrightarrow[\text{THF}]{H_2O}$	34	66
Equilibrium		97	3

With such an unusual result in hand, we were curious as to whether all bis-cyclooctatetraene complexes might hydrolyze in this manner, forming mostly 1,3,6-cyclooctatriene. Perhaps the first ring in the hydrolysis of uranocene is protonating 1,4, resulting in 100% 1,3,6-cyclooctatriene, while the second ring protonates as in the dianion case (mostly 1,3,5-cyclooctatriene formed). However, as can be seen in Table 1-12, there is a complex continuum of product ratios which result from the hydrolysis of bis-[8]annulene actinide and lanthanide complexes. No known physical properties can be confidently correlated with these

results, although one can note a general trend of the more "ionic" complexes hydrolyzing to larger amounts of the 1,3,5-cyclooctatriene.

Table 1-12: Ratio of Cyclooctatriene Products of Bis-[8]annulene Complexes in 1M H<sub>2</sub>O/THF

Complex	% 1,3,6	% 1,3,5
K <sub>2</sub> COT <sup>=</sup>	24	76
K <sub>2</sub> Ca(II)(COT) <sub>2</sub>	29	71
Ce(IV)(COT) <sub>2</sub>	38	62
KYb(III)(COT) <sub>2</sub>	40	60
KSm(III)(COT) <sub>2</sub>	44	56
K <sub>2</sub> Yb(II)(COT) <sub>2</sub>	45	55
Th(COT) <sub>2</sub>	51	49
U(COT) <sub>2</sub>	64	36

If the product ratio in the hydrolysis is effected by the central metal of the complex, would the percent isomers formed also be effected by other factors, such as the proton source, as well? A variety of protic reagents (varied based on pKa values) were used to protonate uranocene and thorocene (Table 1-13). Acidic reagents tend to give mostly the 1,3,5-cyclooctatriene, even more than observed in the hydrolysis of K<sub>2</sub>COT. Interestingly, protonating K<sub>2</sub>COT with different reagents demonstrated a different trend. The lower the pKa of the protic reagent, the

Table 1-13: %1,3,5-cyclooctatriene isolated from  
hydrolysis of actinide complexes

<u>Proton Source</u>	<u>Uranocene</u>	<u>Thorocene</u>	<u>(COT)ThCl<sub>2</sub></u>
MeOH	48		
EtOH	45	52	47
H <sub>2</sub> O	34	49	48
MeSO <sub>3</sub> H	93	72	
CF <sub>3</sub> COOH	73	62	
CH <sub>3</sub> COOH	88	84	91

Table 1-14: Cyclooctatriene Product Ratio for  
K<sub>2</sub>COT Protonations

<u>Protic Reagent</u>	<u>1,3,5</u>	<u>1,3,6</u>
CH <sub>2</sub> (CN) <sub>2</sub>	52	48
CH <sub>3</sub> SO <sub>3</sub> H	56	44
CF <sub>3</sub> COOH	44	56
CH <sub>3</sub> COOH	49	51
H <sub>2</sub> O	76	24
CH <sub>3</sub> OH	78	22
C <sub>2</sub> H <sub>5</sub> OH	73	27
1-C <sub>3</sub> H <sub>7</sub> OH	86	14
(CH <sub>3</sub> ) <sub>3</sub> COH	99	1
Fluorene	91	9

closer to a 50:50 ratio of isomers resulting from the protonation of  $K_2COT$  (Table 1-14). Alcoholic reagents and high  $pK_a$  proton sources (i.e., fluorene) tended to give large amounts of 1,3,5-cyclooctatriene. Explanations for these observations can only be speculative, but perhaps in the case of the dianion, comparatively slower hydrolysis by the alcohols (compared to the acetic and methylsulfonic acids) may allow for some sort of prior coordination to potassium (figure 1-23). This coordinated alcohol, may then somehow, differentiate between protonating 1,2 and 1,4, in contrast to the random protonation resulting from the protons of a highly dissociated acetic acid.

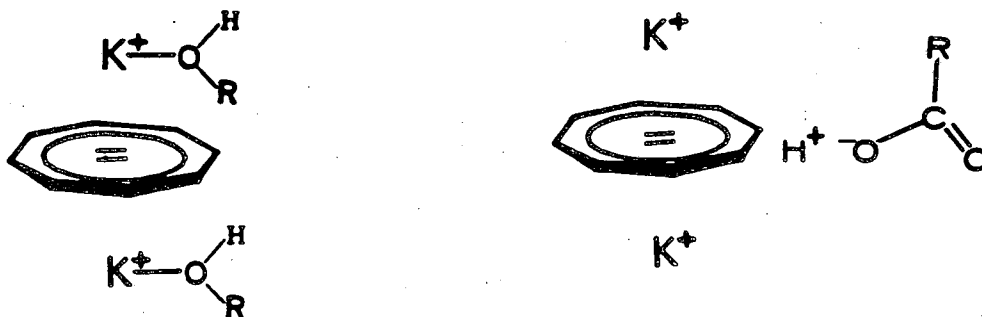
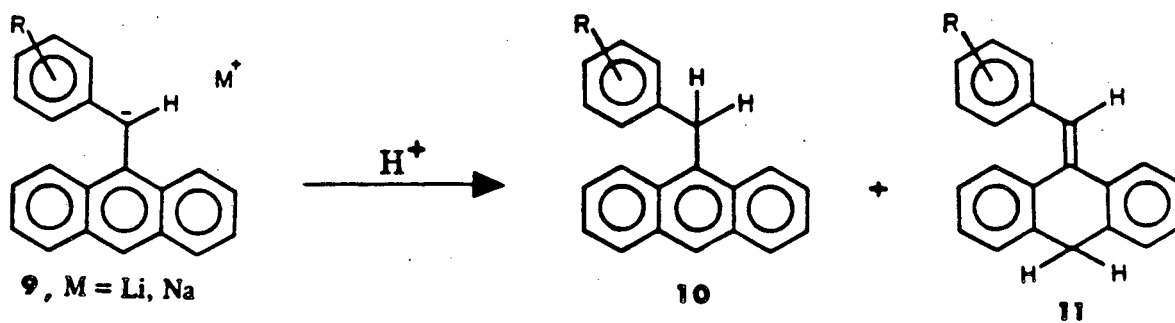


FIGURE 1-23

Changes in the regiochemistry of a protonation when the proton source is varied is not a unique observation to this system. Nojima<sup>49</sup> and co-workers found the nature of the proton

donor to be important in determining the protonation regiochemistry of anion **9** (eq. 1-23). Protonation of the sodium anion **9** with "strong" oxygen acids, trifluoroacetic acid, acetic acid, and phenol (pKa 0.2, 4.7 and 10.0, respectively), yielded less **10** (and more of **11**) than did protonation with "weak" oxygen acids, trifluoroethanol, water, ethanol, and 2-methyl-propanol (pKa 12, 14, 16, and 19, respectively). The effect of the proton source was even more pronounced in the case of the lithium anion of **9**, which led the authors<sup>49</sup> to deduce the coordination of oxygen acids toward lithium cation as a probable reason for the appearance of the counteraction effects on the protonation regiochemistry.



eq. 1-23

Not surprisingly, varying the counterion in the cyclooctatetraene dianion complex also had an effect on the amount of 1,3,6-cyclooctatriene formed upon protonation (Table 1-15). Perhaps prior coordination to the cation could account for the differences in product ratios. Alternative explanations for the

variation in regiochemistry could be the differences in the way the ion pair is solvated (contact vs. solvent separated),<sup>50</sup> or the size of the cation. In any case, simple predictions of product formation are not possible at this time.

Table 1-15: Cyclooctatetraene Dianion Hydrolysis  
Product Analysis

$M_2COT$	% 1,3,5 cyclooctatriene	% 1,3,6
$Li_2COT$	43	57
$K_2COT$	76	24
$Cs_2COT$	79	21

Even though the amount of information that was obtained from the product ratios was somewhat limited, perhaps examination of the amount of deuterium incorporated into the products might give us some insight into the large kinetic isotope effects observed for the hydrolysis of uranocene. It was still postulated, at this point, that the large kinetic isotope effects observed were unique to the slow hydrolysis of uranocene (as opposed to the immediate hydrolysis of the bis-[8]annulene lanthanide and  $M_2COT$  complexes) and that the effect was due primarily to the slow transfer of the first proton to the uranocene ring. If we did find that an isotope effect existed for only the first

protonation, then we might be able to 'label' its position in a substituted cyclooctatriene product and perhaps be able to study electrophilic aromatic substitution in a coordinated 10  $\pi$ -electron system. Or, we might be able to distinguish separate isotope effects in each of the four protonations of the sandwich complexes. In either case, it was necessary to determine deuterium incorporation in the hydrolysis/deuterolysis of the alkali metal dianions in order to standardize the analysis procedure and compare it to the unusual uranocene hydrolysis reaction.

The experiment was carried out by recovering the volatile cyclooctatriene products via vacuum transfer after adding a THF solution of the dianion or sandwich complex to a 50/50 mixture of  $H_2O/D_2O$  in THF. The organic products were then extracted with hexane. The hexane was removed in vacuo, and the two triene isomers were isolated by preparative GLPC. The analysis for deuterium incorporation into the triene isomers was carried out by low voltage (approx. 10 eV) mass spectrometry. The percent deuterium incorporated into the products was calculated from the relative intensities of the  $d_0$ ,  $d_1$ , and  $d_2$  molecular ion peaks (given as a percentage of the base peak) after a small correction for C-13 (eq. 1-24). The %D thus resulting refers to the percent probability that an individual protonation site will have incorporated a deuterium.

$$\%D = 1/2[2d_2 + d_1] \times 100\%$$

eq. 1-24

A low deuterium incorporation could be due to exchange of deuterium in the products with the hydrogen in the solvent, with the walls of the chromatograph or mass spectrometer, or with some other source in the isolation procedure. As a check of the isolation technique and as a way of establishing standards for the mass spectral analysis,  $K_2COT$  was quenched separately by 100%  $H_2O$  and by "100%" (99.998%)  $D_2O$  and handled in the same manner that all of the hydrolyses of cyclooctatetraene complexes were handled. No isomerization (<1%, the limit of experimental reproducibility) was detected for either isomer under the conditions of isolation. In addition, no exchange of deuterium for hydrogen was found with the mild GC conditions and low voltage mass spectral analysis employed. With "100%"  $D_2O$  as the quenching reagent, the molecular ion peak at 106 ( $d_2$  for cyclooctatriene) dominates (>98%) the spectrum. A small peak at 105 ( $d_1$ ) (approx. 2%) could be due to some minor M-1 fragmentation, trace  $H_2O$  impurity, or perhaps there is a minor amount of hydrogen exchange for deuterium. In any case, any large isotope effects observed by this method are significant and reliable.

When the alkali metal dianions ( $Li_2COT$ ,  $K_2COT$ , and  $Cs_2COT$ ) were quenched in a 50/50 mixture of  $H_2O/D_2O$ , the isolated cyclooctatrienes were all found to have much lower than expected (<50%) deuterium incorporation (Table 1-16). Both the products from the potassium and cesium dianion quenchings have only 15% deuterium incorporation, a 6 to 1 preference for hydrogen over deuterium, quite remarkable since hydrolysis of the salts occurs immediately upon addition to water. Even upon addition of  $K_2COT$



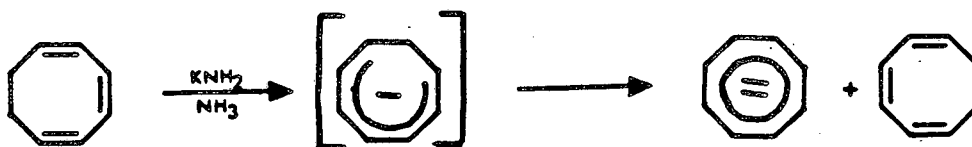
to an 8 to 1 ratio of  $D_2O$  to  $H_2O$  in THF, a preference for hydrogen over deuterium is demonstrated (44% deuterium incorporated into the cyclooctatriene products). It is worthy to note that no significant difference (<2%) was found in the amount of deuterium incorporated in the two cyclooctatriene isomers (1,3,6 and 1,3,5).

Table 1-16: Percent Deuterium Incorporated into  
Cyclooctatetraene Dianion

$M_2COT$	%D in 1,3,5	%D in 1,3,6
$Li_2COT$	32	31
$K_2COT$	15	16
$Cs_2COT$	15	15

As the data in Table 1-16 demonstrates, there is a substantial difference in the amount of deuterium incorporated in the cyclooctatriene products resulting from the  $Li_2COT$  quenching and those from the  $K_2COT$  and  $Cs_2COT$  quenchings. This product difference can be due to a difference in ion pairing, or perhaps due to the size of the cation itself. Both of these factors will influence the cation's environment and if there is prior coordination to the cation by the water molecule there will be a significant effect on the deuterium incorporation.

It would be desirable to be able to distinguish between the two isotope effects of the two protonations. Since the percent deuterium incorporated into the products is less than 25%, it appears as if both protonations have significant isotope effects. Quenching cyclooctatrienyl anion in the  $H_2O/D_2O$  mixture would give us the desired information. Unfortunately, efforts to isolate the unsubstituted mono-anion by Pearl and Staley<sup>51</sup> were unsuccessful (eq. 1-25).



eq. 1-25

The problem of deprotonation of the mono-anion to the dianion is eliminated in the case of the 8,8-dimethylcyclooctatrienyl anion, 12, since it does not contain a hydrogen on the 8-position.<sup>51</sup> The synthetic scheme for the preparation of 12 (Figure 1-24) involved the dialkylation of cyclooctadiene, followed by halogenation, and dehydro-halogenation.<sup>51</sup> In general, the yields were poor (those yields quoted are maximum yields) and the first reaction was not reproducible. Thus, it would be advantageous to produce the gem-substituted cyclooctatriene in a much higher yielding reaction. In the presence of a catalyst, trimethylaluminum has been found to gem-dimethylate ketones in satisfactory yields.

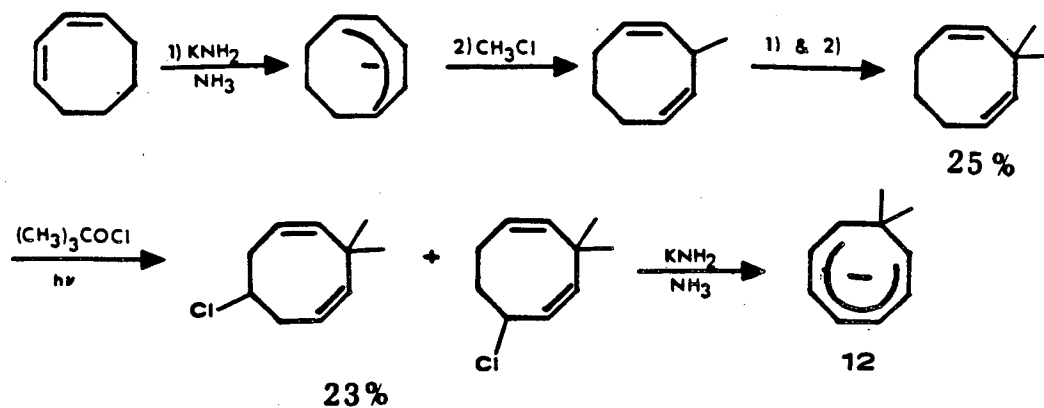


FIGURE 1-24

Dimethylation was first attempted directly on the epoxide, 13, (Figure 1-25). IR and NMR data, however, confirmed that methyl addition had occurred 1,4, resulting in compound 14. Efforts thus turned towards dimethylation of the ketone 15. Addition of  $\text{AlMe}_3$  to 15, however, also failed to produce the desired dimethylation product (8,8-dimethylcycloocta-1,3,5-triene), thus the project

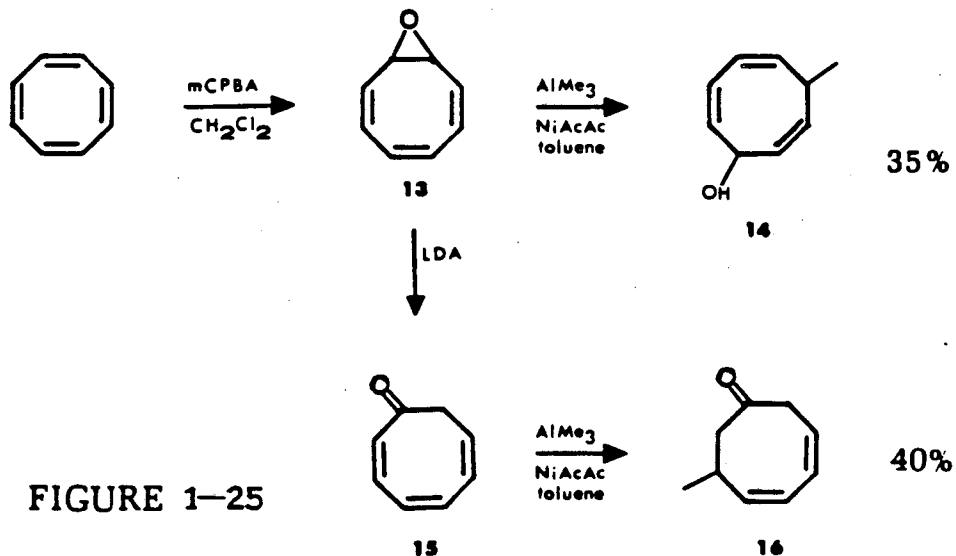


FIGURE 1-25

was abandoned in favor of other methods (see half-sandwich section results) which might distinguish between the isotope effects of the two protonations.

Although a study of competitive isotope effects for other carbanions won't provide us with information on cyclooctatetraene dianion isotope effects, it would be convenient to be able to make comparisons with other types of anions. Remarkably, there is no mention in the literature of an isotope effect determined simply by taking a carbanion and quenching it in a mixture of  $\text{H}_2\text{O}$  and  $\text{D}_2\text{O}$ . Thus, if we are to make a comparison between anions and dianions, we must carry out our own experiments.

Selecting a system in which an anion is formed completely, without decomposition, and without exchange of protons during the work-up was not completely trivial. Triphenylmethane (TPM) was the selected hydrocarbon, since it contained a proton in the desired range ( $\text{pK}_a=30-40$ ) and could be easily handled. Unfortunately, selecting the proper base was not as simple. Cleaving bibenzyl with potassium to form the respective benzyl anion that will deprotonate TPM resulted in less than 50% TPM anion formation (checked by quenching with  $\text{D}_2\text{O}/\text{THF}$ ). Use of *n*-butyllithium was found to result in sufficient formation of the TPM anion. Addition of 1.1 equivalents of *n*-butyllithium to 1 equivalent of TPM in THF, followed by quenching in a 10-fold excess of  $\text{H}_2\text{O}-\text{D}_2\text{O}$  in THF resulted in 40% deuterium incorporation by mass spectral analysis. Thus, the quenching study demonstrates that simple anions such as the anion of TPM do not demonstrate as large an

isotope effect during protonation as do the potassium or lithium cyclooctatetraene dianion salts.

Changing the protic reagent used to quench the cyclooctatetraene complexes had a varying effect on the amount of deuterium incorporated in the cyclooctatriene products. For  $K_2COT$ , the more acidic protic reagents ( $CF_3COOH$ ;  $CF_3COOD$ ) resulted in a much higher deuterium incorporation. Since much of the quenching of the dianion complex probably occurs via "free" protons and deuterons, there is a much lower isotope effect (Table 1-17). In the case of the uranocene complex (Table 1-18), there is no variation in deuterium incorporation upon a change in the proton source, indicating perhaps that protonation of the [8]-annulene ring occurs primarily from protic reagents complexed to the metal center (whether water, methanol, or acetic acid). For thorocene (Table 1-19), there is an intermediate increase in the amount of deuterium incorporated, suggesting that while some of the protonations of the rings are occurring via complexed protic reagent, some of the protons (after the initial protonation) are transferred from external (uncomplexed) sources (Figure 1-26). Interestingly, for the majority of the deuterium incorporation experiments carried out, 1,3,6-cyclooctatriene had higher amounts of deuterium incorporated, implying that there is a distinct isotope effect for each of the two isomers formed.

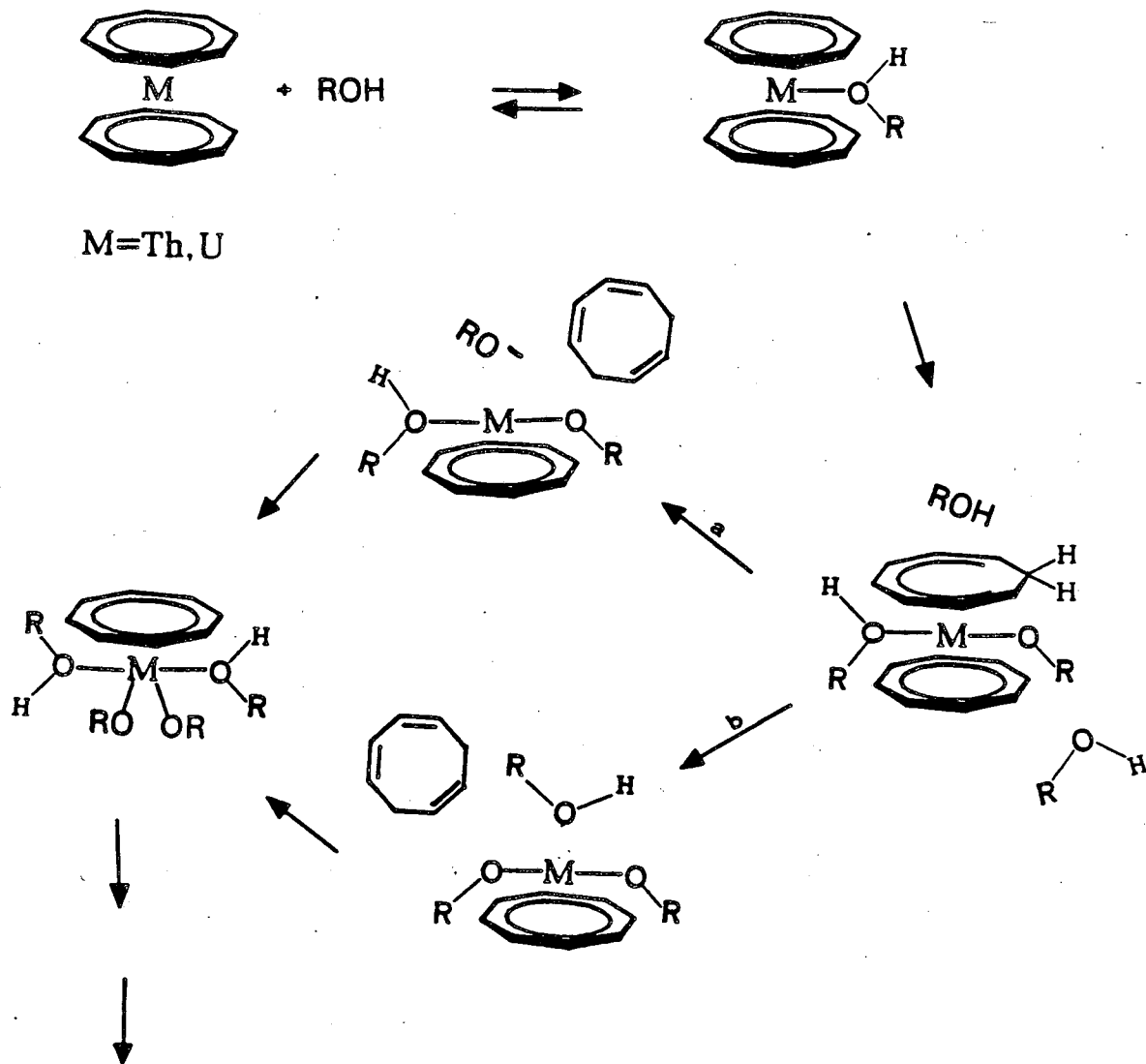


FIGURE 1-26



a-proton source is uncomplexed;

no isotope effect

b-proton source is complexed;

isotope effect results

Table 1-17: Percent Deuterium Incorporated into Cyclooctatriene  
Products of  $K_2COT$  After Quenching

<u>Protic Reagent</u>	<u>1,3,5</u>	<u>1,3,6</u>
$CF_3COOH/CF_3COOD$	43	47
$CH_3OH/CH_3OD$	25	24
$H_2O/D_2O$	15	16

Table 1-18: Percent Deuterium Incorporated into Cyclooctatriene  
Products of Uranocene After Quenching

<u>Protic Reagent</u>	<u>1,3,5</u>	<u>1,3,6</u>
$CF_3COOH/CF_3COOD$	15	---
$CH_3OH/CH_3OD$	17	22
$H_2O/D_2O$	16	18

Table 1-19: Percent Deuterium Incorporated into Cyclooctatriene  
Products of Thorocene After Quenching

<u>Protic Reagent</u>	<u>1,3,5</u>	<u>1,3,6</u>
$CF_3COOH/CF_3COOD$	33	40
$CH_3OH/CH_3OD$	26	29
$H_2O/D_2O$	29	31

The analysis of the inorganic products formed in the hydrolysis turned out to be a more difficult task. The solid that precipitates out of the solution after the hydrolysis is a polymeric and/or oligomeric material which was found to be insoluble in all common solvents (organic or aqueous). However, reaction of acetic acid with uranocene and thorocene did allow us some small glimpse of the type of materials forming. The inorganic uranium product reacted upon exposure to oxygen (probably oxidizing to U(VI)), while the thorium product did not appear to change oxidation states. However, both materials were treated as air-sensitive. Elemental analysis (Table 1-20) of the solid indicates there are four acetate molecules per actinide ion. Thus, it is justified to postulate in Figure 1-26 that an average of four bidentate (some bridging acetates, such as those found in binuclear transition metal compounds, are likely to be present<sup>53</sup>) acetates are complexed to uranium and thorium. What is most comforting about this result is that there are no changes in the oxidation state (both metal center remain in the IV oxidation state) during the hydrolysis.

Table 1-20: Elemental Analysis of the Inorganic Products from the Reaction of  $(C_8H_8)_2M$  with 1M Acetic Acid

Calcd. for $U(OOCCH_3)_4$	Found
C, 20.26 H, 2.55	C, 20.70 H, 2.69
Calcd. for $Th(OOCCH_3)_4$	Found
C, 20.52 H, 2.58	C, 19.66 H, 3.04



## Results: Half-Sandwich Hydrolysis

Even with the deuterium incorporation experiments indicating that protonation of the bis-[8]annulene complexes is complicated, an investigation of the hydrolysis of mono-[8]annulene, or "half-sandwich" compounds, might demonstrate that protonation of the second ring was distinct in its mechanism from protonation of the first ring. After all, the half-life for hydrolysis of uranocene is almost 20 hours, while a half-sandwich with non-sterically demanding ligands should hydrolyze rapidly, if not immediately. If we examine the amount of deuterium which is incorporated in the cyclooctatriene products from the competitive quenching of the known thorium half-sandwich (and its uranium analog), a comparison can be made with the products of hydrolysis of uranocene and thorocene. Unfortunately, no "half-sandwich" uranium complex was known, which left out an important intermediate to analyze in terms of the mechanism. Thus, it became necessary for us to find a method of preparation for the complex, which would afford us an opportunity to hydrolyze the complex and determine separate isotope effects for each of the four protonations.

Details of the preparation of ([8]annulene)uranium dichloride bistetrahydrofuran will be left to the second chapter. In this section, we will discuss the assumptions made in using this complex as a model for an intermediate in the hydrolysis of uranocene.

In his dissertation, Lyttle<sup>33</sup> postulated that an [8]annulene-oxouranium complex (Figure 1-27) was an intermediate in the hydrolysis. Whether such a discrete species is present is certainly suspect; however, it is quite reasonable to suppose that at some point in the hydrolysis, one ring has already been

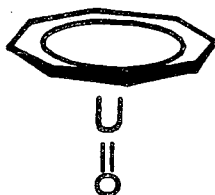


FIGURE 1-27

protonated off of the metal, while the other ring remains coordinated. It is believed that the newly synthesized ([8]annulene)uranium dichloride complex is, at the least, a rough model of this mono-ring intermediate. Sterically, the chlorides should occupy approximately the same amount of coordination space as would oxo or hydroxy ligands. The electronic demands of the chlorides could change the Lewis acidity of the uranium from that of an oxouranium complex. However, we have seen from earlier results that even with large changes in reaction rates (several orders of magnitude), large constant isotope effects still result (see Tables 1-4 and 1-7). Therefore, we should be able to derive information about the mechanism from our deuterium incorporation experiments, at least in the context of whether there is but a single isotope effect, or a number of complex protonations.

The hydrolyses of the half-sandwich complexes were carried out in the same manner as described in the product analysis section. Solutions of the half-sandwich in THF were added rapidly to an equal volume of a 2M H<sub>2</sub>O/THF solution (to make a 1M solution). It was noted that discoloration of the solution was not immediate, the hydrolysis of the uranium half-sandwich requiring over fifteen minutes for completion. The percent 1,3,5-cyclooctatriene isolated from the hydrolyses of the half-sandwich complexes are presented in Table 1-21, along with the full sandwich results which are listed for comparison. Note that for three of the complexes, an essentially equal amount of both cyclooctatrienes are isolated. Only uranocene hydrolyzes uniquely to the 1,3,6-cyclooctatriene as the major product.

Table 1-21: Comparison of Organic Products from the Hydrolysis of Half-Sandwich and Bis-Actinide Complexes

<u>complex</u>	<u>%1,3,6 cyclooctatriene</u>	<u>%D incorp. 1,3,6(1,3,5)</u>
(COT)UCl <sub>2</sub>	52	15(12)
(COT) <sub>2</sub> U	65	18(16)
(COT)ThCl <sub>2</sub>	52	23(21)
(COT) <sub>2</sub> Th	51	31(29)

Table 1-22: Deuterium Incorporated into the Products of Acidolysis and Alcoholysis of the Half-Sandwich Complexes

complex	quenched with	%1,3,6 cyclooctatriene	%D; 1,3,6(1,3,5)
(COT)UCl <sub>2</sub>	A	15	--(19)
(COT)ThCl <sub>2</sub>	A	38	29(27)
(COT)ThCl <sub>2</sub>	B	25	22(20)

A=50/50 CF<sub>3</sub>COOH/CF<sub>3</sub>COOD

B=CH<sub>3</sub>OH/CH<sub>3</sub>OD

Table 1-21 also lists the percent deuterium incorporated upon quenching the complexes in a solution of 0.5M H<sub>2</sub>O and 0.5M D<sub>2</sub>O in THF. Note that there are significant isotope effects even for the relatively rapid hydrolyses of thorocene, uranium half-sandwich, and the thorium half-sandwich. For the uranium half-sandwich, the 15% deuterium incorporation implies that there is, on the average, an approximate 6 to 1 preference for hydrogen over deuterium or an isotope effect of 6. The question remains, however, as to whether this value is indicative of the isotope effect of both protonations, or is it merely an average of two isotope effects (ex. 9 and 4).

To deduce the effect on the two protonations, we could examine the mass spectrum which had been used to calculate the percent incorporation. Algebraic manipulation of d<sub>0</sub>, d<sub>1</sub>, and d<sub>2</sub> values from the mass ion peak, can separate out the percent incorporation in the two protonations. Unfortunately, due to the significant error in the relative intensity of the mass spectrum

(1%), particularly in relation to the relatively small, but critical  $d_2$  peak (the relative intensity of the  $d_2$  peak was typically 3% to 5%), the method was deemed unreliable and non-reproducible.

A more fruitful method requires an assumption. If we assume that the large kinetic isotope effect measured for these complexes is due to the slow first protonation, then the second protonation can be deduced from the first (determined from kinetic measurement) and the total isotope effect (determined from deuterium incorporation). Fortunately, the complex reacts slowly enough for a kinetic measurement to be made in both  $H_2O$  and  $D_2O$  and those results are shown below.

$$k(H_2O) = 2.2 \times 10^{-3} \text{ s}^{-1}$$

$$k(D_2O) = 3.5 \times 10^{-4} \text{ s}^{-1}$$

The ratio of the two kinetic rates results in an isotope effect of about 6, the same as the value derived from deuterium incorporation. Thus, if our assumption holds true, the two protonations of a single ring, even in rapid hydrolyses, both have a large isotope effect.

### Conclusions from the Product Analyses

One of the frustrating aspects of these product analyses was the discovery that the formation of products is dependent on a variety of factors, some of which could not be accounted for easily. While it may not be possible to make simple predictions on the products which form, the generalizations we do make on the hydrolysis increase our understanding of electrophilic reactions in actinide organometallic chemistry. All of the protonations in the decomposition of the half-sandwich and full complexes have substantial isotope effects ( $>5$ ), which makes the first protonation unique only in that it is much slower than the protonations that follow. No intermediates, other than the starting complex, are found in the visible spectrum during the hydrolysis. No firm evidence pinpoints the source of the isotope effect, but it is hypothesized that it results from the protonation by protic reagents which are coordinated to the cation, whether an actinide or an alkali metal. Finally, while both protonations of the half-sandwich have substantial and approximately ( $\pm 2?$ ) the same isotope effect, it is difficult to reliably determine the specific isotope effect of each step.

## Experimental

General. Unless otherwise indicated, materials were obtained from commercial suppliers and used as supplied. Tetrahydrofuran (THF) and ethyl ether were distilled immediately before use from sodium/benzophenone. Toluene was distilled from sodium. Hexane was distilled from  $\text{CaH}_2$  after refluxing overnight. All air and moisture sensitive compounds were handled either in an argon atmosphere glovebox, or by standard Schlenk techniques.  $^1\text{H}$  NMR spectra were recorded on the UCB-200 (200 MHz, FT) or UCB-250 (250 MHz, FT) spectrometers. Significant  $^1\text{H}$  NMR data are tabulated in order: multiplicity (s, singlet; d, doublet; m, multiplet), number of protons, coupling constant in Hertz. Chemical shifts are referenced to tetramethylsilane (TMS) either directly with TMS as internal standard or indirectly by resonance of solvents referenced to TMS. Elemental analyses were performed by the Microanalytical Laboratory operated by the College of Chemistry, University of California, Berkeley. Infrared spectra were determined on a Perkin-Elmer Model 297 spectrometer. Visible spectra of THF solutions of the organometallic compounds were determined with a Cary Model 118 spectrophotometer. Low voltage mass spectra were obtained with the AEI MS-12 mass spectrometer. Mass spectral data are expressed as m/e (intensity expressed as percent of total ion current). All weights, unless otherwise specified, are  $\pm 0.01$  g.

Kinetic Runs. Approximately 5 to 10 mg of the uranocene was loaded into a UV-VIS mixing cell and dissolved in 4 mL of degassed 1M H<sub>2</sub>O or D<sub>2</sub>O in THF solutions. Mixing occurred after allowing ten minutes for solvent-temperature bath equilibration. Decomposition rates were determined by following the decrease in absorbance at  $\lambda_{\max}$  for the compound over three half-lives. The measurements were stored by a PET 4016 computer, interfaced to a Cary 118 UV-VIS spectrometer. Correlations for the plots of  $\ln(A/A_0)$  vs. time were greater than 0.999 in most cases and greater than 0.995 in all cases.

$\lambda_{\max}$  for the uranocenes were determined by "Curvalyzer 26",<sup>54</sup> a program designed to analyze a spectrum and assign a wavelength at maximum absorbance. Three scans for each uranocene in THF were made over a 10 nm range (620 to 630 nm). The scan rate was 0.1 nm/sec.

Plots for the kinetic data were made by a least-squares fit on a Tektronix 4052 computer equipped with zeta plotter. Activation parameters for the decomposition were determined by the program ACTENG.<sup>55</sup>

1,1'-Diphenyluranocene. To a flask under argon containing 0.89 g (0.005 moles) of phenylcyclooctatetraene (prepared by the method of DeKock<sup>42</sup>) in 125 mL of anhydrous THF, was added 0.41 g (0.105 moles) of potassium cut into small chunks. The solution was stirred for 18 hr and brought into the dry box where it was added over a 10 min period to a solution of 0.96 g (0.0025 moles) of UCl<sub>4</sub> in 100 mL of dry, degassed THF. After stirring for an



additional 30 min, the flask was connected to a vacuum line and the solvent was pumped off. The blackish powder was brought back into the box and extracted with 100 mL of toluene, which upon solvent removal by vacuum pumping to dryness, left a green, amorphous solid. Recrystallization by dissolving the solid in 25 mL of hot THF and adding hexane until cloudy, afforded 0.62 g (41%) of dark green crystals of 1,1'-diphenyluranocene and 0.28 g (19%) of a green powder which failed to crystallize.  $^1\text{H}$  NMR ( $\text{C}_7\text{H}_8$ , 250 MHz)  $\delta$  -33.99 (s, 2H), -35.74 (s, 2H), -35.98 (s, 2H), -36.69 (s, 1H), -13.66 (s, 2H), 0.87 (s, 1H), 0.96 (s, 2H) at 30 °C.

Anal. Calcd. for  $\text{C}_{28}\text{H}_{24}\text{U}$ : C, 56.19; H, 4.04; Found: C, 55.96; H, 4.14.

p-Trifluoromethylphenyllithium<sup>56</sup>. To a solution of 0.02 moles of *n*-butyllithium in 20 mL of ether/hexane at -78 °C, was cannulated 4.5 g (0.02 moles) of *p*-bromobenzotrifluoride. After two minutes, the clear, yellow solution was cloudy with a white precipitate, but the solution was stirred for 15 min to allow for complete reaction. An aliquot was quenched in freshly crushed Dry Ice, acidified with 6N  $\text{H}_2\text{SO}_4$  and extracted with ether (3x10 mL). The combined organic extract was extracted with 1N NaOH (3x15 mL) and the basic salt solution was acidified with 6N HCl. The resulting white precipitate was filtered and dried to yield a microfine white powder identified by spectroscopy and melting point to be *p*-trifluoromethylbenzoic acid, mp 220 °-225 °C (lit. 222 °-224 °C);  $^1\text{H}$  NMR ( $\text{C}_3\text{D}_6\text{O}$ , 90 MHz)  $\delta$  7.81 (d, 2H, J=12),

8.22 (d, 2H, J=12);  $^1\text{H}$  NMR ( $\text{CDCl}_3$ , 90 MHz)  $\delta$  7.74 (d, 2H, J=12), 8.21 (d, 2H, J=12), 6.7 (broad). To the remainder of the lithium reagent under argon was then added 1.22 g of cyclooctatetraene in 10 mL of ether. The solution was allowed to warm to room temperature, at which time it became red. The solution became dark overnight, but reaction times of up to 96 hr resulted in no arylcyclooctatetraene products.

m-fluorophenylcyclooctatetraene. To a 100 mL 3-neck flask, equipped with a condenser and addition funnel and charged with 0.80 g (0.033 moles) of Mg was added 5.25 g (0.03 moles) of m-bromofluorobenzene in 60 mL of THF. As the reaction occurred over a 0.5 hr period, a total of 0.2 g of dibromoethane was required to maintain the reaction, after which the reaction was refluxed for an additional 0.5 hr to ensure completion. Titration of the reagent (quenching with water and titrating with standard 0.96M HCl) showed a concentration of 0.25M (yield: 80%). The Grignard reagent was added via cannulation into a 500 mL 3-neck flask charged with 0.164 g of [1,3-bis-(diphenylphosphino)-propyl]nickel(II) dichloride,<sup>57</sup> 40 mL of dry ether and 4.58 g (0.025 moles) of bromocyclooctatetraene (an additional 40 mL of dry THF was added to the Grignard solution to dissolve the reagent which precipitated upon cooling). The reaction was slightly exothermic upon addition and formed a white precipitate. After stirring the red-brown solution for 24 hr, the reaction was quenched with 1M HCl, separated and extracted with ether (2x20 mL). The organic portions were combined, washed with water

(50 mL), dried over  $\text{MgSO}_4$ , and the solvent was removed by rotary evaporation. The residue was distilled, affording 2.59 g of an impure yellow oil, bp  $69^\circ\text{--}71^\circ\text{C}/0.2\text{ mm}$ . Further purification was achieved by formation of the silver nitrate complex, followed by decomposition of the complex with  $\text{NH}_4\text{OH}$  (aq) (yield: 40%).  $^1\text{H}$  NMR ( $\text{CDCl}_3$ , 90 MHz)  $\delta$  5.73–6.31 (m, 7H), 6.87–7.32 (m, 4H).  $^{19}\text{F}$  NMR (with respect to  $\text{CFCl}_3$ )  $\delta$  +114.5 (multiplet).  
 Anal. Calcd. for  $\text{C}_{14}\text{H}_{11}\text{F}$ : C, 84.81; H, 5.60; Found: C, 84.57; H, 5.66.

m-Fluorophenyluranocene. To a flask under argon containing 0.50 g (0.0025 moles) of m-fluorophenylcyclooctatetraene in 25 mL of THF was added 0.23 g (0.0059 moles) of potassium cut into small chunks. The cleanly cut potassium permitted rapid reduction, thus reaction was complete within 4 hr. This solution was rapidly cannulated into 0.47 g of  $\text{UCl}_4$  in 15 mL of THF. After stirring for an additional 1 hr, the solvent was removed in vacuo, and the remaining solid was extracted with 200 mL of toluene. Solvent removal by vacuum pumping to dryness left a green, amorphous solid which upon recrystallization from hot hexane produced a light green, powdery material (yield: 50%).  $^1\text{H}$  NMR ( $\text{C}_7\text{D}_8$ , 250 MHz) -37.23 (s, 1H), -36.43 (s, 2H), -35.87 (s, 2H), -33.63 (s, 2H), -14.92 (s, 1H), -12.67 (s, 1H), 0.26 (s, 1H), 0.47 (s, 1H) at  $30^\circ\text{C}$ .  
 Anal. Calcd. for  $\text{C}_{28}\text{H}_{22}\text{UF}_2$ : C, 52.98; H, 3.50; Found: C, 53.27; H, 3.82.

Other substituted uranocenes used in the kinetic experiments were obtained as previously prepared materials.

Preparation of 1-t-butyl-1-phenyluranocene. To an argon flushed 50 mL one-necked flask containing 0.40 g of t-butylcyclooctatetraene (2.5 mmol) and 0.45 g of phenylcyclooctatetraene (2.5 mmol) in 30 mL dry, degassed THF was added 0.43 g of potassium (11 mmol) cut into small chunks. Both substituted cyclooctatetraenes had been prepared by the method of DeKock<sup>42</sup>. The reaction was stirred for 12 hr, although reduction was probably complete within 4 hr. The dianion solution was then cannulated into an argon-flushed, 100 mL Schlenk flask containing 0.95 g of  $UCl_4$  (2.5 mmol) in 20 mL THF at  $-78\text{ }^\circ\text{C}$ . The solution was initially purple, but was green upon completion of the 15 min addition period. The solution was stirred for an additional 20 min at room temperature, the solvent was removed in vacuo, and the remaining solid was extracted with 100 mL of toluene. Solvent removal by vacuum pumping to dryness left a dry, chunky, green powder. Recrystallization from hot hexane precipitated 0.65 g (yield: 45%) of a deep green powder (mixed uranocene + diphenyluranocene) plus 0.25 g (yield: 17%) of a hexane soluble fraction consisting primarily of di-t-butyluranocene. Pure t-butylphenyluranocene was obtained by dissolving 0.50 g of the precipitated mixture in 18 mL of 1M  $H_2O/THF$ , then adding  $MgSO_4$  after 14 hr. The solution was filtered and the THF was removed in vacuo. After washing with hexane, 0.10 g of a green powder was isolated, and was found by  $^1H$  NMR to be >95% pure mixed

uranocene, and <5% di-*t*-butyluranocene.  $^1\text{H}$  NMR ( $\text{C}_7\text{D}_8$ , 200 MHz)  $\delta$  1.2 (s, 2H), 1.0 (s, 1H), -11.58 (s, 9H), -13.51 (s, 2H), -33.15 (s, 2H), -33.74 (s, 2H), -34.44 (m, 4H), -34.97 (s, 1H), -36.10 (s, 2H), -38.18 (s, 2H), -41.61 (s, 1H).

Competitive Deuterium Incorporation Between  $\text{K}_2(\text{PhCOT})$  and  $\text{K}_2(\text{t-BuCOT})$ . A 100 mL flask under argon was charged with 244 ( $\pm 2$ ) mg (1.024 mmol) of  $\text{K}_2(\text{t-BuCOT})$ , 263 ( $\pm 2$ ) mg (1.019 mmol) of  $\text{K}_2(\text{PhCOT})$  and 30 mL of THF. To the dianion solution was added dropwise, 42 ( $\pm 2$ ) mg (2.1 mmol) of degassed  $\text{D}_2\text{O}$  in 5 mL of THF. The flask was swirled for 2 min (10 min, the second time the quenching was carried out) to allow for reaction with the deuterium, before completely quenching with excess water. The organic products were extracted into hexane (2x50 mL), dried over  $\text{MgSO}_4$  and the solvent was evaporated. Separation of the phenylcyclooctatriene products from the *t*-butylcyclooctatriene products was carried out by eluting the mixture with 10% ether/hexane on silica gel. The percent deuterium incorporated into the products was calculated from the relative abundance of the  $d_0$ ,  $d_1$ , and  $d_2$  molecular ion peaks according to equation 1-24.

Analysis of Hydrolysis Products. Experiments on the analysis of hydrolysis products were all carried out under oxygen-free conditions. A solution of uranocene (0.5 g) in 100 mL of 1M  $\text{H}_2\text{O}/\text{THF}$  was allowed to stand for 3-4 days (4 half-lives), then

hydrolyzed to completion by addition of approximately 5M H<sub>2</sub>O/THF. A small sample had been removed before quenching and allowed to stand for 3 weeks for complete hydrolysis in 1M solution. No significant difference in the GC ratio of the products was found. Work-up consisted of removal of all volatile liquids from the uranium solids by vacuum transfer, extraction with hexane of the liquid, followed by drying of the organic layer in MgSO<sub>4</sub> after separation from water. Slow distillation of the THF and hexane under aspirator pressure, such that the temperature did not reach above 40 °C, resulted in a mixture of cyclooctatrienes which could be easily separated by a six meter, 1/8 in. dia. 20% carbowax on chromasorb column on a HP5880A GC at 80 °C. <sup>1</sup>H NMR (CDCl<sub>3</sub>, 200 MHz) 1,3,5-cyclooctatriene, δ 5.89 (m, 4H), 5.72 (m, 2H), 2.41 (m, 4H); cyclooctatetraene, δ 5.78 (s, 8H); 1,3,6-cyclooctatriene, δ 6.11 (d, 2H), 5.62 (t, 2H), 5.47 (q, 2H), 2.72 (m, 4H).

The other metal complexes hydrolyzed more quickly than uranocene; thus to avoid surface reactions, the complexes were dissolved in THF and rapidly added to a 2M H<sub>2</sub>O/THF solution. The products were worked-up as above, with recovery of the triene products typically being 80% to 85% of theoretical yield. In most cases, the protonating species was at least in 10-fold excess of the complex.

Competitive deuterium incorporation experiments were carried out by quenching the metal complex in a 50/50 mixture of H<sub>2</sub>O/D<sub>2</sub>O or in the appropriate protic reagent. Work-up was identical to the hydrolysis procedure above, except for acidic reagents such

as  $\text{CF}_3\text{COOD}$ , when a neutralization step with  $\text{NaHCO}_3$  was added during the extraction procedure. Separation of the two cyclooctatriene isomers for mass spectral analysis was carried out on a six meter, 1 in. Dow 710 on 60/80 chromasorb column on a Varian Model 920 aerograph at 90 °C.

Potassium Cyclooctatetraene Dianion. All of the alkali metal dianion complexes were prepared according to established literature procedures.<sup>47</sup> After stirring cyclooctatetraene in THF with the appropriate metal (Li, K, Cs), the solvent was removed in vacuo, and the solid was brought into the box and washed with hexane to remove any remaining traces of unreacted cyclooctatetraene. The solid was stored under argon atmosphere in the box until it was used in the appropriate hydrolysis experiment.

Uranocene,<sup>58</sup> thorocene,<sup>59</sup> and the thorium half-sandwich<sup>60</sup> are all previously prepared compounds; however, the procedure for their preparation was somewhat modified. The Schlenk techniques used in their preparation were developed by Ken Smith<sup>61</sup> and Steve Kinsley<sup>62</sup> and were found to be highly convenient and successful in obtaining good yields of the desired material.

Bis-([8]annulene)uranium(IV).<sup>58</sup> To a Schlenk flask under argon containing 1.04 g (0.01 mol) of cyclooctatetraene in 100 mL of anhydrous THF, was added 0.82 g (0.021 mol) of cleanly cut potassium. After stirring for 4 to 6 hr (or when the potassium

had completely reacted) at room temperature, the red dianion solution was cannulated into a Schlenk flask containing 1.90 g (0.005 mol) of  $UCl_4$  in 75 mL of dry, degassed THF. The reaction was stirred for 1 hr, and the solvent was removed in vacuo. The remaining solid was extracted for 2 days with toluene in a greaseless extractor to typically yield 50% to 60% of an emerald green, air-sensitive solid, whose spectroscopic ( $^1H$  NMR, UV-VIS) characteristics were identical to the known compound, uranocene.

Bis-([8]annulene)thorium.<sup>59</sup> The preparation of thorocene is identical to that of uranocene, except that 1.87 g of  $ThCl_4$  is substituted for  $UCl_4$ , and the resulting yellow solid, after removal of solvent, is extracted with THF, to remove thorocene from the THF insoluble  $ThCl_4$ .

([8]-Annulene)thorium dichloride bistetrahydrofuran.<sup>60</sup> To an argon flushed 250 mL Schlenk flask containing 4.67 g (0.045 mol) of cyclooctatetraene in 100 mL of THF was added 4.1 g (0.105 mol) of cleanly cut potassium. After 3 hr of stirring, the reaction was cooled to  $-78$  °C and cannulated over a 45 min period to a suspension of 18.9 g (0.05 mol)  $ThCl_4$  in 100 mL of THF, also cooled to  $-78$  °C. The reaction was stirred for 3 hr, and the solvent was removed in vacuo. Extraction of the remaining solid with toluene for six days resulted in 8.4 g of a yellow powder (38% yield based on unsolvated complex). Dissolving the yellow powder in THF, followed by slow evaporation of the solvent



resulted in yellow crystals which analyzed correctly for the bis-tetrahydrofuran complex.  $^1\text{H}$  NMR ( $\text{C}_4\text{D}_8\text{O}$ , 250 MHz)  $\delta$  6.68 (s, 8H)  
Anal. Calcd. for  $\text{C}_{16}\text{H}_{24}\text{Cl}_2\text{O}_2$ : C, 34.86; H, 4.39; Found: C, 34.93; H, 4.49.

Preparation and Quenching of Triphenylmethyl Anion. To 2.44 g (0.01 mol) of triphenylmethane in 50 mL of THF under argon was added 6.5 mL of  $n\text{-BuLi}$  (1.6M) (0.0104 mol) at  $-78^\circ\text{C}$ . The reaction was allowed to slowly warm to room temperature when it turned dark red. After stirring for one hour at room temperature (or 15 min after the solution stopped bubbling), about 3/4 of the solution was quenched in 100 mL of 2M  $\text{H}_2\text{O}-\text{D}_2\text{O}/\text{THF}$ , while the remainder was quenched in 25 mL of 2M  $\text{D}_2\text{O}/\text{THF}$ . Both mixtures were extracted with benzene (2x30 mL), dried over  $\text{MgSO}_4$ , and the solvent was evaporated. Mass spectral analysis of the remaining solids was accomplished by comparison of the relative abundance of the  $m/e=244$  ( $d_0$ ), and 245 ( $d_1$ ) peaks of triphenylmethane.

Bis-([8]annulene)lanthanides. The complexes chosen for the hydrolysis were previously prepared materials supplied as generous gifts from S. Kinsley<sup>62</sup> (La=Ce, Yb) and K. Hodgson<sup>63</sup> (La=Sm).

Cyclooctatetraene Oxide.<sup>33</sup> To a solution of 18.4 g (0.176 mol) of cyclooctatetraene in 275 mL of methylene chloride, was added 20 g of 80% mCPBA. The solution was cooled to  $0^\circ\text{C}$  for the

first hour, then allowed to stir unattended overnight. The yellow slurry was washed successively with 3N NaOH (3x100mL), 60 mL of water, and 60 mL of brine. The yellow solution was dried over  $\text{MgSO}_4$  and the solvent was evaporated. The residue was distilled with a 10 cm fractionating column. The first fraction was collected at  $<35\text{ }^\circ\text{C}/6\text{ torr}$ , which by  $^1\text{H}$  NMR spectroscopy was identified as the starting material, COT (yield: 9.91 g, 54%). A second fraction was collected at  $68\text{ }^\circ\text{--}70\text{ }^\circ\text{C}/5\text{ torr}$ , which, by  $^1\text{H}$  NMR, was identified as the desired product, COT oxide (yield: 6.27 g, 30%).  $^1\text{H}$  NMR ( $\text{CDCl}_3$ , 250 MHz)  $\delta$  3.45(s, 2H), 5.89(s, 2H), 5.95–6.15(m, 4H).

4-Methylcycloocta-2,5,7-trienol. (Attempted direct dimethylation of COT oxide). A 100 mL Schlenk flask was charged with 155 mg (0.6 mmol) of anhydrous nickel acetoacetonate (the hydrate was heated under 1 mm vacuum at  $105\text{ }^\circ\text{C}$  for 50 min), 20 mL of toluene, and 1.80 g of COT oxide (15 mmol). After cooling the flask to  $-15\text{ }^\circ\text{C}$ , 8 mL of commercial (Aldrich)  $\text{AlMe}_3$  (2M toluene solution, 16 mmol) was cannulated into the reaction flask over a 5 min period. The reaction was exothermic, turning the green color of the Ni catalyst to a muddy brown. After the addition was complete, stirring was continued for 12 hr at  $0\text{ }^\circ\text{C}$ , then at room temperature for 11 hr. The reaction was cooled in an ice bath before quenching with 15 mL of HCl. The reaction was extracted with hexane (3x20 mL) and the combined organic portion was washed with  $\text{NaHCO}_3$ . After drying over  $\text{MgSO}_4$ , the solvent was removed by rotary evaporation. Distillation of the residue resulted in the

isolation of 0.71 g (35% yield) of a yellow oil identified by  $^1\text{H}$  NMR and infrared spectroscopy as not the desired gem-dimethylcyclooctatrienone, but rather the mono-methyl product, 4-methyl-cycloocta-2,5,7-trienol.  $^1\text{H}$  NMR ( $\text{CDCl}_3$ , 250 MHz)  $\delta$  1.30 (d, 3H,  $J=7.1$  Hz), 1.72 (q, 1H,  $J=7.0$  Hz), 1.78 (s, 1H), 4.0-4.1 (m, 1H,  $J=7.1$  Hz), 5.2-5.5 (m, 2H), 6.2-6.35 (m, 2H), 6.6-6.7 (m, 2H). Infrared (neat) 3400 (broad), 3020 w, 2970 w, 2920 vw, 2860 vw, 1445 vw, 1400 vw, 1370 vw, 1140 w, 1060 w, 740 w, 725 w, 700 s, 665 w.

Cycloocta-2,4,6-trien-1-one.<sup>33</sup> A solution of lithium diisopropylamide in THF was prepared by adding 4.72 g (46.7 mmol) of diisopropylamine to 125 mL of dry THF under argon followed by 19 mL (46.5 mL) of 2.45M *n*-butyllithium in hexane at 0 °C. The light yellow solution was stirred for 15 min, then cooled to -78 °C. A solution of 2.50 g (20.8 mmol) of COT oxide in 15 mL dry THF was added slowly, during which time the solution turned a clear, deep red. The reaction mixture was stirred for 30 min at -78 °C and allowed to warm to -20 °C, whereupon it was quenched by adding 60 mL of saturated ammonium chloride solution. To the yellow mixture was added 100 mL of ether and the layers were separated. The organic portion was washed with water (2x60 mL), brine (30 mL), dried over  $\text{MgSO}_4$  and evaporated. Distillation of the crude product resulted in 1.89 g (76%) of a yellow liquid. A 250 MHz  $^1\text{H}$  NMR spectrum of the product was identical to that of the known product.<sup>33</sup>

7-methyl-cycloocta-3,5-dienone. To 0.16 g (0.6 mmol) of anhydrous nickel acetoacetonate in 20 mL of toluene was added 1.80 g (15 mmol) of cycloocta-2,4,6-trien-1-one under argon. The flask was cooled to -15 °C and 8 mL of commercial 2M  $\text{AlMe}_3$ /toluene solution (16 mmol) was cannulated into the Schlenk flask. After the addition was complete, the reaction was stirred at 0 °C to -3 °C for 14 hr, and at room temperature for 10 hr. The reaction was cooled in an ice bath and quenched with 15 mL of HCl. The mixture was extracted with hexane (3x20 mL) and the extracted organic phase was washed with  $\text{NaHCO}_3$ . After drying over  $\text{MgSO}_4$ , the solvent was removed by rotary evaporation. Distillation caused severe polymerization, therefore purification was carried out by eluting the remaining oil with hexane/ether (5 to 1, respectively) on 50 g of silica gel. Spectroscopic data indicated that the 0.83 g (40%) of oil recovered was not the desired gem-dimethyl product, but rather the mono-methyl ketone, 7-methyl-cycloocta-3,5-dienone.  $^1\text{H}$  NMR ( $\text{CDCl}_3$ , 250 MHz)  $\delta$  1.08 (d, 3H,  $J=7.1$  Hz), 2.3-2.6 (m, 2H), 2.9 (broad, 1H), 3.0-3.3 (m, 2H), 5.5-6.0 (m, 4H). Infrared (neat) 3010 w, 2960 s, 2930 w, 1722 s, 1450 w, 1420 w, 1320 w, 1280 w, 1130 w, 1030 w, 760 w, 690 s. Mass Spectrum m/e (rel. intensity) 136 (32.98), 121 (5.24), 107 (4.96), 94 (93.51), 79 (100), 66 (75.51).

Inorganic Products;  $^{\text{m}}(\text{CH}_3\text{COO})_4\text{U}^{\text{m}}$ . To a flask containing 1M acetic acid in degassed THF was added 0.89 g (0.002 mol) of bis-([8]annulene)uranium. After one week (over five half-lives), an

excess of degassed acetic acid was added to complete the quenching. All volatile liquids were removed in vacuo and the remaining solid was pumped to dryness. The insoluble solid was washed once with THF and twice with hexane, then pumped to dryness again. The submitted, air-sensitive solid analyzed correctly for one uranium per four acetate molecules.

Anal. Calcd. for  $C_8H_{12}O_8U$ : C, 20.26; H, 2.55; Found: C, 20.70; H, 2.69.

"(CH<sub>3</sub>COO)<sub>4</sub>Th". The yellow, insoluble solid was handled in a similar manner to the uranium solid.

Anal. Calcd. for  $C_8H_{12}O_8Th$ : C, 20.52; H, 2.58; Found: C, 19.66; H, 3.04.

FOOTNOTES AND REFERENCES

1. Marks, T. J. and Fischer, R. D., eds. "Organometallics of the f-elements", D. Reidel Publishing Company, Holland; 1979.
2. Seyam, A. M.; Kolb, J. R.; Marks, T. J. J. Am. Chem. Soc. 1973, 95, 5529.
3. Whitesides, G. M.; Casey, C. P.; Krieger, J. K. J. Am. Chem. Soc. 1971, 93, 1379.
4. Wachter, W. A. and Marks, T. J., J. Am. Chem. Soc. 1976, 98, 703.
5. Gilman, H.; Jones, R. G.; Bindschalder, E. J. Am. Chem. Soc. 1956, 78, 2790.
6. Seyam, A. M. and Marks, T. J. J. Organometal. Chem. 1974, 67, 61.
7. Kalina, D. G.; Marks, T. J.; Wachter, W. A. J. Am. Chem. Soc. 1977, 99, 3877.
8. Bruno, J. W.; Kalina, D. G.; Mintz, E. A.; Marks, T. J. J. Am. Chem. Soc. 1982, 104, 1860.
9. Fagan, P. J.; Manriquez, J. M.; Maatta, E. A.; Seyam, A. M.; Marks, T. J. J. Am. Chem. Soc. 1981, 103, 6650.
10. Moloy, K. G.; Marks, T. J.; Fagen, P. J. J. Am. Chem. Soc. 1981, 103, 6959.
11. Moloy, K. G. and Marks, T. J. J. Am. Chem. Soc. 1984, 106, 7051.
12. Since the author was unable to predict how the pre-equilibrium (CO coordination) is affected by a change in the steric and electronic properties of the R and X substituents on thorium, this can be said to be only a rough ranking of migratory aptitudes of alkyl and hydride ligands.
13. Bruno, J. W.; Marks, T. J.; Morss, L. R. J. Am. Chem. Soc. 1983, 105, 6824.
14. Maatta, E. A. and Marks, T. J. J. Am. Chem. Soc. 1981, 103, 3576.
15. Grant, C. B. Ph.D. Thesis U.C. Berkeley, 1977.

16. Grant, C. B. and Streitwieser, A., Jr. J. Am. Chem. Soc. 1978, 100, 2433.
17. Harmon, C. A. and Streitwieser, A., Jr. Inorg.Chem. 1972, 12, 1102.
18. Streitwieser, A., Jr. "Organometallics of the f-Elements", Marks, T. J. and Fischer, R. D., eds., D. Reidel Publishing Company, Holland, 1979, p. 159.
19. Wailes, P. C.; Coutts, R. S. P.; Weigold, H. "Organometallic Chemistry of Titanium, Zirconium, and Hafnium", Academic Press, New York, 1974.
20. Ref. 19. p. 151.
21. Rohl, H.; Lange, E.; Gossl, T.; and Roth, G. Angew. Chem., Int. Ed. Engl. 1962, 1, 117.
22. Ref. 19. p. 91.
23. Samuel, E. J. Organometal. Chem. 1969, 19, 87.
24. Samuel, E. Bull. Soc. Chim. Fr. 1966, 3548.
25. Breil, H. and Wilke, G. Angew. Chem., Int. Ed. Engl. 1966, 5, 898.
26. Schwartz, J. and Sadler, J. E. J. Chem. Soc. Chem. Commun. 1973, 172.
27. Kablitz, H. J. and Wilke, G. J. Organometal. Chem. 1973, 51, 241.
28. Kablitz, H. J.; Kallweit, R.; Wilke, G. J. Organometal. Chem. 1972, 44, C49.
29. Ref. 18. p. 158.
30. Yoshida, N. Masters Thesis U.C. Berkeley, 1972.
31. Greco, A.; Cesca, S.; Bertolini, G. J. Organometal. Chem. 1976, 113, 321.
32. Walker, R. unpublished results
33. Lyttle, M. Ph.D. Thesis U.C. Berkeley, 1982.
34. Preliminary experiments by Lyttle (ref. 33) also revealed the presence of a substantial isotope effect.

- 35 Lyttle, M. unpublished results
- 36 Jaffe, H. H. Chem. Rev. 1953, 53, 191.
- 37  $\sigma^{\circ}$  and  $\sigma^{\circ}$  values were derived from Wold, S., and Sjostrom, M. Correlation Analysis in Chemistry, Plenum Press: New York, 1978.
- 38 Values from Lowry, T. H. and Richardson, K. S. Mechanism and Theory in Organic Chemistry, Harper and Row: New York, 1981.
- 39 extrapolated from lower concentrations of water
- 40 Harmon, C. A.; Streitwieser, A., Jr. J. Org. Chem. 1973, 38(3), 549.
- 41 Cope, A. C.; Kinter, M. R. J. Am. Chem. Soc. 1951, 73, 3424.
- 42 DeKock, C. W.; Miller, J. T.; Brault, M.A. J. Org. Chem. 1979, 44, 3508.
- 43 Wang, Hsu-Kun: unpublished results
- 44 Glaser, R. Masters Thesis U.C. Berkeley, 1983.
- 45 Bell, R. P. Chem. Soc. Rev. 1974, 3, 513.
- 46 This assumes, of course, that the rate determining step and isotope effect are due primarily to the first protonation.
- 47 Roth, W. R. Ann. 1964, 671, 25.
- 48 Assuming they took precautions to exclude O<sub>2</sub> from the hydrolysis.
- 49 Takagi, M.; Kusabayashi, S.; Nojima, M. J. Am. Chem. Soc. 1983, 105, 4676.
- 50 Hogen-Esch, T.E.; Smid, J. J. Am. Chem. Soc. 1966, 88, 307.
- 51 Pearl, N.J. Ph.D. Thesis Univ. of Maryland, 1973.
- 52 Mole, T.; Meisters, A.; Jeffery, E. A. Aust. J. Chem. 1974, 27, 2569.
- 53 Cotton, F. A.; Rice, G. W. Inorg. Chem. 1978, 17, 2004.



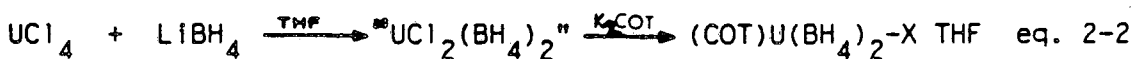
- 54 Written by Jon Swanson.
- 55 DeTar, D. F., Department of Chemistry, Florida State University, Tallahassee, FL 32306.
- 56 Parker, J.; Ladd, J. A. J. Chem. Soc., Dalton Trans. 1972, 930.
- 57 Tamao, K.; Sumitani, K.; Kiso, Y.; Zembayashi, M.; Fujioka, A.; Kumada, M. Bull. Chem. Soc. Jpn. 1976, 49, 1958.
- 58 Streitwieser, A., Jr.; Muller-Westerhoff, U. J. Am. Chem. Soc. 1968, 90, 7364.
- 59 Streitwieser, A., Jr.; Yoshida, N. J. Am. Chem. Soc. 1969, 91, 7528.
- 60 Streitwieser, A., Jr.; LeVanda, C.; Solar, J. P. J. Am. Chem. Soc. 1980, 102, 2128.
- 61 Smith, K. Ph.D. Thesis U.C. Berkeley, 1984.
- 62 Kinsley, S. Ph.D. Thesis U.C. Berkeley, 1984.
- 63 Hodgson, K. Ph.D. Thesis U.C. Berkeley, 1972.

## Chapter 2. The Preparation of ([8]Annulene)uranium Dichloride Tetrahydrofuran

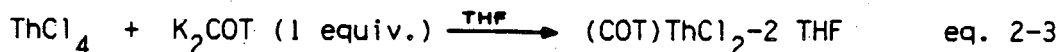
### Introduction

With the hope of furthering our understanding of the mechanism of hydrolysis of uranocene, the preparation of a mono-[8]annulene-uranium complex, or "half-sandwich", was undertaken. In addition, preparation of a uranium half-sandwich might also serve as an important precursor to a number of new species, some of them potentially catalytic.

Initial investigations of half-sandwich actinides by LeVanda<sup>1</sup> and Solar<sup>2</sup> (reviewed previously by Ken Smith<sup>3</sup>) resulted in some novel chemistry (eq. 2-1, 2-2). Unfortunately, the products themselves were incompletely characterized due apparently to loss of coordinating THF and changes in their physical properties.<sup>3</sup>



Despite these early setbacks, a number of methods were developed for the preparation of half-sandwich actinides, which were primarily successful for the thorium analog. Addition of one equivalent of  $\text{K}_2\text{COT}$  to a stirred THF suspension of  $\text{ThCl}_4$  resulted in the isolation of ([8]annulene)thorium dichloride bis-tetrahydrofuran, 1 (eq. 2-3). The structure of 1 as determined by



x-ray diffraction analysis is depicted in figure 2-1. If the 10  $\pi$ -electron, [8]annulene ring is given a formal coordination number of 5, then a dichloride complex is 7-coordinate. A 7-coordinate complex is sterically unsaturated, thus two additional solvent molecules are required to saturate the compound.

Since addition of one equivalent of the dianion to  $\text{ThCl}_4$  is successful in preparing a half-sandwich thorium complex, the same type of methodology was applied to attempt a preparation of the uranium analog. Unfortunately, the investigators,<sup>2,3</sup> despite using a wide variety of reaction conditions and complexing agents (TMEDA, DME), were unsuccessful in isolating any mono-[8]annulene uranium products. In his dissertation,<sup>3</sup> Ken Smith mentions that the reaction of  $[\text{UCl}_3\text{-(tmeda)}_2]_n$  with excess  $\text{K}_2\text{COT}$  produced an unstable red-brown compound whose  $^1\text{H}$  NMR consisted of two resonances in the "COT region" (-30 to -40 ppm). The resonance at -36 ppm was assigned to uranocene, while the peak slightly downfield of the uranocene resonance was assigned to the reduced uranocene,  $\text{K}(\text{COT})_2\text{U}$ . The red-brown solid isolated was unstable, yielding uranocene with time.

The second type of method used to prepare the thorium half-sandwich is a simple redistribution process between  $\text{ThCl}_4$  and thorocene, first reported by LeVanda (eq. 2-4).<sup>1</sup> However,

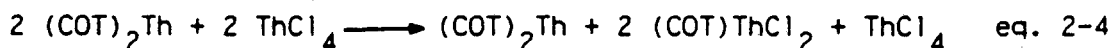
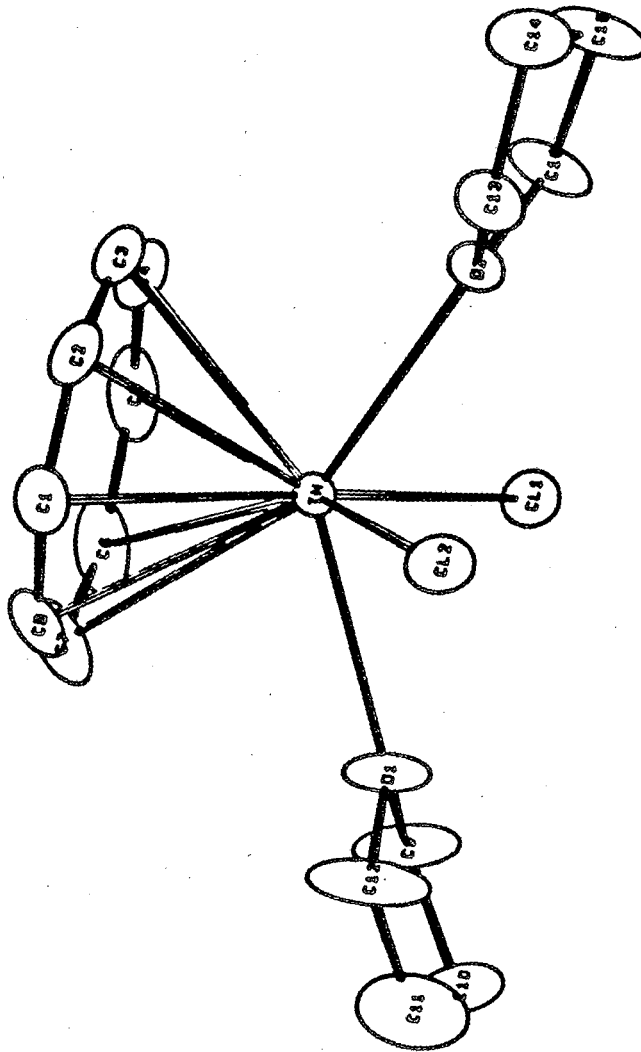
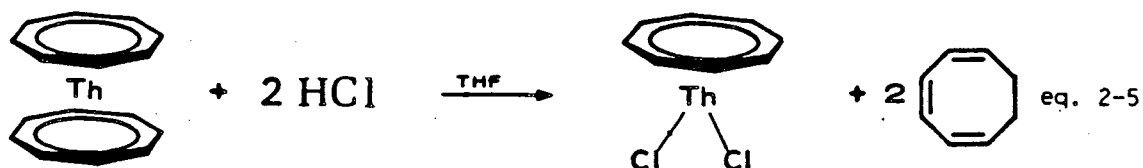


Figure 2-1: Crystal Structure of  $(\text{COT})\text{ThCl}_2 \cdot 2 \text{ THF}$  1



despite a report by LeVanda<sup>1</sup> that a redistribution reaction was observed for  $\text{UCl}_4$  and  $(n\text{-BuCOT})_2\text{U}$  by heating them at reflux in THF for prolonged times, the products were never completely characterized. Ken Smith<sup>3</sup> attempted redistribution by heating a mixture of  $\text{K}_2\text{COT}$  and one equivalent of  $\text{UCl}_4$ . The purple solid isolated had two resonances by  $^1\text{H}$  NMR at 28 °C, one at -36.4 ppm, assigned to uranocene and one at -32.1 ppm with a peak width at half-height of 20 Hz, believed to be  $\text{K}(\text{COT})_2\text{U}$ . The same resonance at -32.1 ppm was observed when equimolar amounts of uranocene and  $\text{UCl}_4$  were refluxed for 48 hr.<sup>3</sup> The redistribution reaction to prepare the uranium half-sandwich, thus appeared to be unsuccessful.

The final method used in the preparation of the thorium half-sandwich involves protonation of a single ring of thorocene to liberate cyclooctatriene and the [8]annulenethorium dichloride complex (eq. 2-5).<sup>1</sup> Addition of two equivalents of HCl to



$(n\text{-BuCOT})_2\text{U}$  also was reported to have resulted in a half-sandwich complex,  $(n\text{-BuCOT})\text{UCl}_2$ ,<sup>2</sup> although solutions of the isolated solid were reported as being unstable.<sup>4</sup> The investigator was able to obtain a suitable  $^1\text{H}$  NMR of the solid (Table 2-1), which was found to exhibit a resonance pattern markedly different from that

of the analogous uranocene. In particular, the single proton opposite the ring from the substituent (H5) has its resonance shifted much further (>10 ppm) downfield from the H5 proton in *n*-butyluranocene. Although no suitable elemental analysis of the material was obtained, the preparation remained, until the present investigation, the best evidence for the existence

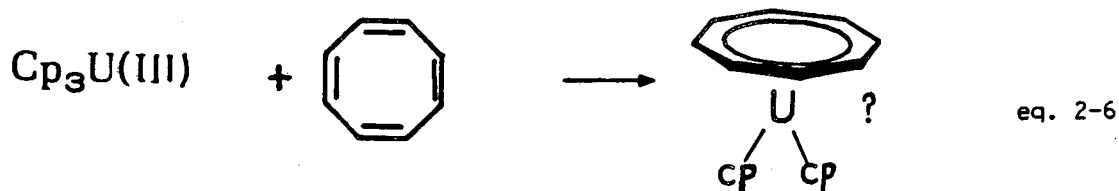
Table 2-1:  $^1\text{H}$  NMR Chemical Shifts of the Ring Protons of the (*n*-Butyl-[8]annulene)uranium Complexes

<u>Compound</u>	<u>Chemical Shifts</u>
( <i>n</i> -BuCOT)UCl <sub>2</sub>	-33.0, -44.7, -29.0, -21.5 (H5)
( <i>n</i> -BuCOT) <sub>2</sub> U	-36.22, -39.74, -32.64, -34.1 (H5)

of the complex ([8]annulene)uranium dichloride. For this reason, initial investigations by myself concentrated on reactions which would protonate one of the rings of uranocene with a sterically hindered reagent in order to isolate a half-sandwich uranium product.

While these experiments were commencing, however, other investigators<sup>5,6</sup> obtained results which would lead this chemistry in a new and interesting direction. Steve Kinsley had found that when COT is added to a red suspension of UCl<sub>3</sub> in THF and stirred overnight, the reaction turns green and the presence of UCl<sub>4</sub> is detected by visible spectroscopy. Unfortunately, the reaction was not investigated further. A few months later, John Brennan<sup>6</sup> found that the addition of cyclooctatetraene to tris-

cyclopentadienyluranium(III) resulted in a complex whose crude  $^1\text{H}$  NMR suggests the presence of a cyclooctatetraene-bound uranium complex (eq. 2-6). It thus appeared as if some sort of electron transfer process is taking place between uranium(III) and the ligand. Thus, the decision was made to investigate the reaction in the hopes of isolating a half-sandwich uranium complex.



### Results: Preparation of the Half-Sandwich

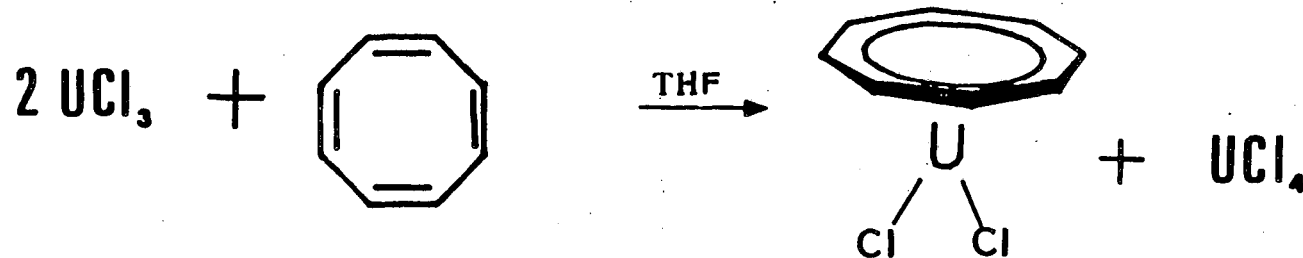
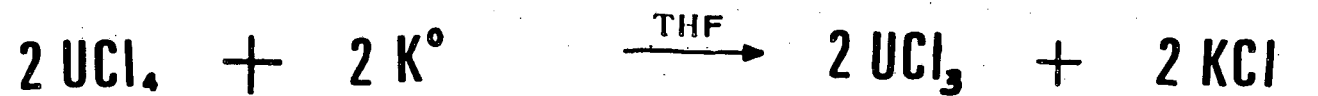
As was mentioned above, the initial attempts to isolate the half-sandwich complex concentrated on the protonation reaction. A half-sandwich complex which contained sterically bulky alkoxy or phenoxy groups might hinder further attack by a protic reagent. Earlier efforts<sup>3</sup> had determined that no reaction would occur between a sterically bulky alcohol such as *t*-butanol (see also Table 1-8); thus a reaction between uranocene and thiophenol

was carried out. It was believed that the sulfur might provide soft-base stabilization for the half-sandwich complex, while the phenyl group would provide the steric hindrance desired. Unfortunately, the addition of two equivalents of thiophenol to one equivalent of di-(*t*-butoxycarbonyl)uranocene resulted in the recovery of a tetrathiophenoxy uranium complex, substituted cyclooctatrienes, and unreacted starting materials. Apparently, the thiophenol was protonating the half-sandwich faster than it protonates the full complex.

It was at this point that the results of Kinsley<sup>5</sup> and Brennan<sup>6</sup> were presented. Since the protonation reactions had failed to be productive, an entirely new approach involving an electron transfer reaction seemed both aesthetically appealing and sensible enough to attempt. Thus, reducing a green solution of  $UCl_4$  in THF with potassium resulted in a red THF suspension of  $UCl_3$ . Addition of cyclooctatetraene to the  $UCl_3$  gradually turned the red suspension back to green, which, when confirmed by visible spectroscopy, indicated the presence of  $UCl_4$  (Figure 2-2). The net result is, therefore, electron transfer from two equivalents of uranium(III) to one equivalent of cyclooctatetraene with formation of  $UCl_4$  and a cyclooctatetraene complex postulated to be a half-sandwich compound. A  $^1H$  NMR (Figure 2-3) of the mixture confirms the presence of an [8]annuleneuranium complex by the singlet present at  $-31.6$  ppm ( $30^\circ C$ ). Uranocene has a singlet at  $-35.9$  ppm ( $30^\circ C$ ) in the  $^1H$  NMR which is much broader (90 Hz) than the relatively sharp singlet (20 Hz) of the uranium(IV) half-sandwich complex.



Figure 2-2: Reactions Used In the Preparation of  
the Uranium Half-Sandwich



OR

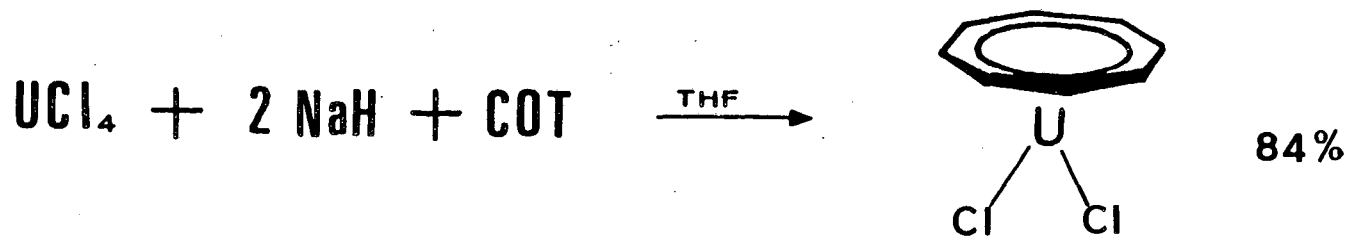
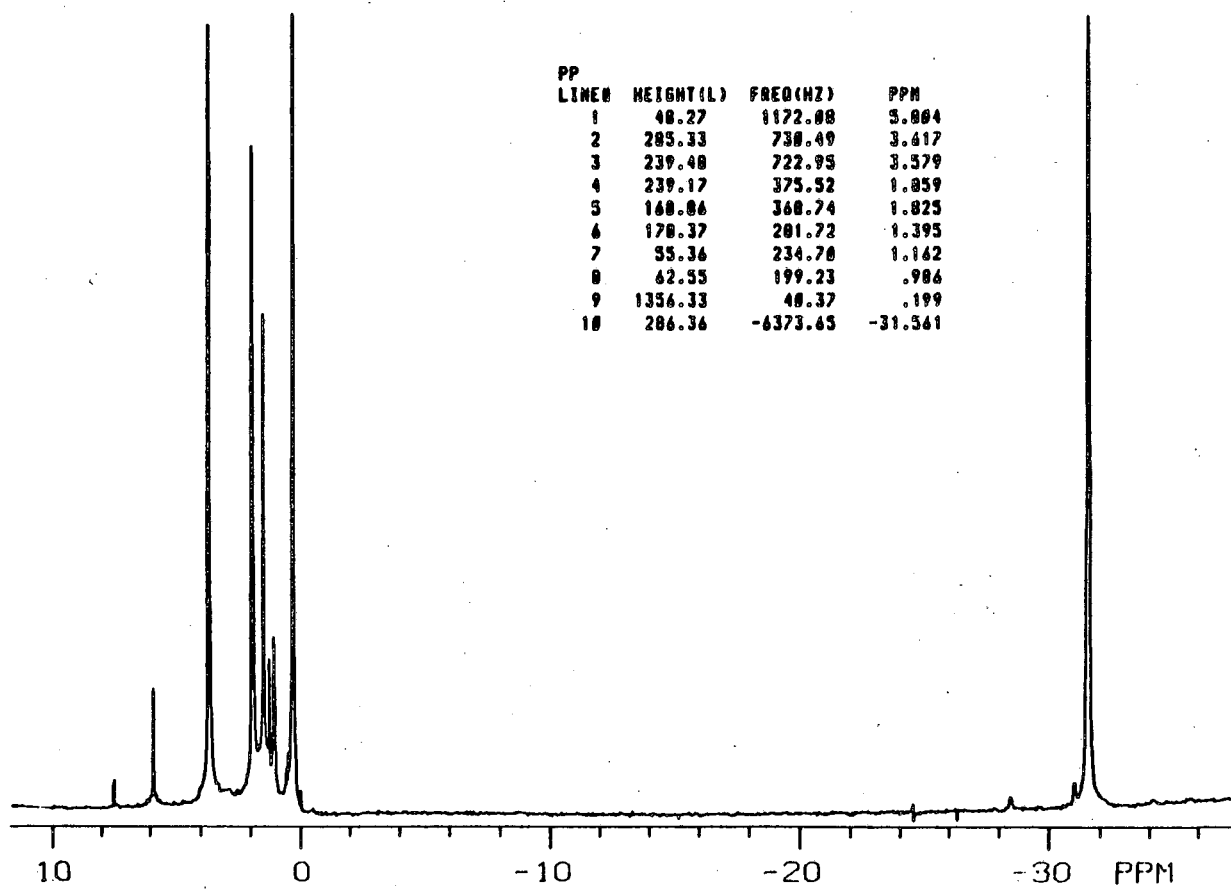


Figure 2-3:  $^1\text{H}$  NMR of  $(\text{COT})\text{UCl}_2 \cdot 2 \text{ THF}$  at  $30^\circ\text{C}$  in  $\text{THF-d}_8$



Unfortunately, efforts to separate the complex from  $UCl_4$  proved to be difficult due, primarily, to the similar solubility properties. Both species are soluble in THF and only slightly soluble in hydrocarbon solvents. Thus, slow crystallizations resulted only in the recovery of mixtures of the two complexes.

What was needed was a method to convert all the  $UCl_4$  being formed into half-sandwich. In order to do this, excess reducing agent could be added to re-convert the  $UCl_4$  to  $UCl_3$ . Unfortunately, if excess potassium is added, conversion of cyclooctatetraene to its dianion would also take place, which would add to the half-sandwich and form unwanted uranocene. Thus, a reducing agent was required which could carry out the uranium reduction, but would not reduce the cyclooctatetraene to the dianion. That reducing agent turned out to be sodium hydride. To one equivalent of  $UCl_4$  and 2.2 equivalents of NaH suspended in THF was added one equivalent of cyclooctatetraene. Since the reaction was primarily a surface reaction, the mixture was stirred at least 18 hr. The majority of the recovered organometallic material is the desired ([8]annulene)uranium dichloride.

The complex can be purified by washing out any remaining  $UCl_4$ -THF complex with toluene. An even more efficient purification method is to prepare the  $UCl_4$ -TMEDA complex, which is hexane soluble, by stirring the mixture of starting material and product with excess TMEDA (tetramethylethylenediamine) at room temperature. The half-sandwich complex does not appear to form a TMEDA complex under these conditions.

Once the purified half-sandwich complex was obtained, further characterization could be undertaken. A large amount of structural information was obtained from the infrared spectrum. Comparison of the absorbances in the infrared spectrum of the uranium half-sandwich with the absorbances of the known thorium half-sandwich (Table 2-2) demonstrates that the two compounds are structurally similar.

Table 2-2: Observed IR Frequencies For (COT)MCL<sub>2</sub>-2THF (in cm<sup>-1</sup>)

<u>(COT)UCl<sub>2</sub>-2THF</u>	<u>(COT)ThCl<sub>2</sub>-2THF</u>
1340	1342
1259	1260
1163	
1070	
1032(shoulder)	1039
1008(s)	1010(s)
920	907
900	900
840(s)	852(s)
805(s)	835(s)
720(s)	729(s)
660	668

(s)=strong

all samples are nujol mulls

Since the infrared spectrum suggests that the two compounds are structurally similar, it would be informative to obtain a crystal structure of the uranium half-sandwich in order to make a comparison of the metal-ligand bond distances between it and its thorium analog. Unfortunately, the uranium complex apparently desolvates upon removal of THF. The red crystalline solid that remains after initial removal of the solid is transformed into a green powder in a matter of minutes under an argon atmosphere. An x-ray powder pattern (Table 2-3) of the green powder demonstrates that it is not isostructural with the thorium half-sandwich. The similar infrared spectra were possible because of rapid mill preparation. Also, the coordinated THF molecules do not affect the infrared spectrum (which is influenced by strongly bonded ligands) as much as they would affect an x-ray pattern. Thus, without an x-ray structure we can only assume from the thorium half-sandwich structure and the IR spectra, that two THF molecules also coordinate to uranium.

The visible spectrum of [8]annuleneuranium dichloride is shown in Figure 2-4. Uranocene has a distinct cascade of absorbances between 600 and 700 nm. The uranium half-sandwich, on the other hand, is of much lower symmetry.<sup>8</sup> The lower symmetry means there will be a breakdown in the forbiddenness of a number of the transitions resulting in a general broad absorbance for the compound.

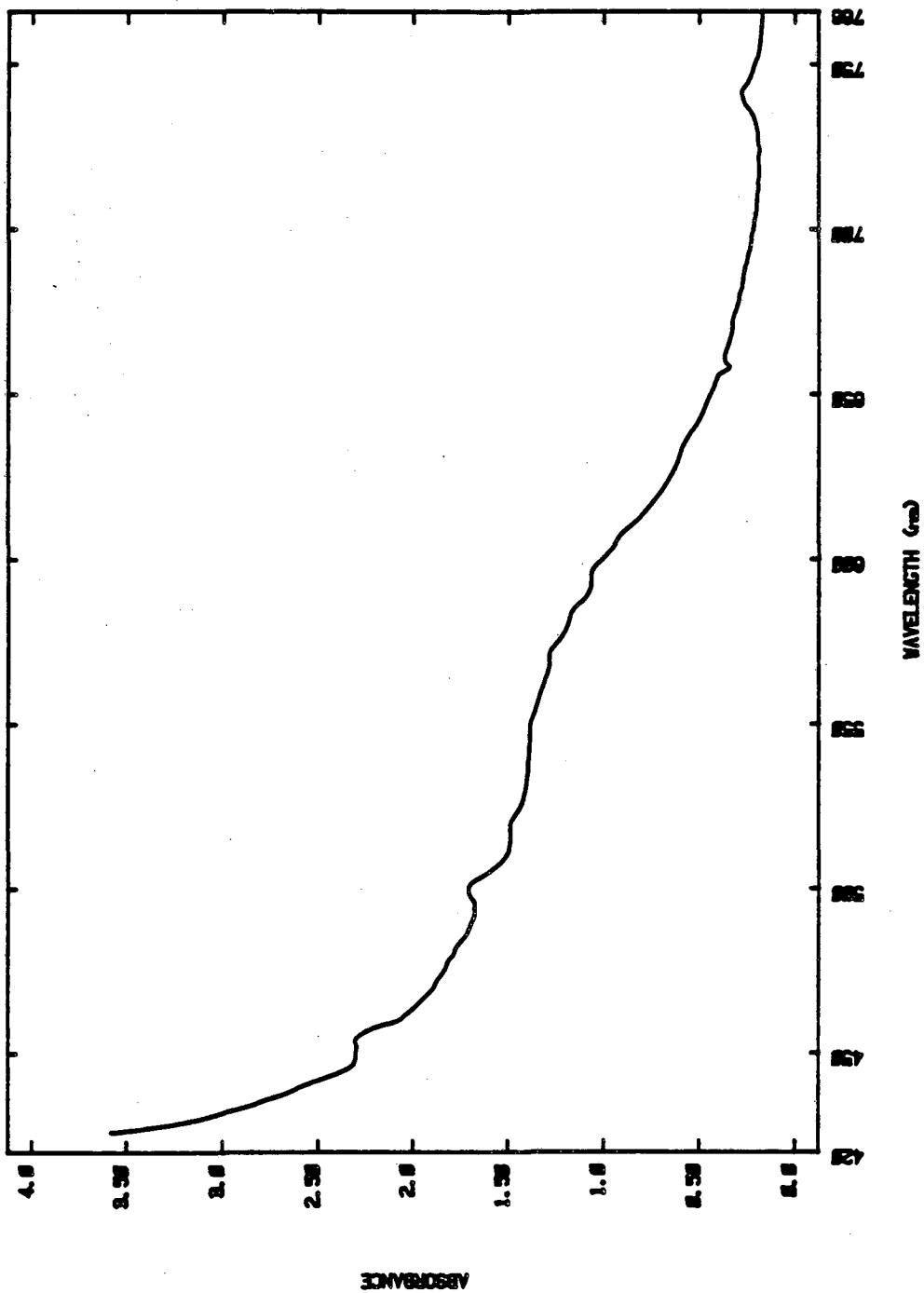
Table 2-3: X-Ray Powder Pattern Data on (COT)MCl<sub>2</sub>-X THF

(COT)UCl <sub>2</sub>		(COT)ThCl <sub>2</sub>	
d(A)	I <sup>a</sup>	d(A)	I <sup>a</sup>
11.37	s-	11.53	w+
		8.49	m+
		7.53	m
		6.49	m
		6.17	m
		5.86	m
		5.22	w+
4.30	w	4.59	w-
		3.93	w
3.15	m		
2.81	w	2.88	w
2.73	w-	2.64	w-
2.00	w-	2.21	w-
1.93	m-	1.92	w-
1.65	m		
1.26	w-		
1.22	w-		
0.773 <sup>b</sup>	w+	0.773 <sup>b</sup>	w

a Estimated relative intensity

b Back reflection

Figure 2-4: Visible Spectrum of (COT)UCI<sub>2</sub>-2 THF in THF

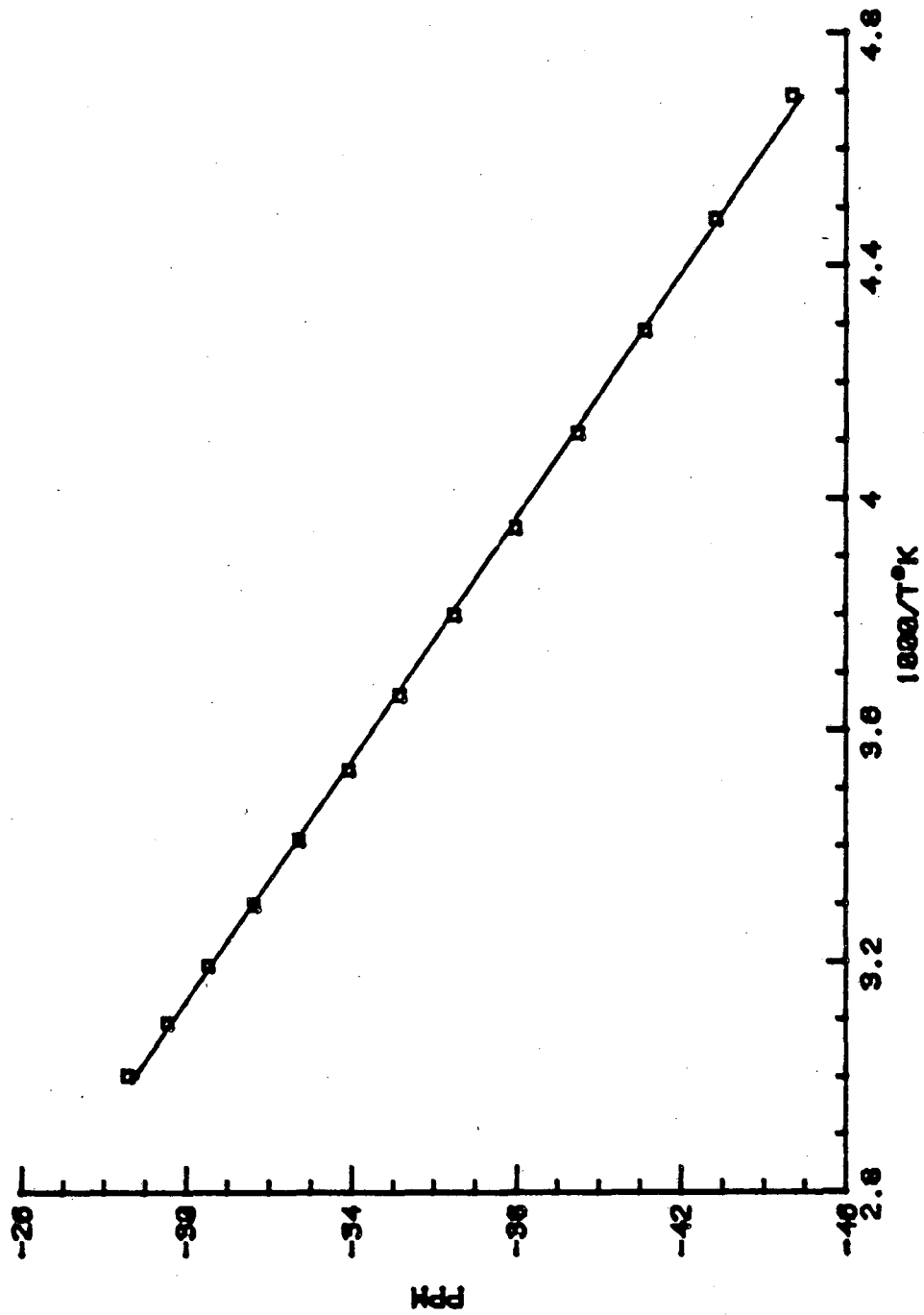


Unfortunately, elemental analyses for the purified complex were poor. In general, they suffered from the same problem that has plagued other highly air-sensitive compounds; low carbon contents.<sup>9,10</sup> In one analysis of the uranium half-sandwich, the hydrogen and chlorine contents were respectable, but the carbon content was still almost four percent away from the calculated value (see experimental section).

Finally, a variable temperature  $^1\text{H}$  NMR indicates there are no dynamic processes occurring on the  $^1\text{H}$  NMR time scale with the THF solvated half-sandwich complex. A plot of chemical shifts versus inverse temperature is strictly linear (exhibits approximate Curie-Weiss behavior) over the temperature range studied ( $-60\text{ }^\circ\text{C}$  to  $+60\text{ }^\circ\text{C}$ ) (Figure 2-5). Its slope is determined as  $-9,556$ , which is lower than the slope determined for uranocene (slope =  $-12,940$ ).<sup>7</sup> The steeper slope for uranocene could be due to a shorter metal to ring bond distance than in the half-sandwich. This is assuming that the difference is due to the through-space (pseudo-contact shift)<sup>7,11</sup> interaction, rather than a through-bond interaction (contact shift).<sup>7</sup> However, without a crystal structure of a uranium half-sandwich complex it is difficult to determine the precise reason for the differences in their slopes. The y-intercept is near zero ( $-0.1\text{ ppm}$ ), in accordance with the prediction by theory.<sup>7</sup>



Figure 2-5: Plot of Chemical Shift vs. Inverse Temperature  
for  $(\text{COT})\text{UCl}_2 \cdot 2 \text{ THF}$



### Preparation of a Substituted Uranium Half-Sandwich

Despite the successful preparation of ([8]annulene)uranium dichloride bistetrahydrofuran, the limited solubility in hydrocarbon solvents might hinder the reaction chemistry that could be undertaken. Thus, an attempt was made to prepare a substituted half-sandwich that might demonstrate greater solubility in aromatic and aliphatic hydrocarbon solvents.

One of the best substituted cyclooctatetraenes to use in an organometallic complex, based on the solubility properties of its respective uranocene and on its ease of preparation<sup>12</sup>, is *n*-butylcyclooctatetraene. Unfortunately, when an excess of sodium hydride was added to a stirred solution of  $UCl_4$  and *n*-butylcyclooctatetraene in THF and stirred for almost three days at room temperature, no reaction resulted. Perhaps under these conditions, no electron transfer takes place between  $UCl_3$  and *n*-butylcyclooctatetraene. This was confirmed by stirring  $UCl_3$  (prepared by the reduction of  $UCl_4$  with potassium) with *n*-butylcyclooctatetraene. After three days, the only organometallic product which had formed was a trace amount of *n*-butyluranocene. As Table 2-4 indicates,<sup>13</sup> alkyl groups raise the reduction potential of cyclooctatetraenes, thus electron transfer from uranium(III) to the ligand becomes more difficult.

The next attempt at a substituted half-sandwich was made with a cyclooctatetraene containing an electron-withdrawing substituent which would lower the reduction potential, and

Table 2-4: CV Reduction Potentials of Cyclooctatetraenes in DMF<sup>13</sup>

Compound	E1/2	E2/2
COT	-1.65V	-1.89V
ethylCOT	-1.76V	-1.96V
<u>n</u> -butylCOT	-1.79V	-1.96V
<u>t</u> -butylCOT	-1.90V	-2.03V
methoxyCOT	-1.76V	-1.94V
phenylCOT	-1.64V	-1.74V
benzyl ester of COT	-1.26V	-1.58V
<u>t</u> -butyl ester of COT	-1.34V	-1.65V
1,3,5,7-tetramethylCOT	-2.11V (2e)	-
1,3,5,7-tetra- <u>t</u> -butylCOT	(*)	-
naphthalene	-2.46V	-

(\*)-reduction potential not observed

therefore, facilitate electron transfer to the ligand. The ligand of choice was the previously prepared,<sup>14</sup> highly electron-withdrawing ligand, m-fluorophenylcyclooctatetraene. The presence of the phenyl group should also result in greater solubility in toluene for the uranium complex.

When an excess of sodium hydride was added to  $UCl_4$  and m-fluorophenylcyclooctatetraene in THF, the green solution turned red within an hour, indicating the presence of the half-sandwich complex. After stirring for six more hours to ensure completion, a red solid was recovered which, by  $^1H$  NMR spectroscopy, was demonstrated to be the desired substituted uranium half-sandwich.

The  $^1\text{H}$  NMR spectrum of the compound is interesting because the [8]annulene absorbances follow the same pattern reported by Solar<sup>2</sup> (Table 2-5) for the ( $n$ -butyl-[8]annulene)uranium dichloride. Although the compound was found to be only sparingly soluble in toluene, the synthesis does demonstrate the feasibility of the preparation of substituted uranium half-sandwich complexes.

Table 2-5: Chemical Shifts of the [8]Annulene Protons  
of Substituted Half-Sandwich Complexes

---

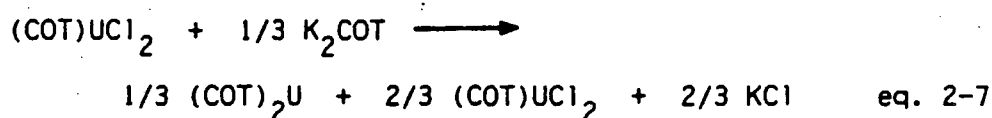
$(n\text{-BuCOT})\text{UCl}_2$ <sup>2</sup>	-33.0, -44.7, -29.0, -21.5 (H5)
$(m\text{-FPhCOT})\text{UCl}_2$	-33.1, -33.9, -30.9, -23.9 (H5)

### Reactions of the Uranium Half-Sandwich

Some reactions of ([8]annulene)uranium dichloride were carried out to begin an investigation into the interesting chemistry which the complex might demonstrate. The preliminary goals of this research were to establish that first, replacement of the chloride ligands could occur both easily and cleanly,

and second, that reaction with alkyl anions would result in stable uranium-carbon sigma-bonded complexes. Recent work by Marks<sup>15</sup> would indicate that both of these goals are feasible, although the differences between the reaction chemistry of the half-sandwich and the uranium complexes of Marks are bound to result in interesting comparisons.

Initially, displacement of the chlorides was carried out simply by adding cyclooctatetraene dianion to an excess of the half-sandwich (eq. 2-7). Certainly it is not the most efficient way of preparing uranocene, but what it did prove was that ligand addition to uranium can occur a single ring at a time, with no

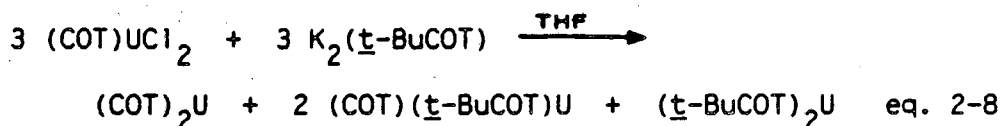


inherent stability problems with the half-sandwich, except when in the presence of cyclooctatetraene dianion. What was also demonstrated was the lack of ligand exchange between uranocene and the half-sandwich in THF-d<sub>8</sub> solution on the <sup>1</sup>H NMR time scale. When a <sup>1</sup>H NMR spectrum is obtained on a mixture of uranocene and the half-sandwich, both peaks are clearly observed at 30 °C (-35.9 ppm for uranocene, -31.6 ppm for the half-sandwich), with no signs of peak broadening.

A practical application of the addition of cyclooctatetraene dianion to the half-sandwich, would be the preparation of a mixed uranocene in good yield. Previously, mixed uranocene preparation required the simultaneous addition of the two different cyclooctatetraene dianions to UCl<sub>4</sub>, followed by difficult isolation and

separation techniques (for example, see Chapter 1). But by adding, for example, t-butylcyclooctatetraene to the unsubstituted half-sandwich, it might be possible to isolate pure mono-t-butyluranocene.

Unfortunately, the addition of one equivalent of t-butylcyclooctatetraene dianion to a solution of ([8]annulene)-uranium dichloride in THF resulted in a statistical mixture of the unsubstituted uranocene, mono-t-butyluranocene, and di-t-butyluranocene (23%, 53%, and 24%, respectively) (eq. 2-8). Apparently, ligand exchange catalyzed by the presence of cyclooctatetraene dianion occurs more rapidly than simple addition of the ligand to uranium. Thus, preparation of a mixed uranocene by this method does not appear to be as straightforward as it was hoped.



The second phase of the reaction chemistry of the uranium half-sandwich has not yielded any immediate successes. Addition of two equivalents of methyllithium to one equivalent of the half-sandwich in THF resulted only in decomposed materials. Apparently, the methyllithium is too harsh a methylating reagent for the complex.

If lithium reagents are too reactive, then perhaps a milder alkylating reagent, such as benzylmagnesium chloride, might result in a uranium- $\sigma$ -carbon complex. Addition of two equivalents of the Grignard reagent to one equivalent of the

half-sandwich at low temperature resulted in a complex whose  $^1\text{H}$  NMR suggested the presence of an  $\eta^3$ -bound benzyl group, similar to the thorium complexes postulated by Ken Smith (Figure 2-6).<sup>3</sup> Unfortunately, further manipulation of the crude material resulted in decomposition of the complex. The same difficulties were encountered previously in the dibenzylthorium half-sandwich<sup>3</sup> and might be due to thermal stability problems, although further work in this area is necessary.

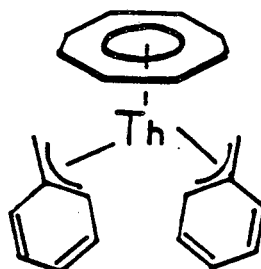


Figure 2-6: ([8]Annulene)thorium- $\eta^3$ -Dibenzyl

Since there appeared to be problems with the reaction chemistry of the THF solvated half-sandwich, a better coordinating reagent ( $\text{PMe}_3$ ) was complexed to the uranium with the hope that it might eventually result in better behaved chemistry from the ([8]annulene)uranium complexes. When trimethylphosphine ( $\text{PMe}_3$ ) was vacuum transferred onto a THF solution of the uranium half-sandwich a precipitate gradually formed overnight. The precipitate was filtered from the solution, and from the dark red

solution a red solid was isolated whose  $^1\text{H}$  NMR spectrum is shown in figure 2-7. The two relevant peaks in the spectrum (at  $-28.7$  ppm and  $-0.1$  ppm) integrate to a ratio of 8 to 9, respectively. This is consistent with a trimethylphosphine adduct of the uranium half-sandwich.

What is particularly interesting about the complex's behavior in the  $^1\text{H}$  NMR occurs at lower temperatures. As the probe was cooled below  $+60$  °C, the peak at  $-0.1$  ppm (attributed to  $\text{PMe}_3$ ) broadened until it was obscured by the baseline at  $5$  °C. At  $0$  °C, two peaks reappeared (Figure 2-8), one further upfield at approximately  $-4$  ppm, and one downfield at  $+1.25$  ppm (broad peak underneath solvent peaks). As the sample was cooled further to  $-40$  °C, the peaks narrowed as they approached the slow exchange limit (Figure 2-9). The upfield resonance at  $-5$  ppm ( $-40$  °C) follows approximate Curie-Weiss behavior and can be attributed to complexed  $\text{PMe}_3$ , while the chemical shift values for the free  $\text{PMe}_3$  peak at  $+1.25$  ppm remain constant with varying temperature. At higher temperatures ( $+10$  °C to  $+70$  °C), the average resonance signal for the rapidly exchanging  $\text{PMe}_3$  was observed.

Much further upfield from the  $\text{PMe}_3$  peaks, are the resonances attributed to the protons of the [8]annulene ring. Only a single peak was detected at temperatures above  $0$  °C, but as the probe was cooled, this peak also broadened and coalesced. At temperatures below  $-10$  °C, two major peaks were observed. One peak is assigned to the [8]annulene ring protons of the  $\text{PMe}_3$  complex,



Figure 2-7:  $^1\text{H}$  NMR of ([8]Annulene)uranium Dichloride  
Trimethylphosphine in  $\text{THF-d}_8$  at  $+60^\circ\text{C}$

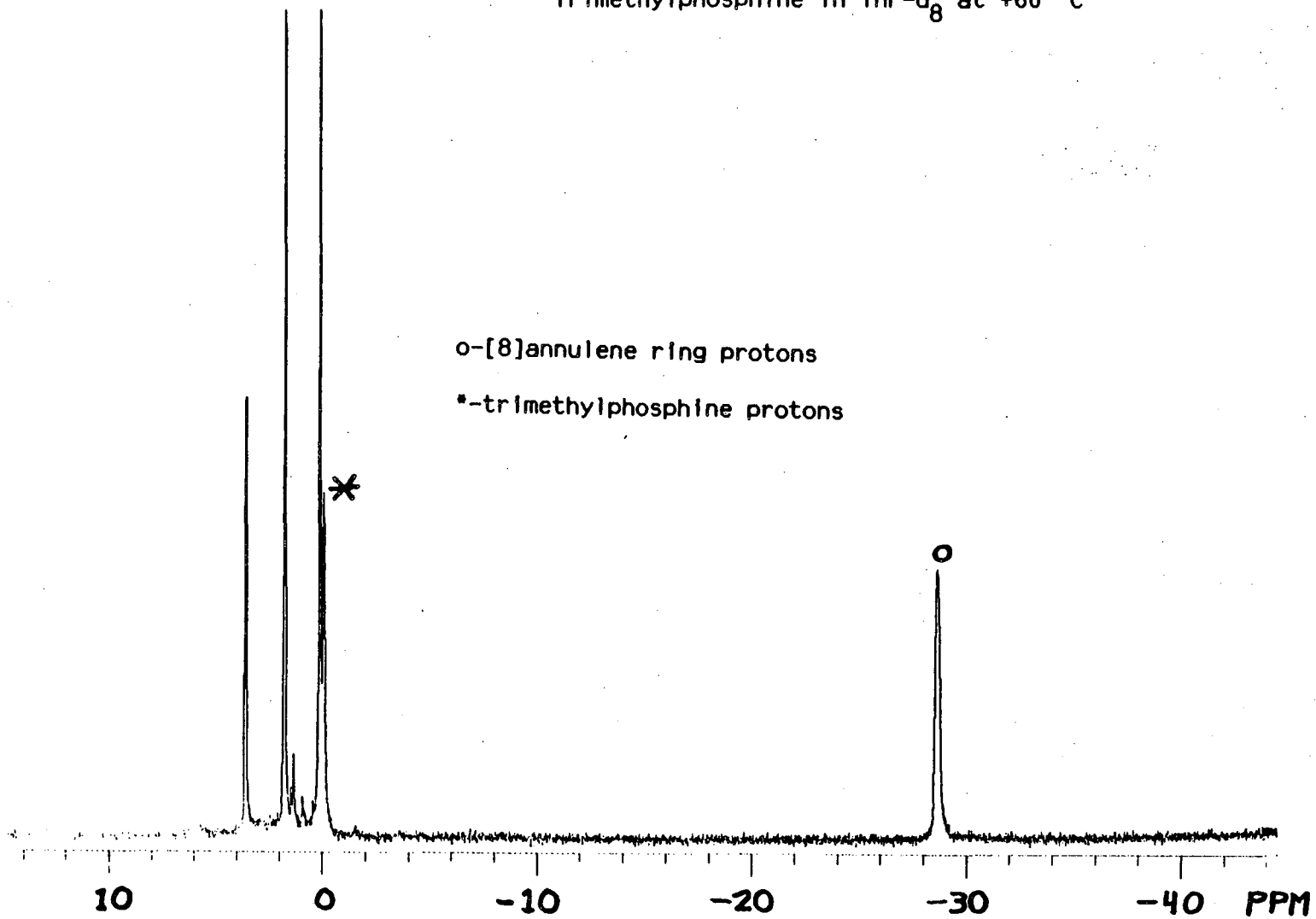


Figure 2-8:  $^1\text{H}$  NMR of ([8]Annulene)uranium Dichloride  
Trimethylphosphine in  $\text{THF-d}_8$  at  $0^\circ\text{C}$

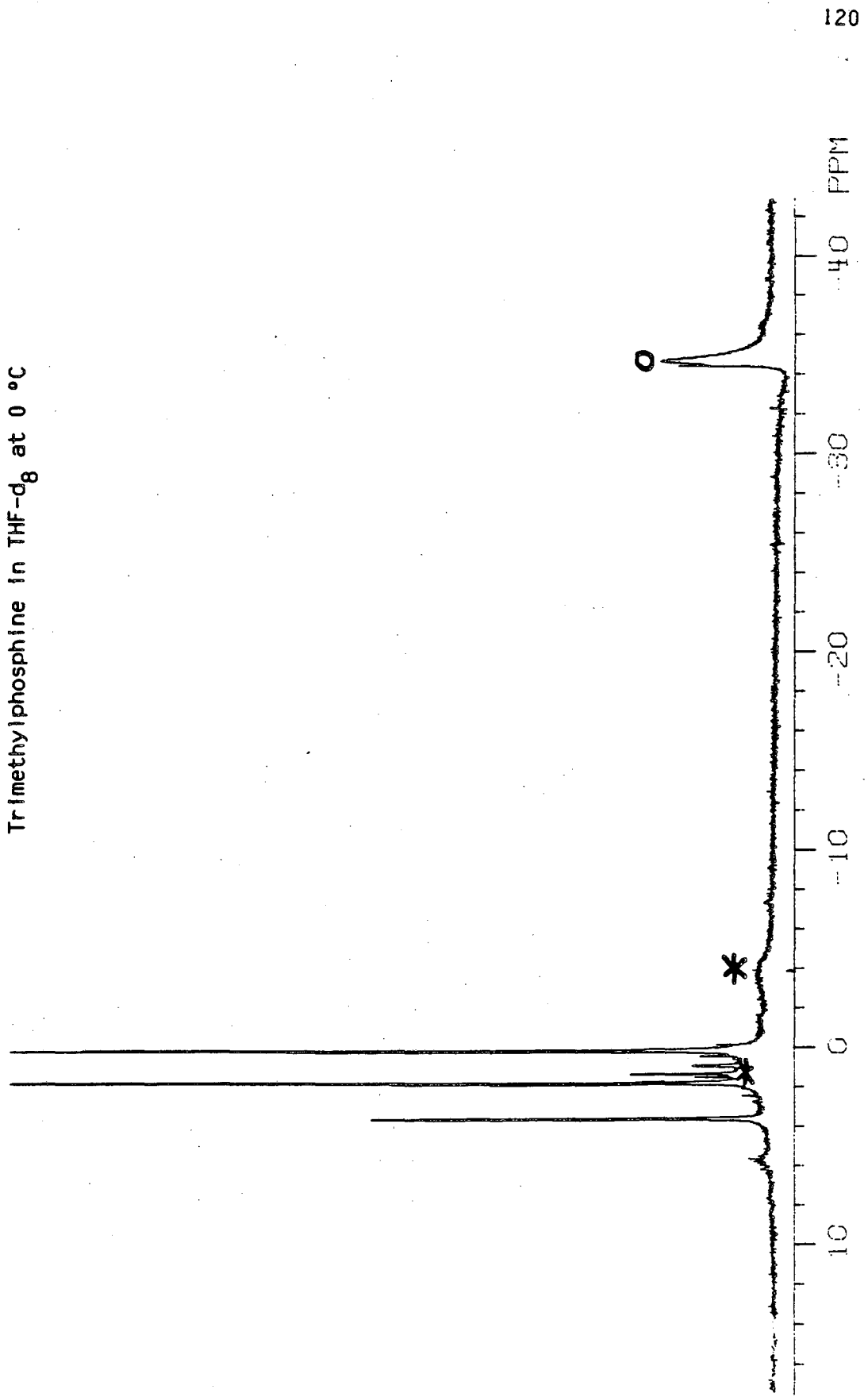
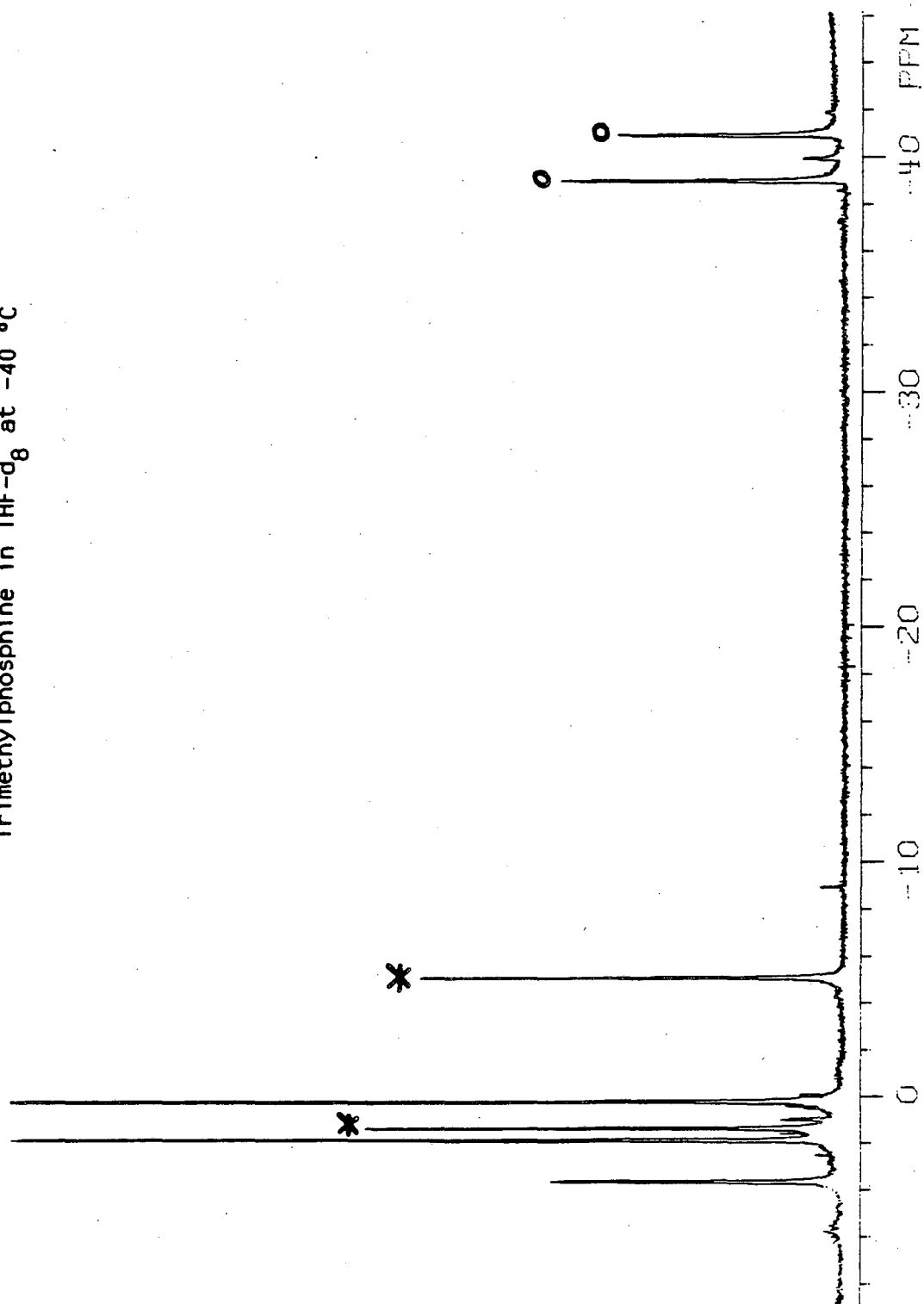


Figure 2-9:  $^1\text{H}$  NMR of ([8]Annulene)uranium Dichloride  
Trimethylphosphine in  $\text{THF-d}_8$  at  $-40^\circ\text{C}$



while the other peak is assigned to the [8]annulene protons of the THF solvated half-sandwich complex. Chemical shift values for the latter peak (from  $-10\text{ }^{\circ}\text{C}$  to  $-60\text{ }^{\circ}\text{C}$ ) correspond to those of the known ([8]annulene)uranium dichloride bistetrahydrofuran complex (within 0.2 ppm). The slope of the line from a plot of chemical shift versus inverse temperature is virtually identical with the slope from figure 2-5.

If we estimate the coalescence temperature of the  $\text{PMe}_3$  to be  $+5 \pm 3\text{ }^{\circ}\text{C}$ , then by use of the approximate formula in equations 2-9 and 2-10 ( $\Delta\nu=1016\text{ Hz}$ ), we can determine the free energy of activation for exchange between free and complexed  $\text{PMe}_3$  to be  $11.9 \pm 0.2\text{ kcal/mol}$ .

$$k = 2^{-0.5} \pi \Delta\nu \quad \text{eq. 2-9}$$

$$-\Delta G^{\ddagger} = RT \ln(kh/Kk_{\text{B}}T) \quad \text{eq. 2-10}$$

Activation parameters for the exchange process can also be determined by computer simulated line-shape analysis of the broadened exchange peaks. By inputting frequency values for non-exchanging peaks, along with natural line widths, and best fitting the computer generated curve for specific mean nuclei lifetimes ( $\tau$ ) to the actual nmr peak,  $\tau$  values for a series of temperatures were determined (Figure 2-10). Converting the  $\tau$  values to rate constants and plotting against inverse temperature (Figure 2-11) results in the following activation parameters for this temperature range:

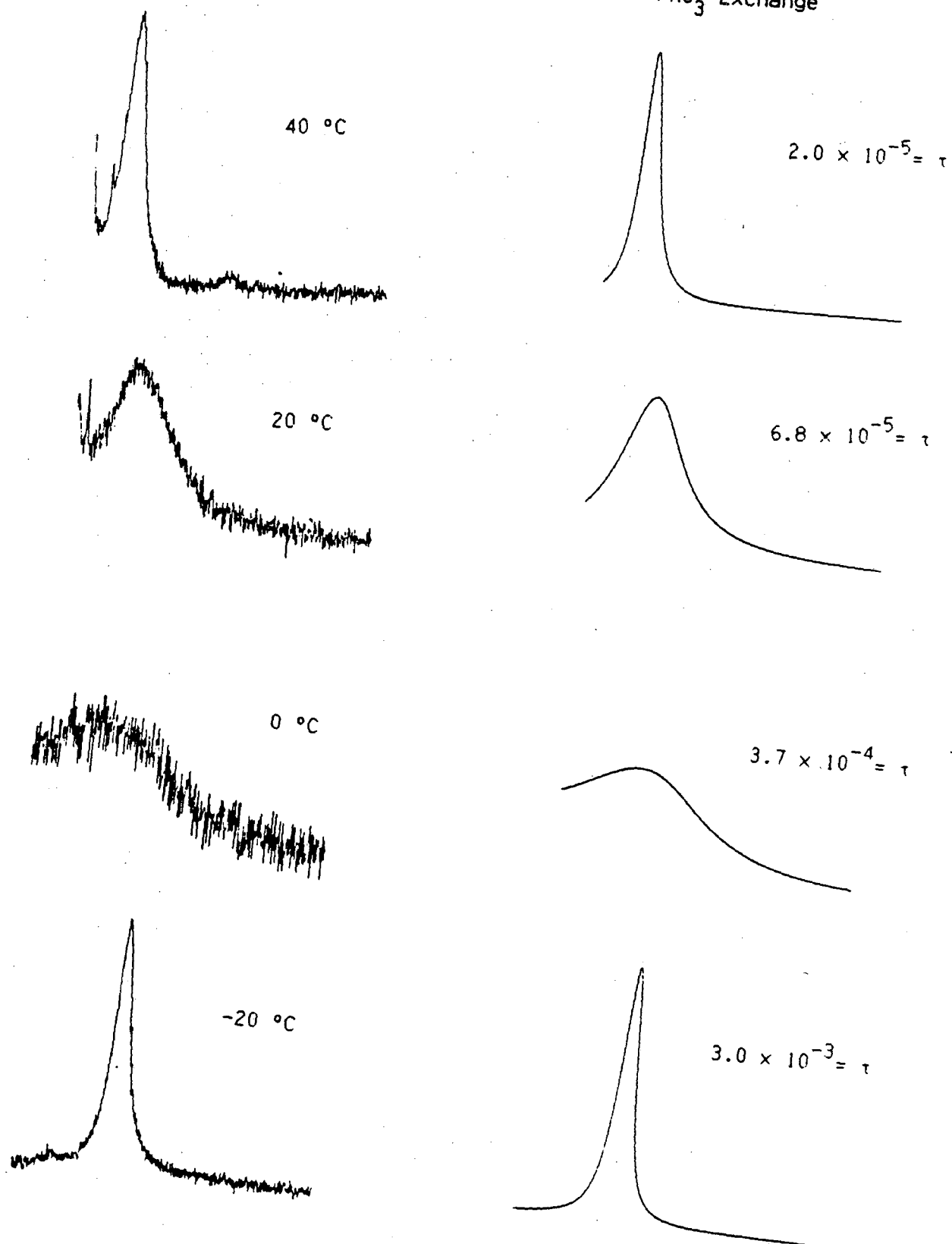
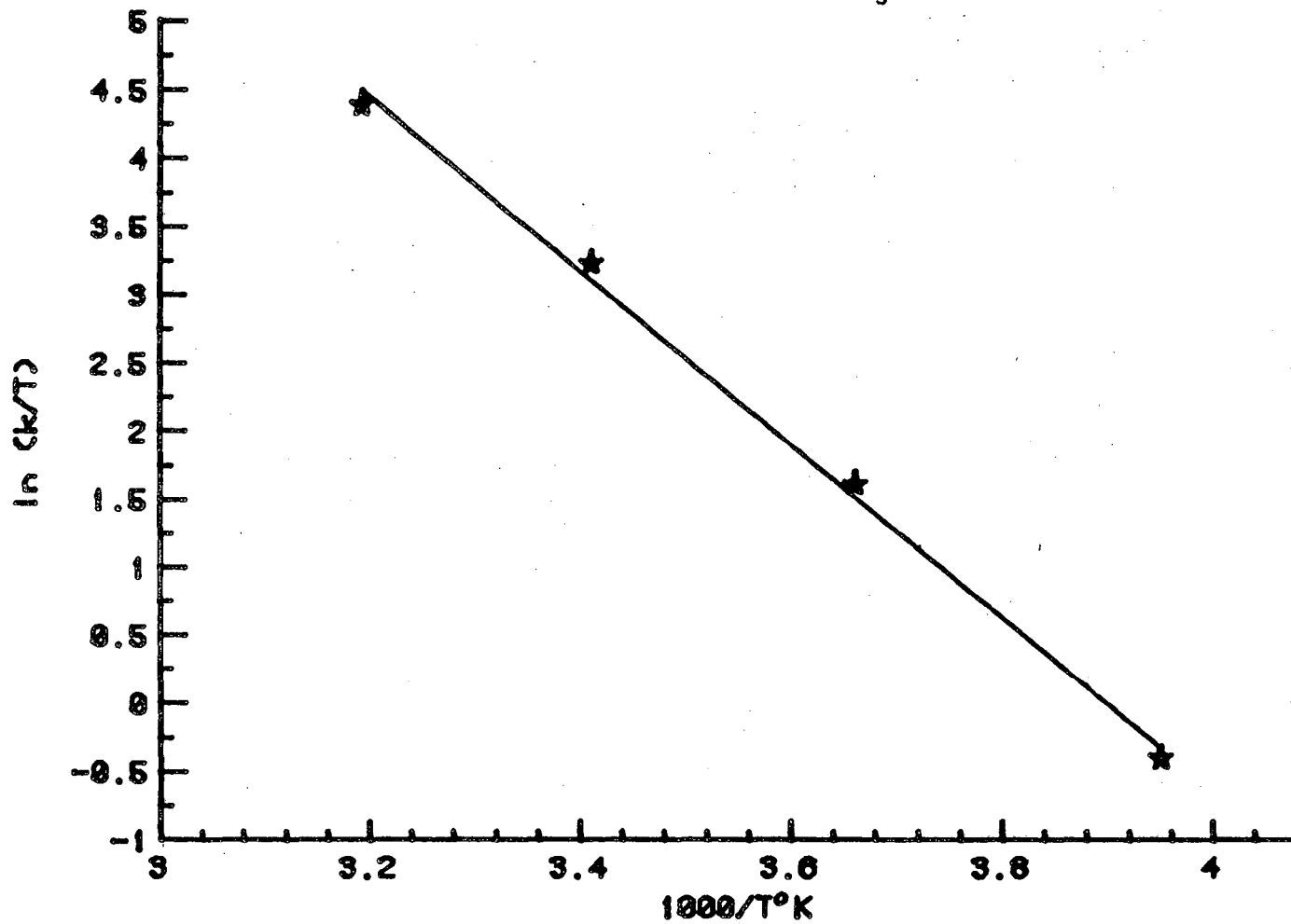
Figure 2-10: Line Shape Analysis for  $\text{PMe}_3$  Exchange

Figure 2-11: Eyring Plot of Rate Constants Determined from  
Line Shape Analysis for  $\text{PMe}_3$  Exchange



$$\Delta H^\ddagger = 12.7 \pm 0.4 \text{ kcal/mol}$$

$$\Delta S^\ddagger = 2.2 \pm 1.3 \text{ e.u.}$$

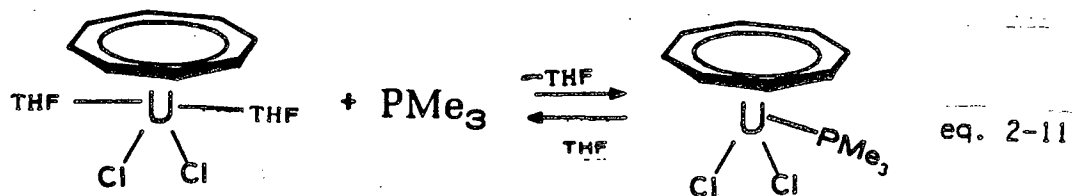
$$\Delta E^\ddagger = 13.2 \pm 0.4 \text{ kcal/mol}$$

$$A = (4.8 \pm 3.0) \times 10^{13} \text{ s}^{-1}$$

The free energy of activation can be determined from the  $\Delta H^\ddagger$  and  $\Delta S^\ddagger$  values. With a coalescence temperature of +5 °C, the free energy of activation is calculated to be  $12.1 \pm 0.5$  kcal/mol, which compares favorably with the  $\Delta G^\ddagger$  value of 11.9 kcal/mol estimated earlier.

An estimate for the free energy of activation for the exchange process can also be determined from the coalescence temperature of the [8]annulene ring protons. Though the single peak never collapses completely into the baseline, but rather broadens and "divides" into separate peaks, estimating the coalescence temperature as  $-5 \text{ °C} \pm 5^\circ$  is still possible. Using equations 2-9 and 2-10 ( $\Delta\nu = 212 \text{ Hz}$ ), a free energy of activation ( $\Delta G^\ddagger$ ) of  $12.3 \pm 0.3$  kcal/mol results. The value is somewhat higher than that derived from the  $\text{PMe}_3$  peaks and might be attributed to the uncertainty in the coalescence temperature (the values are within the error bars). In any case, the exchange process appears to have an activation barrier of about 12.0 kcal/mol.

In addition to the activation parameters for the process, we can also determine the free energy and entropy of the equilibrium between the trimethylphosphine half-sandwich complex and the solvated half-sandwich (eq. 2-11). Since the solvent is in



excess, the equilibrium constant can be determined from the relative concentrations of the solvated half-sandwich, free  $\text{PMe}_3$ , and the  $\text{PMe}_3$  complex (eq. 2-12).

$$K = \frac{[(\text{COT})\text{UCl}_2\text{-PMe}_3]}{[(\text{COT})\text{UCl}_2\text{-2 THF}][\text{PMe}_3]} \quad \text{eq. 2-12}$$

By integrating the relevant peaks in the  $^1\text{H}$  NMR spectrum at temperatures below the coalescence point, equilibrium constants for the process could be obtained (Table 2-6). A plot of

Table 2-6: Equilibrium Constants Determined  
from Equation 2-11

T°C	K
-30	0.0093
-40	0.0099
-50	0.0114
-60	0.0125
-70	0.0178
-80	0.0154



the log of the equilibrium constants versus inverse temperature (Figure 2-12) gives the enthalpy and entropy of the process:

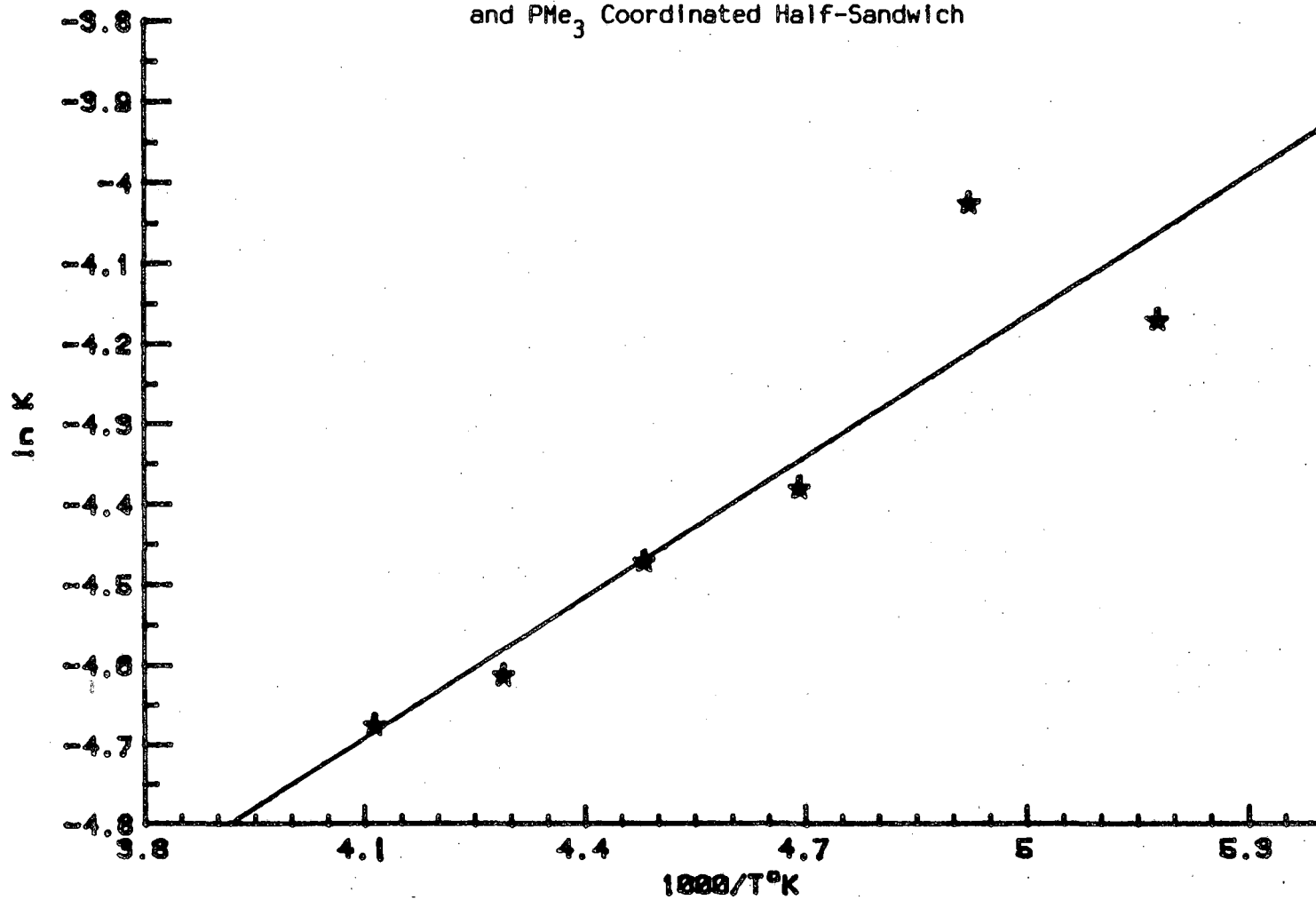
$$\Delta H^\circ = -1.2 \pm 0.4 \text{ kcal/mol}$$

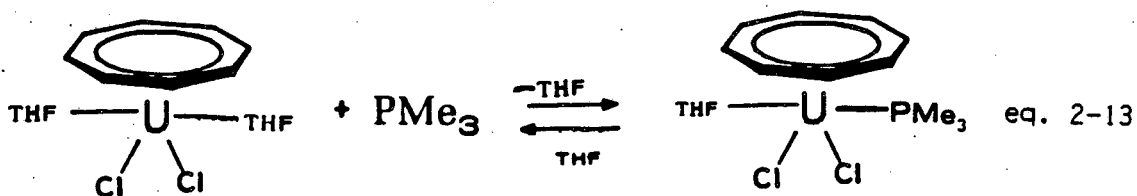
$$\Delta S^\circ = -14.1 \pm 1.5 \text{ e.u.}$$

$$\Delta G^\circ = +3.0 \pm 0.5 \text{ kcal/mol}$$

Though there is some scatter of points in the plot, due to the uncertainty in integration values, the enthalpy and entropy values derived will permit us to make a few conclusions on the  $\text{PMe}_3$  complexation process. Surprisingly, the free energy for the process is positive. The phosphorous ligand should favor coordination to uranium<sup>6,16</sup> over the solvent molecules, and this is reflected in the negative enthalpy value. However, the negative entropy factor results in the equilibrium (eq. 2-12) favoring coordination to THF, at least at the concentrations studied ( $10^{-2}$  M in half-sandwich and  $\text{PMe}_3$ ,  $\text{THF-d}_8$  as bulk solvent). The negative entropy value also suggests that one  $\text{PMe}_3$  is not displacing two THF molecules, since that would result in a positive entropy value. Instead,  $\text{PMe}_3$  might be displacing only one solvent molecule (eq. 2-13), with the increased steric crowding reducing the ligand's degrees of freedom.

Figure 2-12: van't Hoff Plot of Equilibrium between THF Solvated and  $\text{PMe}_3$  Coordinated Half-Sandwich





The entropy of activation is nearly zero, thus solvent is moving out of the coordination sphere to allow free  $\text{PMe}_3$  to diffuse in and coordinate to uranium. The transition state apparently occurs during this solvent reorganization, before  $\text{PMe}_3$  has entered the coordination sphere and increased steric crowding.

It may be that this THF- $\text{PMe}_3$  half-sandwich complex occurs only under these THF solution conditions. An elemental analysis of the solid compares more favorably with a complex containing no THF. In the solid state, the complex may prefer the less sterically crowded 8-coordinate structure shown in equation 2-11. Perhaps an nmr study in a non-coordinating solvent might demonstrate that the 8-coordinate structure is preferred. Solubility limitations, however, may prevent a conclusive analysis.

Conclusions on the Chemistry of the Half-Sandwich:

It has been demonstrated that formation of a phosphine-coordinated half-sandwich is feasible. The trimethylphosphine ligand increases solubility in toluene, which, in the absence of non-coordinating solvents, will enhance the reactivity of the complex. Time constraints prevent further reaction studies, but perhaps future investigators will find that this phosphine complex reacts more cleanly with alkyl and aryl Grignard reagents. In addition, equilibrium studies with a variety of coordinating ligands (pyridine, TMEDA, etc.) should yield results which would be interesting to compare with recent equilibrium data of the Andersen group.<sup>17</sup> It is encouraging that considerable effort on the part of many investigators is finally beginning to demonstrate that actinide chemistry has as rich and varied a chemistry as that of the transition metals.

## Experimental

General. Unless otherwise indicated, materials were obtained from commercial suppliers and used as supplied. Tetrahydrofuran (THF) and ethyl ether were distilled immediately before use from sodium/benzophenone. Toluene was distilled from sodium. Hexane was distilled from  $\text{CaH}_2$  after refluxing overnight. All operations with the half-sandwich were carried out using either an argon atmosphere glovebox, or standard Schlenk techniques.  $^1\text{H}$  NMR spectra were recorded on the UCB-200 (200 MHz, FT) or UCB-250 (250 MHz, FT) spectrometers. Significant  $^1\text{H}$  NMR data are tabulated in order: multiplicity (s, singlet; d, doublet; m, multiplet), number of protons, coupling constant in Hertz. Chemical shifts are referenced to tetramethylsilane (TMS) either directly with TMS as internal standard or indirectly by resonance of solvents referenced to TMS. Elemental analyses were performed by the Microanalytical Laboratory operated by the College of Chemistry, University of California, Berkeley. Infrared spectra were determined on a Perkin-Elmer Model 297 spectrometer. Visible spectra of THF solutions of the organometallic compounds were determined with a Cary Model 118 spectrophotometer. Samples for x-ray powder pattern determination were prepared by grinding the crystalline sample to a fine powder and sealing the powder into a quartz capillary under argon. X-ray powder pattern data were taken with a Debye-Scherrer camera using nickel filtered copper  $\text{K}\alpha$  x-rays. All weights, unless otherwise specified, are  $\pm 0.01$  g.

([8]Annulene)uranium Dichloride Bistetrahydrofuran

(Potassium Method): To 7.98 g (0.021 mol) of  $UCl_4$  in 250 mL of dry, degassed THF under argon was added 0.82 g (0.021 mol) of potassium. The reduction to  $UCl_3$  required 12 hr of stirring at room temperature. To this suspension of  $UCl_3$  was added 1.09 g (0.105 mol) of cyclooctatetraene. The reaction was stirred for 36 hr at room temperature. After removal of the solvent *in vacuo*, the remaining solid was extracted with toluene. Subsequent identification by spectroscopic techniques ( $^1H$  NMR, visible, IR) revealed that both the extracted material and the toluene insoluble material contained both the starting material ( $UCl_4$ ) and the desired product.  $^1H$  NMR ( $C_4D_8O$ , 250 MHz, 30 °C)  $\delta$  -31.5 (s, 8H), coordinated THF rapidly exchanges with the solvent. Visible (THF): 436 nm ( $\epsilon=421$ ), 450 nm ( $\epsilon=430$ ), 486 nm ( $\epsilon=351$ ), 490 nm ( $\epsilon=348$ ), 552 nm ( $\epsilon=274$ ), 586 nm ( $\epsilon=239$ ), 646 nm ( $\epsilon=376$ ), 664 nm ( $\epsilon=370$ ).

([8]Annulene)uranium Dichloride Bistetrahydrofuran (Sodium

Hydride Method): To 9.50 g (0.025 mol) of  $UCl_4$  and 2.60 g (0.025 mol) of cyclooctatetraene in dry, degassed THF under argon, was added 1.33 g (0.055 mol) of NaH. After magnetically stirring for 7 hr, the solution was filtered and the solvent was removed *in vacuo*. The solid was then washed free of starting materials with hexane, leaving 11.64 g (84%) of an air-sensitive, reddish crystalline material, which within minutes of exposure to a glove box atmosphere, lost coordinated THF to form a greenish powder.

Redissolving the solid in THF resulted in a red solution, indicating recoordination of the THF.  $^1\text{H}$  NMR ( $\text{C}_4\text{D}_8\text{O}$ , 250 MHz, 30 °C):  $\delta$  -31.6 (s, 8H), 1.86 (s), 3.62 (s). Visible (THF): 454 nm ( $\epsilon=281$ ), 500 nm ( $\epsilon=249$ ), 518 nm ( $\epsilon=227$ ), 570 nm ( $\epsilon=206$ ), 582 nm ( $\epsilon=188$ ), 596 nm ( $\epsilon=174$ ), 742 nm ( $\epsilon=32$ ). IR ( $\text{cm}^{-1}$ ): 1340, 1259, 1163, 1070, 1032 (shoulder), 1008 (strong), 920, 900, 840 (strong), 805 (strong), 720 (strong), 660.

Anal. Calcd. for  $\text{C}_{16}\text{H}_{24}\text{Cl}_2\text{O}_2\text{U}$ : C, 34.48; H, 4.34; Cl, 12.72. Found: C, 30.69; H, 4.14; Cl, 14.10.

Attempted Preparation of (n-Butyl-[8]annulene)uranium

Dichloride Bistetrahydrofuran (Potassium Method): To 7.40 g (0.0195 mol) of  $\text{UCl}_4$  in 125 mL of THF was added 0.762 g (0.0195 mol) of potassium. After stirring the suspension overnight at room temperature, 1.40 g (0.0087 mol) of *n*-butylcyclooctatetraene (prepared by the method of DeKock<sup>12</sup>) was added to the suspension of  $\text{UCl}_3$  in THF. Stirring was continued for 72 hr, but the suspension failed to turn green, indicative of the failure to convert  $\text{UCl}_3$  to  $\text{UCl}_4$ . The solvent was removed *in vacuo*. Spectral data ( $^1\text{H}$  NMR, visible) on the crude material indicated that only trace amounts of *n*-butyluranocene and no substituted half-sandwich was present.

Attempted Preparation of (n-Butyl-[8]annulene)uranium

Dichloride Bistetrahydrofuran (Sodium Hydride Method): To 380 mg (1 mmol) of  $\text{UCl}_4$  in 20 mL of THF was added 60 mg (2.5 mmol) of

NaH and 160 mg (1 mmol) of *n*-butylcyclooctatetraene. After stirring for 60 hr, the solution was filtered and the solvent was removed *in vacuo*. No color change had occurred and visible spectroscopy indicated the presence of  $\text{UCl}_4$  only.

(*m*-Fluorophenyl-[8]annulene)uranium Dichloride

Bistetrahydrofuran: To 380 mg (1 mmol) of  $\text{UCl}_4$  and 198 mg (1 mmol) of *m*-fluorophenylcyclooctatetraene<sup>14</sup> in 20 mL THF was added 70 mg (2.9 mmol) of NaH. After stirring for 7 hr, the solution was filtered and the solvent was removed *in vacuo*. The remaining red oil was washed with hexane, leaving 438 mg (67%) of a red powder, which by  $^1\text{H}$  NMR spectroscopy was found to be the desired product.  $^1\text{H}$  NMR ( $\text{C}_4\text{D}_8\text{O}$ , 250 MHz, 30 °C):  $\delta$  -33.9 (s, 2H), -33.1 (s, 2H), -30.9 (s, 2H), -23.9 (s, 1H), -4.7 (s, 1H), -2.3 (s, 1H), 2.6 (s, 1H), 5.0 (s, 1H).

Reaction of ([8]Annulene)uranium Dichloride with Potassium

Cyclooctatetraene Dianion: To 20 mg ( $\pm 2$ ) (0.04 mmol) of  $(\text{COT})\text{UCl}_2 \cdot 2 \text{ THF}$  in 1 mL of  $\text{THF-d}_8$  was added 4 mg ( $\pm 2$ ) (0.02 mmol) of  $\text{K}_2\text{COT}$ . The reddish-green solution was transferred to an nmr tube and sealed under vacuum. A  $^1\text{H}$  NMR spectrum of the solution indicated the presence of both uranocene and unreacted half-sandwich complex (some uranocene precipitated out of the solution). A visible spectrum of the reaction in THF was identical to the known spectrum of uranocene.  $^1\text{H}$  NMR ( $\text{C}_4\text{D}_8\text{O}$ , 250 MHz, 30 °C):  $\delta$  -35.9 (s), -31.7 (s).



Attempted Preparation of Mono-*t*-butyluranocene. To a stirred solution of 160 mg (0.29 mmol) of (COT)UCl<sub>2</sub>-2 THF in 30 mL of THF at room temperature was added 60 mg (0.25 mmol) of K<sub>2</sub>(*t*-BuCOT) in 15 mL of THF. The red solution turned green within 5 minutes after addition had been completed. The THF was removed *in vacuo* and the crude sample was analyzed by <sup>1</sup>H NMR spectroscopy. The resulting <sup>1</sup>H NMR spectrum included twelve peaks that were assigned to the known<sup>7</sup> compounds, di-*t*-butyluranocene (5 peaks), mono-*t*-butyluranocene (6 peaks), and uranocene (1 peak).

Reaction of ([8]Annulene)uranium Dichloride with Methylithium. To 557 mg (1 mmol) of (COT)UCl<sub>2</sub>-2 THF in 10 mL of THF and 50 mL of ethyl ether (the THF was required to dissolve the half-sandwich) was added, via cannulation, 2.2 mL of 1M (2.2 mmol) methylithium (Fluka AG) in ethyl ether at -78 °C. After the exothermic addition was complete, the reaction was allowed to warm to room temperature and stirred for 90 min. After solvent removal *in vacuo*, the crude material was analyzed by <sup>1</sup>H NMR spectroscopy, which indicated that only decomposed metal products and free ligand were present.

Reaction of ([8]Annulene)uranium Dichloride with Benzylmagnesium chloride. To 570 mg (1.0 mmol) of (COT)UCl<sub>2</sub>-2 THF in 30 mL of THF at -78 °C was added, via cannulation, 1.1 mL of a 2.0M commercial (Aldrich) benzylmagnesium chloride in THF

solution (2.2 mmol). The reaction was stirred for 30 min at  $-78$  °C, the solvent was removed *in vacuo*, and the remaining crude solid was analyzed. A  $^1\text{H}$  NMR spectrum of the crude material suggested the presence of an  $\eta^3$ -dibenzyluranium complex.

Extraction of the crude solid with toluene, and a second attempt at reproducing these results, netted only decomposed materials.  $^1\text{H}$  NMR ( $\text{C}_4\text{D}_8\text{O}$ , 250 MHz, 30 °C):  $\delta$  -31.6 (s, 4H), -31.2 (s, 2H), -29.7 (s, 8H), -29.1 (s, 4H), -13.1 (s, 4H).

[[8]Annulene)uranium Dichloride Trimethylphosphine. A flask containing 0.826 g (2 mmol) of the desolvated half-sandwich complex in 20 mL of THF was connected to a Schlenk line and cooled to 77 °K. Two equivalents of  $\text{PMe}_3$  were prepared by decomposing 1.25 g of  $\text{PMe}_3\text{-AgI}$  (4 mmol) complex above 200 °C. The  $\text{PMe}_3$  was vacuum transferred into the flask containing the half-sandwich and the flask was allowed to warm to room temperature. The reaction was stirred overnight, under argon. A large amount of precipitate had formed in the flask (which was insoluble in hexane and THF); thus, the solution was filtered, and the THF was removed *in vacuo*. A  $^1\text{H}$  NMR spectrum at 30 °C of the remaining solid contained two relevant peaks whose areas integrated to a ratio of 9 to 8, suggesting the presence of a  $\text{PMe}_3$  coordinated [8]annulene complex. An analysis of the recovered red solid was mediocre. Yield: (0.435 g, 44%)  $^1\text{H}$  NMR ( $\text{C}_4\text{D}_8\text{O}$ , 200 MHz,  $-40$  °C)  $\delta$  -39.0 (s, 8H), -5.1 (s, 9.7H)

Anal. Calcd. for  $\text{C}_{11}\text{H}_{17}\text{UCl}_2\text{P}$ : C, 27.01%; H, 3.50%;

Cl, 14.50%; P, 6.33%. Calcd. for  $C_{15}H_{25}UCl_2PO$ : C, 32.10%; H, 4.49%; Cl, 12.69%; P, 5.52%. Found: C, 27.90%; H, 4.01%; Cl, 8.22%; P, 3.01%.

Measurement of the Rate of  $PMe_3$  Exchange The  $^1H$  NMR spectra were run on the UC Berkeley FT-NMR 200 MHz spectrometer. The system employs a superconducting magnet, a deuterium lock system, and Nicolet software. Temperature was monitored by a Doric Trendicator 410A. Line shape analyses were performed using an exchange program written for the 1180 Nicolet system as part of the NTCFT software package.<sup>18</sup> All measurements were carried out in approximately  $10^{-3}$  M solutions in  $THF-d_8$ .

The natural line widths were determined from the line widths at  $-60$  °C in the slow exchange limit. The natural line widths were found to be 5 Hz for the free  $PMe_3$  peak and 10 Hz for the complexed  $PMe_3$  peak. Chemical shifts were determined at ten degree intervals from  $-80$  °C to  $+60$  °C. At fast exchange (above the coalescence temperature), the chemical shifts were determined by extrapolating from the slow exchange limit.

Errors in  $\Delta H^\ddagger$  and  $\Delta S^\ddagger$  were calculated by the program ACTENG<sup>19</sup> ( $k$ ,  $\pm 10\%$ ,  $T$ ,  $\pm 0.5^\circ$ ).

Calculation of  $\Delta G^\ddagger$  for the barrier to  $PMe_3$  exchange was made by using the  $\Delta H^\ddagger$  and  $\Delta S^\ddagger$  values from the line shape analysis ( $\Delta G_c^\ddagger = \Delta H^\ddagger - T_c \Delta S^\ddagger = 12.1$  kcal/mole) and also by extrapolating  $\Delta\nu$  values to the estimated coalescence temperature (from chemical shift vs.  $T^{-1}$  plots,  $\Delta\nu = 1016$  Hz), then substituting into

the formulas,  $k = 2^{-0.5} \pi \Delta \nu$  and  $-\Delta G^\ddagger = RT \ln(kh/Kk_B T)$ , where  $K = 1$  ( $\Delta G^\ddagger = 11.9$  kcal/mole).

Determination of the Equilibrium Constants for Equation 2-

11. Determination of the equilibrium constants were made by equation 2-14.

$$K = [(\text{COT})\text{UCl}_2\text{-PMe}_3]/[(\text{COT})\text{UCl}_2\text{-2 THF}][\text{PMe}_3] \quad \text{eq. 2-14}$$

Relative concentrations for the species were determined by integration of the peak areas in the  $^1\text{H}$  NMR spectrum. The peaks chosen for convenient integration were the  $\text{PMe}_3$  protons for the  $\text{PMe}_3$  half-sandwich complex, the [8]annulene protons in the THF solvated complex, and the methyl protons in free  $\text{PMe}_3$ . The error in the equilibrium constants is estimated to be 15%.

Footnotes and References

- 1 LeVanda, C.; Report on Half-Sandwich Actinides, 1978. (b) Zalkin, A.; Templeton, D.H.; LeVanda, C.; Streitwieser, A., Jr. Inorg. Chem. 1980, 19, 2560.
- 2 Solar, J.; Report on Half-Sandwich Actinides, 1979.
- 3 Smith, K. Ph.D. Thesis U.C.Berkeley, 1984
- 4 Probably due to residual HCl.
- 5 Kinsley, S. unpublished results.
- 6 Brennan, J. unpublished results.
- 7 Luke, W. D.; Streitwieser, A., Jr. ACS Symposium Series No. 131, Edelstein, N., ed., p 93.
- 8  $C_{2v}$  is the highest symmetry possible for the half-sandwich. Ufanocene belongs to the symmetry group  $C_{8h}$ .
- 9 Berryhill, S. Ph.D. Thesis U.C.Berkeley, 1975.
- 10 Kinsley, S. Ph.D. Thesis U.C.Berkeley, 1984.
- 11 The reader is encouraged to read a more detailed account of the theory of paramagnetic shifts. See, "NMR of Paramagnetic Molecules: Principles and Applications;" La Mar, G. N.; Horrocks, W., Jr.; Holm, R. H., Eds.; Academic Press, New York, N.Y.; 1973.
- 12 DeKock, C. W.; Miller, J. T.; Brault, M. A. J. Org. Chem. 1979, 44, 3508.
- 13 Hillard, E. S. unpublished results.
- 14 See Chapter 1, p. 25, for preparation.
- 15 Fagan, P. J.; Manriquez, J. M.; Maatta, E. A.; Seyam, A. M.; Marks, T. J. J. Am. Chem. Soc. 1981, 103, 6650.
- 16 Edwards, P. G.; Andersen, R. A.; Zalkin, A. Organometallics 1984, 3(2), 293.
- 17 Stewart, J. unpublished results.
- 18 Reeves, L. W. Advances in Phys. Org. Chem. 1965, 3, 187.
- 19 DeTar, D. F. "Computer Programs for Chemistry, Vol. III", DeTar, D. F., ed.,; W.A. Benjamin, New York, 1969.

## Chapter 3. The Phenyl Rotational Barrier

### In 1,1'-Diphenyluranocene

#### Introduction

Paramagnetic organometallic U(IV)(5f<sup>2</sup>) compounds have served as useful probes in the observation of a variety of nuclear magnetic resonance properties and processes.<sup>1,2,3</sup> The large isotropic shifts can result in greater amplification of chemical shift differences which increase the time resolution of the <sup>1</sup>H NMR experiment, according to the approximate solutions to the modified Bloch equations<sup>4</sup> given in equations 3-1 and 3-2.

$$1/\tau = (\pi\Delta\nu)^2 / 4 [1/T_2^{\text{exch}} - 1/T_2^{\circ}] \quad \text{eq. 3-1}$$

$$1/\tau = \pi\Delta\nu/2^{0.5} \quad \text{eq. 3-2}$$

The increase in time resolution permits observation by <sup>1</sup>H NMR of dynamic processes with free energies of activation lower than the 7 to 8 kcal mol<sup>-1</sup> normally required for observation in diamagnetic complexes. As part of a study of substituted bis-π-[8]annuleneuranium(IV) complexes, this probe has been used to determine the rotational barrier of the phenyl ring about the C-C bond to the [8]-annulene ring in 1,1'-diphenyluranocene, 1.

1,1'-diphenyluranocene was prepared by the addition of phenylcyclooctatetraene dianion to a solution of UCl<sub>4</sub> in THF under argon (see Experimental section, Chapter 1). The recovered solid was extracted with toluene and crystallized in THF/hexane.

The dark green, air-sensitive crystals which formed analyzed correctly for 1,1'-diphenyluranocene.

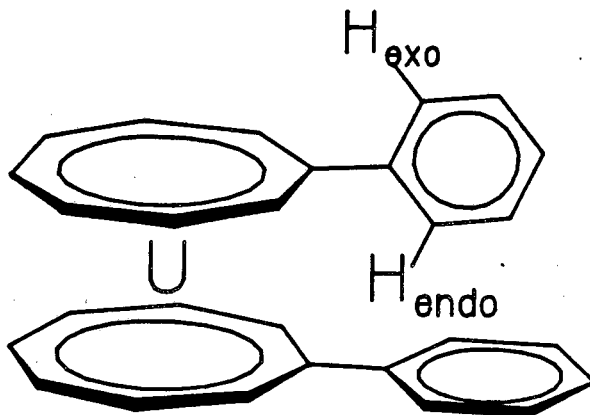


Figure 3-1: 1,1'-Diphenyluranocene, 1

At 30 °C, the  $^1\text{H}$  NMR spectrum of 1 contains seven peaks; three phenyl proton resonances,  $\delta$  -13.95 (ortho, 2H), 0.76 (meta, 2H), 0.85 (para, 1H) and four [8]-annulene ring proton resonances,  $\delta$  -34.29, -36.15, -36.45, -37.13.<sup>1</sup> In particular, the ortho-phenyl proton chemical shift is an average shift position for the endo and exo proton environments (Figure 3-1) since the phenyl ring is not coplanar with the [8]-annulene ring but rotates rapidly about the C-C bond at 30 °C. As the sample is cooled to -40 °C, the ortho proton resonance begins to broaden until it collapses into the baseline at -100 °C. Unfortunately, 1 is poorly soluble in solvents at the temperatures required for observation of the slow exchange limit (below -125°C). It is possible, however, to estimate the chemical shifts of the endo and exo proton positions from the  $^1\text{H}$  NMR data of a recently

prepared analog, 1,1'-di-o-tolyluranocene, 2.

1,1'-di-o-tolyluranocene was obtained by a preparation similar to the synthesis of diphenyluranocene. Addition of o-tolyllithium to cyclooctatetraene resulted in a 30% isolated yield of o-tolylcyclooctatetraene.<sup>5</sup> Reduction of o-tolylcyclooctatetraene with potassium metal resulted in formation of the dianion, which was added to a solution of  $UCl_4$  in THF under argon. Extraction with hexane, followed by recrystallization from a hexane-THF mixture resulted in a dark green, air sensitive solid which was identified to be di-o-tolyluranocene.<sup>5</sup>

The  $^1H$  NMR of di-o-tolyluranocene is similar to diphenyluranocene with regard to the pattern and location of the [8]-annulene ring resonances. There are, however, clear differences in the chemical shifts for the aryl ring protons between diphenyluranocene and di-o-tolyluranocene. The presence of a single proton resonance far upfield ( $\delta$  -71.6 at  $-45^\circ C$ ) indicates that the ortho proton of di-o-tolyluranocene is close to the uranium metal (endo). Due to the bulky ortho-methyl group, rotation of the tolyl ring is restricted, with the methyl group remaining exo to the uranium. Since the contact shift<sup>3</sup> contribution to the chemical shift of the methyl protons will be small, due to the large through-bond distance from uranium to the protons, the chemical shift can be assumed to arise principally from a dipolar (pseudo-contact shift)<sup>3</sup> interaction. Thus, with the methyl proton resonance located at +23.2 ppm, the assignment of the methyl group exo to the uranium is reasonable. The peaks for di-o-tolyluranocene remain sharp from  $-100^\circ C$  to  $80^\circ C$ ,



indicating that the compound is restricted to this single conformation throughout the temperature range studied.

Similar chemical shifts for the para proton on both the aryl rings ( $\delta$  0.85 for 1, and  $\delta$  0.87 for 2) of di-*o*-tolyluranocene and diphenyluranocene suggest that 1 and 2 possess similar conformations, with the exception of the rapidly rotating aryl ring in diphenyluranocene. Therefore, it is likely that the endo-ortho proton of di-*o*-tolyluranocene mimics the behavior of the ortho proton of diphenyluranocene in the slow exchange limit. The chemical shifts of the exo-proton can be extrapolated from the average shift position for both ortho-protons in 1 and the endo-ortho-proton in di-*o*-tolyluranocene.

These shift values could be extrapolated from the chemical shift vs.  $T^{-1}$  plot to the estimated coalescence temperature and a free energy of activation determined by use of the Eyring equation with eq. 3-2. A more dependable method for determining thermodynamic parameters is by computer simulated line-shape analysis of the broadened exchange peaks to determine the mean nuclei lifetimes,  $\tau$ , over a series of temperatures. Values for  $\tau$  were determined by inputting frequency values for non-exchanging peaks, along with natural line widths, and best fitting the computer generated curve for a specific  $\tau$  value to the actual nmr peak. Converting  $\tau$  values to exchange rate constants and plotting against inverse temperature yields values for the activation enthalpy,  $\Delta H^\ddagger$ , and entropy,  $\Delta S^\ddagger$ . The  $\Delta G^\ddagger$  value calculated from the  $\Delta H^\ddagger$  and  $\Delta S^\ddagger$  values is not sensitive to errors in judging the coalescence temperature and is expected to be more reliable.

## Results

The resonance frequency data for the endo-proton of di-o-tolyluranocene and the ortho-protons (average shift position of exo and endo) of 1 are given in Table 3-1. Also included in this table are the calculated frequencies for the exo-proton in the absence of exchange. All of the protons exhibit approximate Curie-Weiss behavior throughout the temperature range studied. Simulation of the broadened fast exchange peak of the ortho protons in 1 (Figure 3-2) provides the mean nuclei lifetimes  $\tau$  given in Table 3-2 for the temperature range -45 °C to -80 °C.

Table 3-1: Resonance Frequency Data (200 MHz) for Diphenyluranocene

<u>T</u> °C	<u>Endo-Proton</u> <sup>x</sup> (Hz)	<u>Ortho-Protons</u> <sup>y</sup> (Hz)	<u>Exo-Proton</u> <sup>z</sup> (Hz)
-45	-14409	-4700	+5009
-50	-14840	-4901	+5038
-55	-15308	-5068	+5160
-60	-15756	-5274	+5208
-65	-16285	-5472	+5341
-70	-17000	-5689	+5422
-75	-17420	-5915	+5590
-80	-17983	-6175	+5633

x experimentally determined from the resonance frequency of the endo-ortho-proton of di-o-tolyluranocene, 2.

y experimentally determined from the average resonance frequency of the endo and exo-ortho-protons of diphenyluranocene, 1.

z extrapolated from the given experimental data

Figure 3-2: Line Shape Analysis for ortho-proton coalescence in 1,1'-Diphenyluranocene

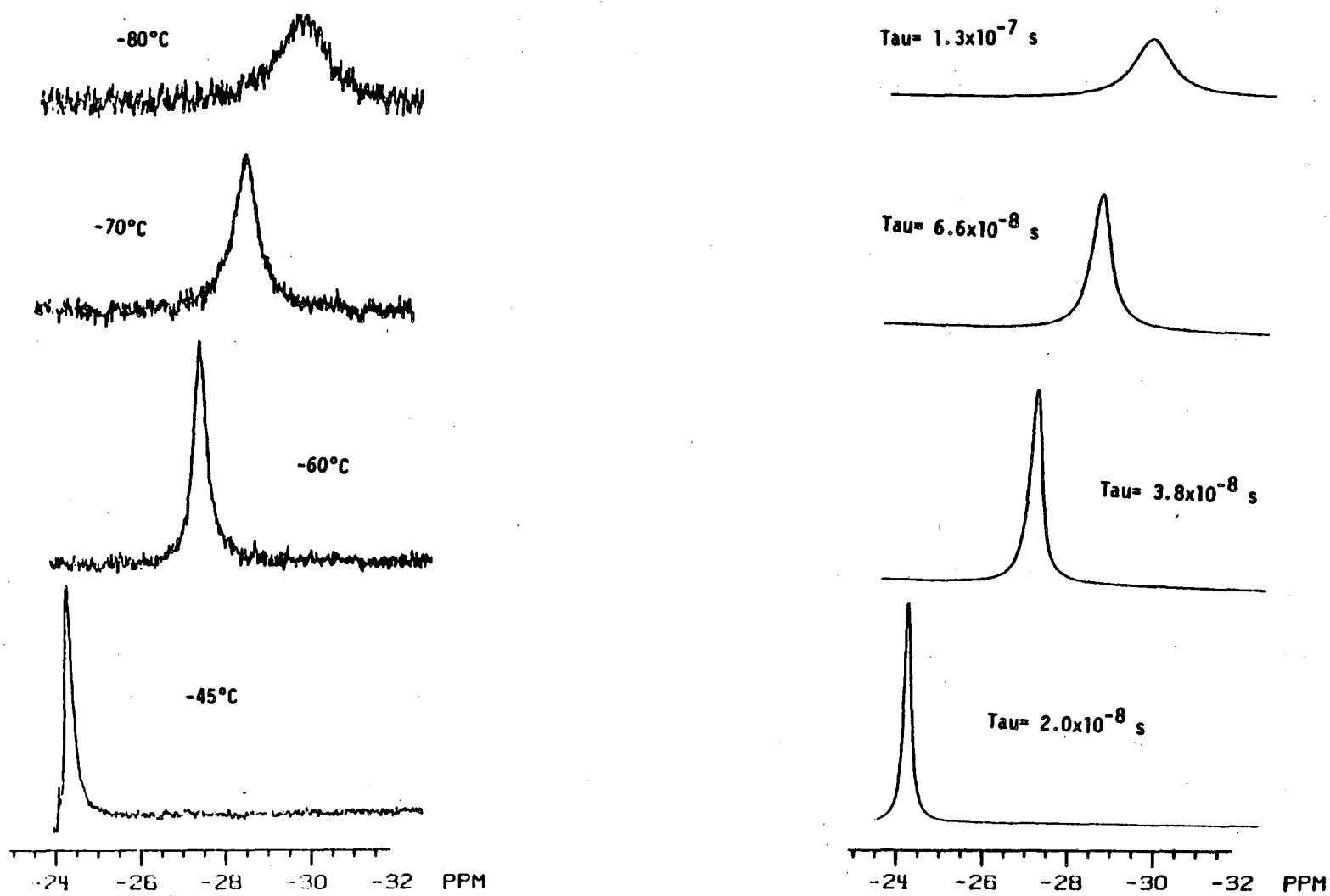


Table 3-2: Results of computer simulation to determine the mean lifetime for rapidly exchanging nuclei in 1

T °C	$\tau \times 10^8$ s	$k \times 10^{-5}$ s <sup>-1</sup>
-45	2.0	250
-50	2.4	210
-55	2.8	180
-60	3.8	130
-65	5.1	98
-70	6.6	76
-75	9.6	52
-80	13	38

An Eyring plot of the rate constants (Figure 3-3) results in the following activation parameters for this temperature range:

$$\Delta H^\ddagger = 4.4 \pm 0.3 \text{ kcal mol}^{-1}$$

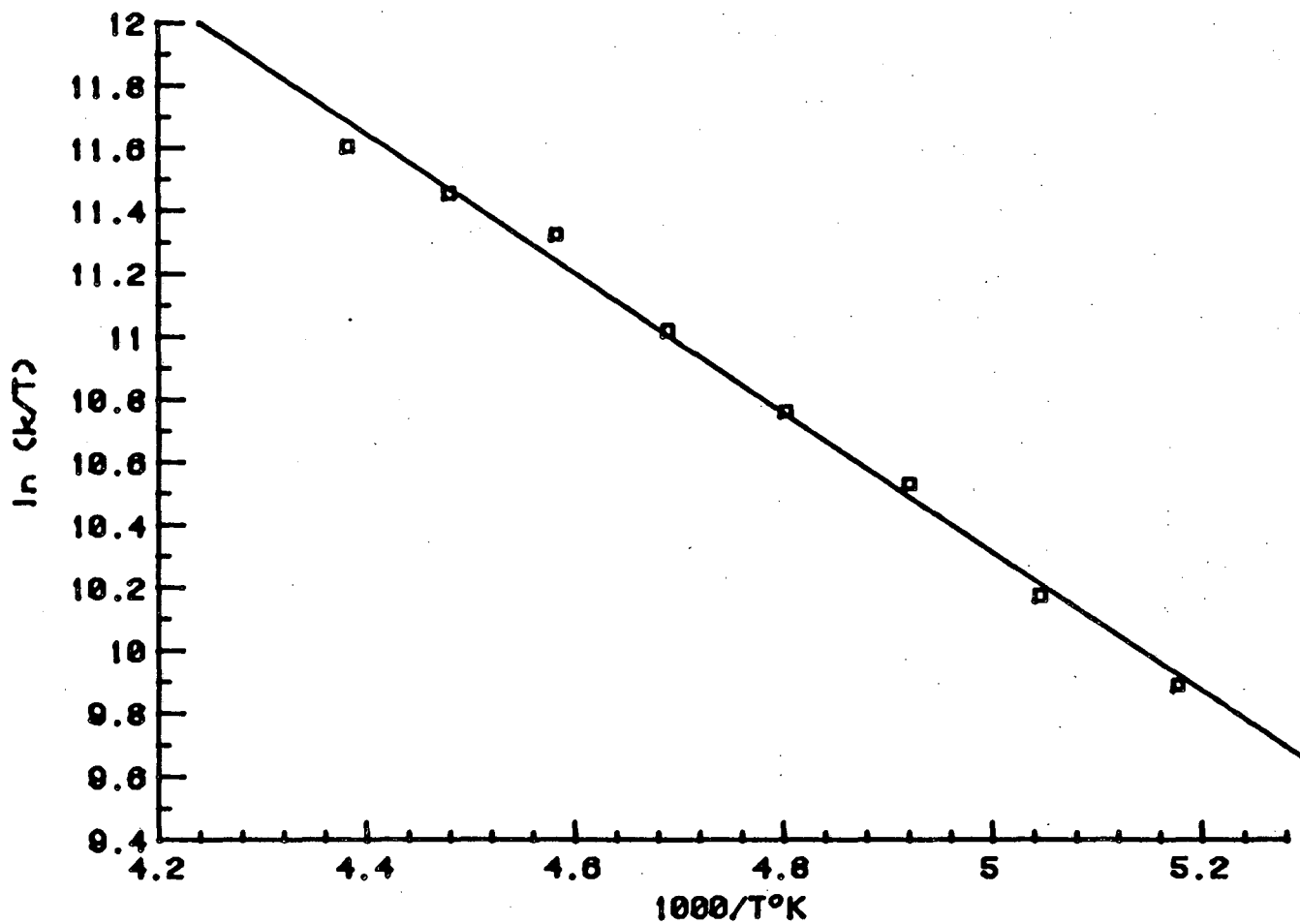
$$\Delta S^\ddagger = -4.7 \pm 1.3 \text{ e.u.}$$

$$E_a = 4.8 \pm 0.3 \text{ kcal mol}^{-1}$$

$$A = (1.1 \pm 0.7) \times 10^{11} \text{ s}^{-1}$$

The free energy of activation can be determined by approximating the coalescence temperature to be 20-30° below the point at which the peak collapses into the baseline, a method used by Marks in estimating the coalescence temperature for exchanging bridging and terminal hydrides in  $(C_5H_5)_3UBH_4$ .<sup>2</sup> Thus, with  $T = (150 \pm 10)^\circ K$ ,  $\Delta G^\ddagger = 5.1 \pm 0.5 \text{ kcal mol}^{-1}$  for rotation of

Figure 3-3: Eyring Plot to Determine Standard Thermochemical Parameters for Phenyl Ring Rotational Barrier



the phenyl ring about the [8]annulene ring plane. As a comparison, calculation of the rotational barrier by extrapolating  $\Delta V$  to the coalescence temperature results in a  $\Delta G^\ddagger$  of 5.2 kcal mol<sup>-1</sup>, in excellent agreement with the value derived from line shape analysis.

Additional substituents on the meta or para positions of the phenyl ring, such as p-dimethylamino, appear to have no effect on the rotational barrier. Mean nuclei lifetime results from line shape analysis of the ortho peak of p-dimethylaminophenyl-uranocene, 3, are given in Table 3-3. The results are virtually identical to those reported in Table 3-2 for 1. The dynamic behavior of 3 appears to mimic that of the parent complex 1.

Table 3-3: Mean nuclei lifetime for exchanging ortho protons in 2

T°C	$\tau \times 10^8$ s
-45	2.1
-55	2.8
-65	5.0
-70	6.6

When line shape analysis was performed on the spectra of 1 and 3 in solutions of THF-d<sub>8</sub>, the rate constants duplicated the values determined in solutions of toluene-d<sub>8</sub>. Changes in solvent have no apparent effect on the rate of peak broadening. In addition, it is difficult to envision a solvent broadening effect which would have such an extreme effect on the ortho proton peak.

while having a relatively smaller effect on the meta proton peak and no effect at all on the peak width of the para proton. The small broadening effect on the meta proton peak are in fact, due to the exchange process. The smaller difference in magnetic environments between exchanging meta protons (compared to ortho),  $\Delta\nu$ , results in a much lower, observed coalescence temperature.

Measuring a dynamic process with such a small barrier by  $^1\text{H}$  NMR spectroscopy is unusual but is made possible by the unique structure and paramagnetism of uranocene which results in widely different magnetic environments of the endo and exo protons ( $\Delta = 20,000\text{--}35,000$  Hz at 200 MHz!). The barrier is substantially larger than the analogous rotation of a phenyl group in unsubstituted biphenyl. Both semi-empirical calculations<sup>6</sup> and experimental results<sup>7</sup> have shown the barrier to rotation in biphenyl to be of the order of 2-3 kcal mol<sup>-1</sup>. Undoubtedly, the higher barrier in diphenyluranocene results from the wider C-C-C bond angle in the [8]annulene ring compared to benzene.

## Experimental

Measurement of the Rotational Barrier. The  $^1\text{H}$  NMR spectra were run on the UC Berkeley FT-NMR 200 MHz spectrometer. The system employs a superconducting magnet, a deuterium lock system, and Nicolet software. Temperature was monitored by a Doric Trendicator 410A. Line shape analyses were performed using an exchange program written for the 1180 Nicolet system as part of the NTCFT software package.<sup>8</sup> All measurements were carried out in approximately  $10^{-3}$  M solutions in toluene- $d_8$  and THF- $d_8$ .

Chemical shifts for 1,1'-diphenyluranocene and 1,1'-di-o-tolyluranocene were determined at ten degree intervals from  $-30$  °C to  $-90$  °C, and are in agreement, within experimental error, with literature values.<sup>1</sup> The line width of the ortho peak at room temperature (fast exchange limit) and of the para-phenyl peak down to  $-85$  °C (no exchange) was found to be 20 Hz. Thus, the natural line width of the ortho peak was taken to be 20 Hz.

Errors in  $\Delta H^\ddagger$  and  $\Delta S^\ddagger$  were calculated by the program ACTENG<sup>9</sup> ( $k$ ,  $\pm 10\%$ ,  $T$ ,  $\pm 0.5^\circ$ ).

Calculation of  $\Delta G^\ddagger$  for the phenyl rotational barrier was made by using the  $\Delta H^\ddagger$  and  $\Delta S^\ddagger$  values from the line-shape analysis ( $\Delta G_c^\ddagger = \Delta H^\ddagger - T_c \Delta S^\ddagger = 5.1$  kcal/mol) and also by extrapolating  $\Delta\nu$  values to the estimated coalescence temperature (from chemical shift vs.  $T^{-1}$  plots,  $\Delta\nu = 31530$  Hz), then substituting into the formulas,  $k = 2^{-0.5} \pi \Delta\nu$  and  $-\Delta G^\ddagger = RT \ln(kh/Kk_B T)$ , where  $K = 1$  ( $\Delta G^\ddagger = 5.2$  kcal/mol).



The preparation of 1,1'-Diphenyluranocene is given in the experimental section of Chapter 1.

1,1'-Di-o-tolylcyclooctatetraene.<sup>5,10</sup> A 250 mL 3-neck flask equipped with condenser, dropping funnel and mechanical stirrer was flame-dried and purged with argon. To this was added 2.0 g (290 mmol) of clean, finely cut lithium wire (1% sodium) and 100 mL of dry ether. Next, 20 g (120 mmol) of o-bromotoluene was slowly dropped in, after which the solution was refluxed for 2 hr. The excess lithium was removed, and 20.5 g of freshly distilled COT (197 mmol) was added. The mechanically stirred solution was slowly warmed to 100°, during which time the ether was allowed to evaporate. The yellow mixture was stirred for 2 hr and was then cooled to 0°, whereupon 100 mL of ether was added to dissolve the mixture. Air was bubbled through for 1 hr, and the reaction was quenched by adding 100 mL of water and 100 mL of hexane. The layers were separated and the organic phase was washed successively with 100 mL of water followed by 60 mL of brine. The yellow solution was dried over calcium carbonate and evaporated to a yellow oil, b.p. 95-98° (0.5 mm). This material was further purified by filtration through a silica column eluted with hexane. <sup>1</sup>H NMR (90 MHz), δ : 6.95 (m, 4H), 5.7 (m, 7H), 2.3 (s, 3H). <sup>13</sup>C NMR (25 MHz) ppm: 144.4, 141.9, 135.2, 132.9, 132.4, 131.7, 130.4, 129.9, 128.8, 127.5, 126.0, 20.1. Anal. Calcd for C<sub>15</sub>H<sub>14</sub>: C, 92.74; H, 7.26. Found: C, 92.51; H, 7.42.

1,1'-Di-o-Tolyluranocene.<sup>11</sup> In an argon-filled glove box 1.75 g (9.1 mmol) of o-tolylcyclooctatetraene dissolved in 135 mL of THF was treated with 0.7 g (18.2 mmol) of clean potassium. The mixture was stirred for 8 hr, whereupon all of the potassium had disappeared leaving a brown solution. To this was added 1.7 g (5 mmol) of uranium tetrachloride dissolved in 100 mL of THF. The solution turned green and was stirred for 3 hr. The THF was removed by vacuum transfer and the residue subjected to high vacuum overnight. The green residue was then loaded into a Soxhlet extractor and extracted with 100 mL of hexane for 10 hr. The hexane was removed leaving 1.1 g (39% yield) of a green solid. A small amount of this material was recrystallized from a hexane-THF mixture. <sup>1</sup>H NMR (180 MHz, toluene-d<sub>8</sub>, 30°): δ 15 (s, 3H), 6.3 (s, 1H), 3.1 (s, 1H), -1.1 (s, 1H), -34 (s, 1H), -33.2 (s, 2H), -34.2 (s, 2H), -37 (s, 2H), -38.3 (s, 1H). Visible spectrum: 623 λ max, 650, 668. Mass spectrum m/e (relative intensity) 626 (M+, 94.32), 433(16.58), 432(100.00), 164(90.80), 179(88.50).  
Anal. Calcd for C<sub>30</sub>H<sub>28</sub>U: C, 57.51; H, 4.50. Found: 57.46; H, 4.70.

Footnotes and References

- 1 Luke, W.; Streitwieser, A., Jr. ACS Symposium Series No. 131, Edelstein, N., ed., P 93.
- 2 Marks, T. J.; Kolb, J. R. J. Am. Chem. Soc. 1975, 1, 27.
- 3 Fischer, R. D. in "Organometallics of the f-elements"; Marks, T. J.; Fischer, R. D., Eds.; D. Reidel Pub. Co., Boston, Mass.; 1979; Pg. 337.
- 4 Gutowsky, H. S.; Jonas, J.; Allerhand, A.; Meinzer, R. A. J. Am. Chem. Soc. 1966, 88, 3185.
- 5 Wang Hsu-Kun, unpublished results.
- 6 Rayez, J. C.; Dannenberg, J. J. Chem. Phys. Lett. 1976, 41(3), 492.
- 7 Poshkus, P. P., Grumadas, A. J. J. Chrom. 1980, 191(1), 169.
- 8 Reeves, L. W. Advances in Phys. Org. Chem. 1965, 3, 187.
- 9 DeTar, D. F. "Computer Programs for Chemistry, Vol. III", DeTar, D. F., ed.; W.A. Benjamin, New York, 1969.
- 10 DeKock, C. W.; Miller, J. T.; Brault, M. A. J. Org. Chem. 1979, 44, 3508.
- 11 Prepared by Matt Lyttle.

This report was done with support from the Department of Energy. Any conclusions or opinions expressed in this report represent solely those of the author(s) and not necessarily those of The Regents of the University of California, the Lawrence Berkeley Laboratory or the Department of Energy.

Reference to a company or product name does not imply approval or recommendation of the product by the University of California or the U.S. Department of Energy to the exclusion of others that may be suitable.

*LAWRENCE BERKELEY LABORATORY  
TECHNICAL INFORMATION DEPARTMENT  
UNIVERSITY OF CALIFORNIA  
BERKELEY, CALIFORNIA 94720*